12
Antibiotics and the Inhibition of Ribosome Function

Daniel N. Wilson

12.1
Introduction

The protein synthetic machinery is a highly complex apparatus that offers many potential sites for functional interference and therefore represents a major target for antibiotics. The knowledge of the structure and function of the ribosome and associated translation factors has progressed enormously in the past five years, which has, in turn, accelerated our understanding of the mechanism of drug action. Conversely, drugs have been used as tools to probe the translation cycle thus providing a means to dissect further the multitude of steps involved in protein synthesis. In an era where bacteria are showing an ever-increasing resistance to many clinically relevant antibiotics the importance to understand their mechanism of inhibition is essential to the development of novel and more effective replacements. Here we attempt to provide a summary of the current understanding of how antibiotics functionally disrupt translation, with an emphasis on antibiotics that have been well-characterized biochemically, and in particular, structurally.

12.1.1
The Inhibition of Protein Synthesis in Bacteria

The translation machinery ensures accurate conversion of the genetic information of the messenger RNA (mRNA) into the corresponding polypeptide sequence. The ribosome provides the platform on which the mRNA can be decoded by transfer RNAs (tRNAs). Each tRNA carries a specific amino acid, which is faithfully incorporated into the growing polypeptide chain. Three tRNA-binding sites exist on the ribosome: The *A-site* is the site at which decoding occurs; here the correct *aminoacyl-tRNA* (aa-tRNA) is selected on the basis of the mRNA codon displayed at this site. Before peptide-bond formation, the *P-site* carries the *peptidyl-tRNA*, the tRNA bearing the elongating polypeptide chain. The *E-site* binds exclusively deacylated tRNAs, i.e., those tRNAs that having undergone peptide-bond formation are ready to *exit* from the ribosome (see Chap. 6 for details).

Protein synthesis can be divided into three distinct phases (Fig. 12.1). The initiation phase results in the necessary binding of the first or initiator tRNA to the P-site

Protein Synthesis and Ribosome Structure. Edited by K. H. Nierhaus and D. N. Wilson

ISBN 3-527-30638-2

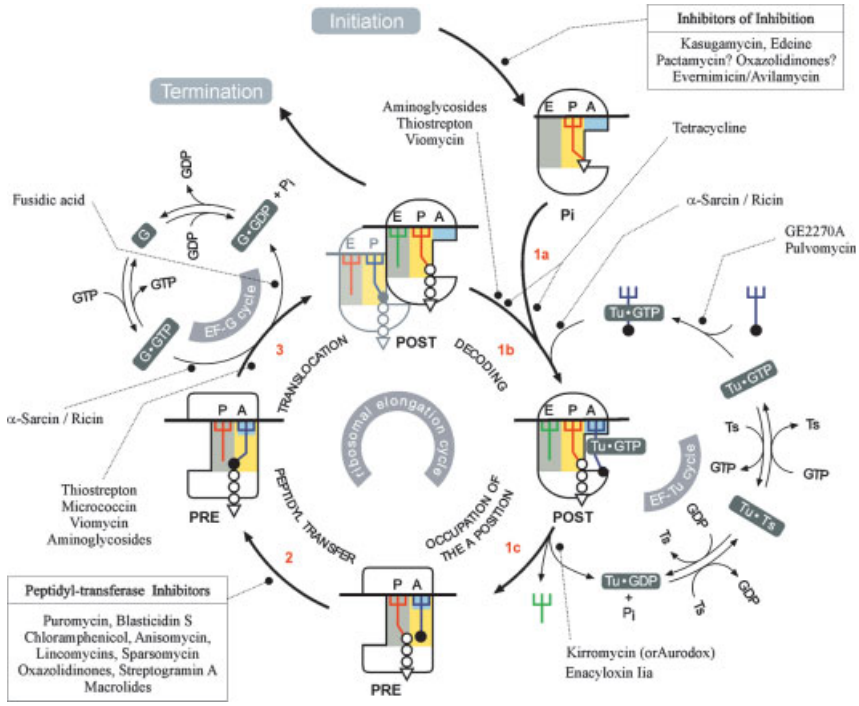

Figure 12.1 Inhibition of the initiation and elongation phases of translation by antibiotics. This figure was updated and modified from [64].

of the ribosome (Chap. 7). The second phase of translation, elongation, involves the movement of tRNAs in a cyclic fashion through the three binding sites on the ribosome, where the number of cycles is dictated by the length of the polypeptide being synthesized (Chap. 8). The first step in the cycle involves binding of the aa-tRNA to the A-site, which is facilitated by a protein factor EF-Tu. During subsequent elongation cycles, binding of the aa-tRNA to the A-site releases the E-site tRNA, maintaining two tRNA per ribosome at any given stage. Peptide-bond formation proceeds, transferring the entire polypeptide chain from the peptidyl-tRNA in the P-site to the aminoacyl moiety of the A-site tRNA. Now the ribosome has a peptidyl-tRNA at the A-site and a deacylated-tRNA at the P-site, a situation that is restored by a process termed translocation. The translocation reaction is catalysed by a second elongation factor, EF-G, and returns the *peptidyl-tRNA* to the *P-site* (although the peptidyl moiety is now extended by one amino acid) and the *deacylated tRNA* to the *E-site* – the outcome being that the *A-site* is now free to bind the next *aa-tRNA*. Thus, in the course of an elongation cycle, the ribosome can be thought to oscillate between two functional states; the pre- (PRE) and post-translocation (POST) states. This oscillation continues until a stop signal in the mRNA

enters the A-site triggering the third and final phase, termination. Stop signals are not generally decoded by tRNAs, but are recognized by protein termination factors, which function to hydrolyse the peptidyl-tRNA bond and release the translated polypeptide from the ribosome (termination is discussed in more detail in Chap. 9).

Every step described above provides a potential target for antibiotics. Indeed, antibiotics have been discovered that target almost every step of translation (as illustrated in Fig. 12.1), although with differing degrees of specificity. Antibiotics are defined as low-molecular-weight metabolic products, usually below 2 kDa, which are produced by microorganisms and inhibit at low concentrations (typically in the μM range) the growth of other microorganisms. The term antibiotic is used here in the broader sense to encompass non-natural chemical compounds that exhibit inhibitory effects against particular microorganisms, such as synthetic and semi-synthetic compounds.

Studies into translation as a target for antibiotics are not recent undertakings and were well advanced early on, as exemplified by the 100-page review of Gale et al. [1] in the early 1970s. Since then few new antibiotics have been uncovered, although numerous "second- and third-generation" derivatives have been developed that are much more potent than their "first-generation" forefathers. However, our understanding of antibiotic action has benefited recently from the exponentially increasing knowledge and understanding of the ribosome itself. Atomic resolution structures for the small and large subunits alone and in complex with ribosomal-substrate-mimics, reveal that the functional centers on the respective subunits are composed almost entirely of rRNA (reviewed in Refs. [2–6]). Thus, the importance of rRNA seems paramount for function, whereas ribosomal proteins may have been acquired somewhat later to "fine-tune" the process.

This is further emphasized by the structures of many small- and large subunit-antibiotic complexes (summarized in Table 12.1; reviewed in Refs. [7, 8]), which have revealed that the binding sites of antibiotics targeting the ribosome are in most cases composed entirely of rRNA, i.e., there is little or no interaction with ribosomal proteins. This is in accord with the observation that antibiotics generally target the functional centers of the ribosome. Bearing in mind the complexity of the ribosome, it is surprising that antibiotics target such a limited number of sites on the ribosome – a generous approximation would be that the antibiotics target 1% of the total volume of the ribosome (Figs. 12.2A and B). In any case, these ribosome–antibiotic complexes have furthered our understanding of both ribosome function and antibiotic inhibition mechanisms enormously. They will be analyzed in more detail as we follow the process of translation, chronologically with respect to the reaction sequence of a synthesizing ribosome. For each of the antibiotics discussed, the chemical structures are presented in Appendices A–F in the order they are discussed in.

Table 12.1 Compilation of pdb files for the antibiotic–ribosome structures

Antibiotic	Class	Species[a]	Res.[b] (Å)	Pdb[c] ID	Reference
Small subunit					
Edeine A	Edeine	T.t	4.5	1I95	24
Compound 2	Aminoglycoside		2.5	1O9M	235
Gentamycin C1a[d]	Aminoglycoside			1BYJ	74
Geneticin[d]	Aminoglycoside		2.4	1MWL	75
Hygromycin B	Aminoglycoside	T.t	3.3	HNZ	29
Pactamycin	Pactamycin	T.t	3.4	1HNX	29
Paromomycin[d]	Aminoglycoside			1A3M	236, 70
Paromomycin[d]	Aminoglycoside		2.5	1J7T	72
Paromomycin	Aminoglycoside	T.t	3.3, 3.0	1IBK, 1FJG[e]	67, 68
Paromomycin + ASL^{Phe}/U_6-mRNA	Aminoglycoside	T.t	3.11	1IBL	68
Paromomycin + ASL^{leu2}/U_6-mRNA	Aminoglycoside	T.t	3.0	1N32	66
Paromomycin + ASL^{Ser}/U_6-mRNA	Aminoglycoside	T.t	3.35	1N33	66
Spectinomycin		T.t	3.0	1FJG[e]	67
Streptomycin	Aminoglycoside	T.t	3.0	1FJG[e]	67
Tetracycline	Tetracycline	T.t	3.4	1HNW	29
Tetracycline	Tetracycline	T.t	4.5	1I97	24
Tobramycin[d]	Aminoglycoside		2.5	1LC4	76
Large subunit					
ABT-773	Ketolide	D.r	3.5	1NWX	143
Anisomycin	PTF inhibitor	H.m	3.0	1K73	112
Azithromycin	Azalide	D.r	3.2	1NWY	143
Azithromycin	Azalide	H.m	3.2	1M1K	145
Blasticidin S	PTF inhibitor	H.m	3.0	1KC8	112
Carbomycin A	Macrolide	H.m	3.0	1K8A	145
Chloramphenicol	PTF inhibitor	D.r	3.5	1K01	127
Chloramphenicol	PTF inhibitor	H.m	3.0	1NJI	112
Clarithromycin	Macrolide	D.r	3.5	1K00	127
Clindamycin	Lincosamide	D.r	3.1	1JZX	127
Dalfopristin	Streptogramin A	D.r	3.4	1SM1	274
Erythromycin	Macrolide	D.r	3.5	1JZY	127
Puromycin[f]	PTF inhibitor	D.r	3.7	1NJ0	108
Puromycin[g]	PTF inhibitor	H.m	3.0	1FG0	104
Puromycin[h]	PTF inhibitor	H.m	3.2	1FFZ	104
Puromycin[i]	PTF inhibitor	H.m	3.1	1KQS	104
Quinupristin	Streptogramin B	D.r	3.4	1SM1	274

Antibiotic	Class	Species[a]	Res.[b] (Å)	Pdb[c] ID	Reference
Roxithromycin	Macrolide	D.r	3.8	1JZZ	127
Sparsomycin	PTF inhibitor	D.r	3.7	1NJN	108
Sparsomycin + ASM	PTF inhibitor	D.r	3.6	1NJM	108
Sparsomycin + CCA-pcb	PTF inhibitor	H.m	2.8	1M90	112, 106
Spiramycin	Macrolide	H.m	3.0	1KD1	145
Telithromycin	Ketolide	D.r	3.4	1P9X	144
Troleandromycin	Macrolide	D.r	3.4	1OND	142
Tylosin	Macrolide	H.m	3.0	1K9M	145
Virginiamycin M	Streptogramin A	H.m	3.0	1N8R	112

a T.t, D.r and H.m correspond to the thermophilic bacterium *T. thermophilus*, the radiation-resistant eubacterium *Deinnoccus radiodurans* and the archaebacterium *Haloarcula marismortui*, respectively.

b Res. value corresponds to the maximum resolution attained in the high-resolution bin. The resolution values for NMR investigations are not given.

c Protein data bank (pdb) files for each antibiotic complex can be downloaded at http://www.rcsb.org/pdb/ and easily viewed with rasmol (http://www.bernstein-plus-sons.com/software/rasmol_2.7.7/ [237]), swiss-pdb-viewer (http://www.expasy.ch/spdbv/ [238]) or VMD (http://www.ks.uiuc.edu/Research/vmd/ [239]).

d The structures for these antibiotics were solved in complex with an RNA fragment mimic of the decoding center of the 30S subunit.

e These antibiotics have the same pdb number since their structures were determined at the same time by soaking crystals in a solution containing a mixture of all three antibiotics, streptomycin, paromomycin and spectinomycin.

f Puromycin is in the form of ACC-puromycin

g Puromycin attached to a 13 bp minihelix and thus mimics a tyrosyl-tRNA acceptor stem

h Puromycin in the form of an analog of A-site aa-tRNA and P-site peptidyl-tRNA covalently linked by the tetrahedral carbonyl carbon intermediate during peptide-bond formation (Yarus inhibitor)

i The products of the PTF reaction where the A-site has CCA and the P-site contains puromycin in the form of CC–Puromycin–phenylalanine–caproic acid–biotin.

12.2 Inhibitors of Initiation

The initiation phase in bacteria differs significantly from that in eukaryotes (see Chap. 7); bacterial transcription and translation are coupled whereas they are compartmentalized into the nucleus and cytosol of the eukaryotic cell, respectively. This segregation is responsible for the increased complexity of events preceding translation initiation itself, these include such processes as mRNA splicing and transport. The complexity of eukaryotic translation initiation is also reflected by the

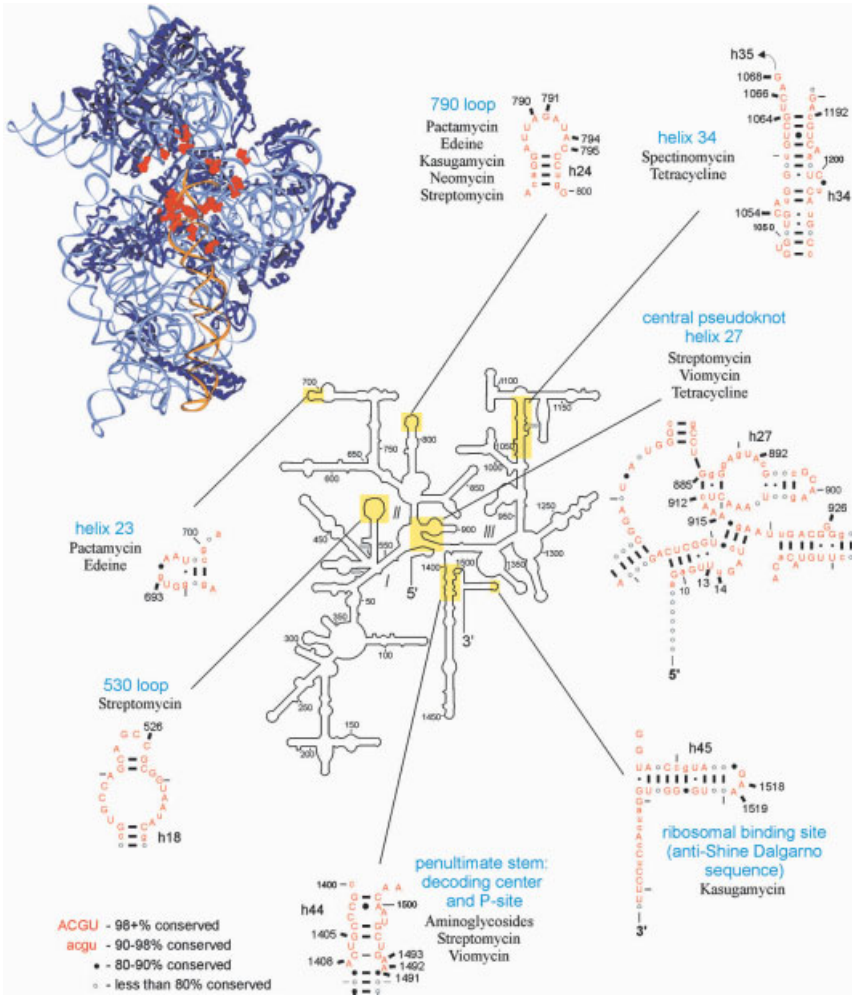

Figure 12.2

large number of protein factors required for this event, at least 13 have been identified so far, whereas in bacteria only three are necessary. In theory, one would think that this disparity could provide an ideal target for drugs, i.e., specific inhibitors of bacterial initiation, which should not have any adverse affects on eukaryotic cells. However, in practice, there are few antibiotics known today that *specifically* block initiation and those that have been identified seem to be universal inhibitors of translation initiation. Surprisingly, it is the drugs that target the conserved functional centers within the ribosome, such as the decoding site or the peptidyl transferase (PTF) center that exhibit differential effects across the three kingdoms (several reasons are discussed below).

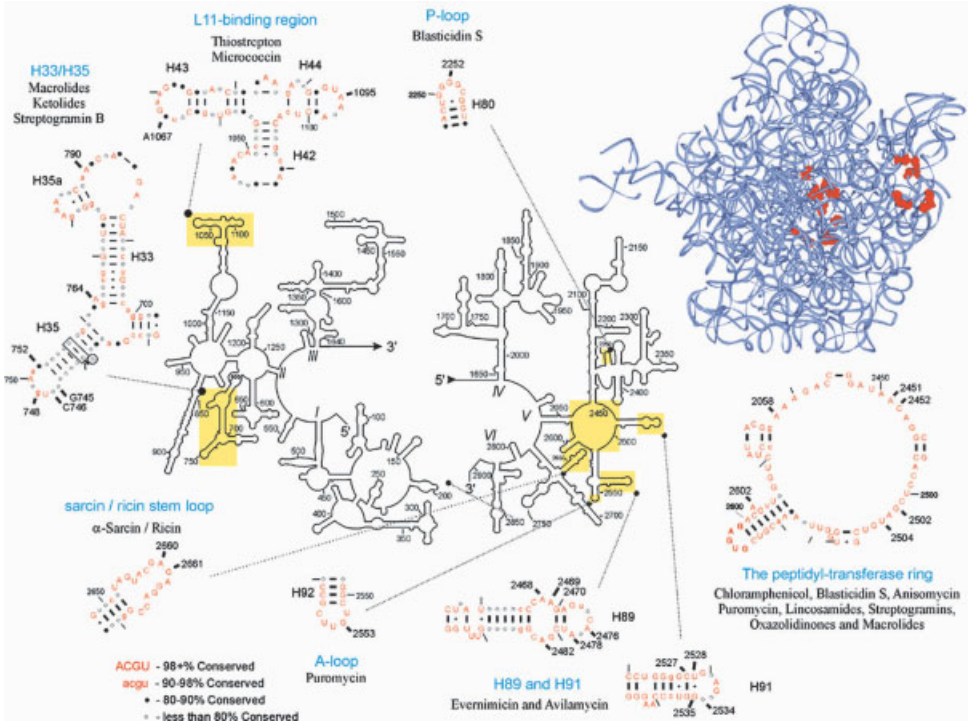

Figure 12.2 Regions of the small and large rRNA associated with various antibiotics. The (A) 16S rRNA and (B) 23S rRNA are schematically represented in the center of each figure, with regions of specific interest enlarged and bases associated with listed antibiotics indicated. The secondary structures were obtained from URL: http://www.rna.icmb.utexas.edu/ and illustrate the conservation in the 16S and 23S rRNA throughout the bacterial phyla, mapped on to the *E. coli* secondary structures [270].

Translation initiation by bacterial ribosomes operates through a pre-initiation complex, consisting of the small ribosomal subunit, mRNA, the initiator fMet-tRNA and three initiation factors, IF1, IF2, and IF3. Association with the large subunit releases the remaining IFs, leaving the initiator tRNA at the P-site, ready for A-site binding (reviewed in Ref. [9]).

There are at least five antibiotics that are commonly referred to as translation-initiation inhibitors. Kasugamycin and edeine both act to inhibit initiator tRNA binding to the 30S subunit but probably do so via different mechanisms. The exact step of initiation by pactamycin is unclear: early reports suggest that it allows initiator tRNA binding to the 30S subunit but prevents association of the pre-initiation complex with the 50S subunit, although recent analysis suggests that pactamycin is in fact a translocation inhibitor. The oligosaccharide antibiotics evernimicin and avilamycin bind the 50S subunit and appear to inhibit association of the pre-initiation complex with the antibiotic bound 50S subunit, thereby preventing 70S ribosome formation.

12.2.1 Kasugamycin

Kasugamycin (Ksg) is thought to inhibit the initiation phase of protein synthesis without affecting elongation [10]. By preventing the binding of fMet-tRNA^{fMet} to the prospective P-site on the 30S subunit, Ksg prevents the formation of the pre-initiation complex, although the exact mechanism by which this is accomplished remains to be determined.

In the early 1970s, resistance to Ksg was shown to arise from mutations of a particular gene, termed *ksgA* because of the resistance phenotype, later shown to encode a methylase responsible for post-transcriptional modification of two adenine residues near the 3′-end of 16S rRNA, namely the universally conserved bases A1518 and A1519 (*Escherichia coli* numbering is used throughout this chapter, unless otherwise indicated) [11–13]. These modifications are the only universally conserved modifications of the rRNAs. A recent study demonstrated that almost any base mutation at position A1519, but none at A1518, could confer resistance to Ksg [14]. This same study also identified two other universally conserved 16S rRNA positions A794 and G926 as conferring Ksg resistance, in agreement with earlier studies demonstrating that binding of Ksg to ribosomes protected these same bases from chemical probing (also the reactivity of C795 was found to be enhanced [15]; Fig. 12.2A). It seems unlikely that a single molecule of Ksg could contact all three regions simultaneously since G926 is located some 15–20 Å from A794 and A1519 in the 30S crystal structure, although contact with the latter two would be possible since they are only 6–7 Å apart (Figs. 12.3A and B).

Ksg does not inhibit translation of leaderless mRNAs at concentrations where translation of canonical mRNAs is abolished [16, 17]. (Canonical mRNAs in prokaryotes are those mRNAs that contain an AUG start codon, upstream of which, is the so-called Shine and Dalgarno (SD) sequence, a region of the mRNA complementary to part of the 3′-end of the 16S rRNA called the anti-SD. Base pairing between these two sequences is thought to help in positioning the start codon in the ribosomal P-site.)

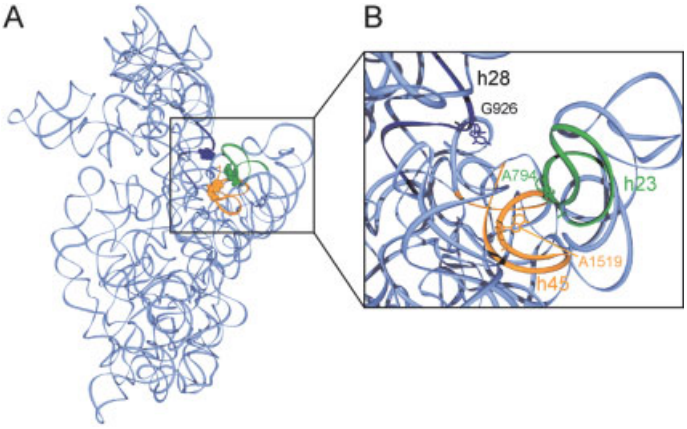

Figure 12.3 The nucleotides of the 16S rRNA associated with the antibiotic kasugamycin. (A) The rRNA of the *T. thermophilus* 30S subunit is shown as a ribbons representation (pale blue) with h28 (blue), the 790-loop (green) and the penultimate helix, h45 (yellow) highlighted. Bases associated with kasugamycin are shown as space fill representation and are detailed in B. (B) Close-up of bases associated with kasugamycin: G926 of h28 (blue), A794 of h24 (green) and A1519 of h45 (yellow). These figures were made from pdb 1fjf [271].

The implication here is that Ksg cannot inhibit P-site tRNA binding when there is no mRNA sequence upstream of the start codon. It is interesting to note that addition of Ksg could remove pre-bound initiator tRNA from 30S subunits, but not from 70S ribosomes [18]. However, although this is an attractive hypothesis, we note that Ksg had no effect on SD-anti-SD interactions nor did it influence the function of IF3 [17].

In addition, Ksg may affect the full maturation of the 30S subunit, since overexpression of the *KsgA* methylase (that when knocked out gives rise to Ksg^R) rescued a temperature-sensitive strain resulting from deletion of a small GTPase called Era [19]. Era has recently been implicated in a final step in the assembly of the 30S subunit, namely the processing of the precursor 17S rRNA to the mature 16S rRNA [20]. Intriguingly, 61S particles are formed in the presence of low concentrations of Ksg that contain normal 50S ribosomal subunits but reduced 30S particles. The latter contain 11 instead of 21 S-proteins and are competent in translating leaderless mRNAs, but not normal SD-sequence carrying mRNAs [21]. Clearly, determination of the Ksg binding site on the 30S subunit would provide much needed help to functional biochemists in elucidating the action of this antibiotic.

12.2.2 Edeine

Edeine A_1 (Ede) is the major active component of one of a number of isomers produced by the bacterium *Bacillus brevis* Vm4 and is composed of an N-terminal

β-tyrosine residue attached to a C-terminal spermidine-like moiety (see Appendix A1). Ede is effective *in vitro* but not *in vivo*. *In vitro* it blocks ribosomes derived from organisms of all kingdoms. Ede has been shown to inhibit specifically mRNA-directed binding of aa-tRNAs to both 30S subunits and 70S ribosomes [22]. Consistent with these observations, the footprints on the 16S rRNA corresponded exactly with those produced by a P-site bound tRNA [23, 15]. Recently, the crystal structure for Ede bound to the *Thermus thermophilus* 30S subunit revealed a single binding site for this antibiotic on the solvent side of the platform sandwiched between h24, h28, h44, and h45 [24]. Binding of Ede induces base-pair formation between C795 and G693 at the tips of h24a and h23b, respectively [24] (see Figs. 12.4A and B). Exactly these same residues were protected from chemical probing upon tRNA binding to the ribosomal P-site [23]. In light of the 70S crystal structure with tRNAs bound at A-, P- and E-sites [25], it is now clear that these bases are located in the E-site and not the P-site as first thought. The conclusion being that the protections most probably result from conformational changes in the rRNA upon tRNA binding and not through direct interaction with the P-tRNA. This suggests (i) that tRNA binding at the P-site requires an open conformation regarding the C795-G693 base-pair, and (ii) because Ede also induced conformational changes in this region, the

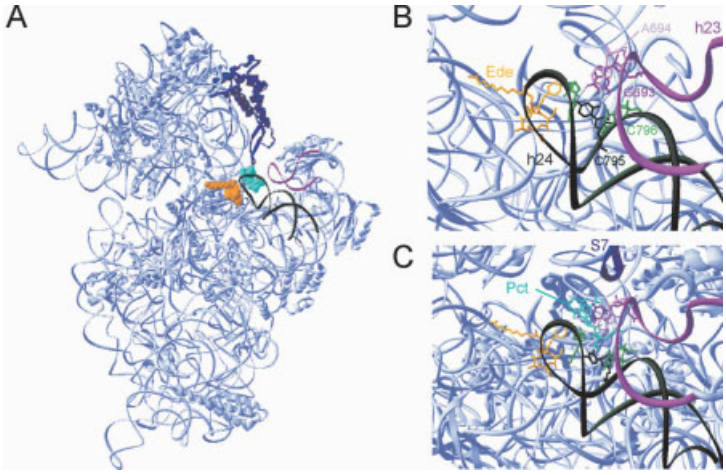

Figure 12.4 The binding site of edeine and pactamycin on the *T. thermophilus* 30S subunit. (A) The 16S rRNA is shown in ribbons (pale blue) with h23 (crimson) and h24 (dark green) and ribosomal protein S7 (blue) highlighted. The relative positions of edeine (yellow) and pactamycin (cyan) are shown with spacefill representations. (B) Close-up view of the G693-C795 base-pair (dark green and crimson, respectively) induced upon edeine (Ede, yellow) binding. Other bases indicated are A694 (pink) and C796 (pale green). Hydrogen bonding is indicated with a dashed blue line. (C) Close-up view of the pactamycin (Pct, cyan) bound between the tip of h23 and h24. The two distal rings of Pct can be seen stacking onto each other and the base of G693, whereas the third ring inserts into the crevice between the helices where it interacts with C795 and C796. All bases and helices are coloured as in (A) and (B). These figures were made from pdb files 1hnx [29] and 1i95[24].

mode of inhibition of Ede may be indirect, i.e., Ede binding may, by inducing the closed conformation (C795-G693 base-pair formation) and locking h23-h24 together, mimic a ribosome already containing a P-site tRNA and therefore prevent the associated conformational changes necessary for stable binding of tRNA to the P-site.

Furthermore, the observation that the predominant contacts between the P-site tRNA and the 30S subunit are due to codon–anticodon interactions [25, 272], suggests that the mechanism of action of Ede is to prevent interaction between codon and anticodon. This is supported by the observation that Ede inhibits the binding of the encephalomyocarditis virus (EMCV) internal ribosome entry site (IRES) to the ribosome but not that of the cricket paralysis virus (CrPV), since the former initiates out of the P-site using Met-tRNAi and eIF2-GTP, whereas the latter initiates out of the A-site [273].

One effect of Ede that had been previously overlooked was its ability to induce translational misreading, at levels comparable with those of the classic misreading antibiotic streptomycin [22]. This represents the first example of an antibiotic that induces misincorporation events from the E-site, supporting the link between E-site and translational fidelity proposed by the α–ε model for elongation (see Chap. 8.1). Consistently, the introduction of site-specific mutations within S7 or S11, both of which are located within the E-site connecting the head and platform, also severely reduced translational fidelity, promoting not only misreading but also frameshifting and nonsense suppression [26]. The site-specific mutations were located at the interface between S7 and S11 and are therefore involved in forming the channel through which the mRNA passes, suggesting that the loss of translational fidelity may operate partly by disturbing the path of the mRNA. Similarly, the base-pair induced by Ede binding would also be expected to disrupt the path of the mRNA through the E-site.

12.2.3 Pactamycin

Pactamycin (Pct) was isolated as a potential anti-tumor agent [27], but subsequently shown to be equally effective against intact cells of both bacteria and eukaryotes therefore limiting its clinical use. Although Pct was extensively studied during the 1960s and 1970s, the exact mode of Pct action remained unclear (reviewed in Ref. [28]). Pct is termed an initiation inhibitor since, under certain conditions Pct has been observed to cause an accumulation of putative pre-initiation complexes when in the presence of crude initiation factors. The conclusion from these experiments was that fMet-tRNA binding to the 30S subunit was not inhibited but that association of the pre-initiation 30S complex with the 50S subunit to form a 70S ribosome was prevented, possibly due to a non-functional P-tRNA orientation. However, these observations were inconsistent with reports where pre-initiation complexes associate to form 70S ribosomes although they were non-functional for translation. Furthermore, in eukaryotes, multiple studies observed accumulation of di- and tripeptides suggesting that Pct targeted, not initiation, but an early elongation step (see Ref. [28]).

The crystal structure of the 30S subunit from *T. thermophilus* in complex with Pct has been resolved to 3.4 Å [29]. A single binding site determined on the 30S subunit revealed that the two distal rings of Pct stack upon each other and with G693 at the tip of h23b of the 16S rRNA, whereas the central ring interacts with C795 and C796 in h24a [29] (Fig. 12.4C). Pct, bound in this position, mimics a dinucleotide of the mRNA in the E-site leading to the proposal that Pct disrupts the path of the mRNA through the ribosome. The implication being that translocation of tRNAs into the E-site may be prevented or may cause the tRNAs to drop off the ribosome.

To understand further the target of Pct inhibition, a systematic study analyzing the effect of Pct on each step of initiation and elongation was performed recently [22]. Surprisingly, Pct exhibited no inhibitory effect during the initiation stage of translation, subunit association nor on A-site binding. The site of action seemed to be translocation of the A and P-tRNA to the P and E-sites. What was unusual was that translocation inhibition was markedly influenced by the tRNA species, such that translocation of Met-tRNA, Val-tRNA or Lys-tRNA was significantly inhibited yet when Phe-tRNA was present little or no inhibition was observed. This was then shown to be consistent with the lack of inhibition of Pct on poly(U)-dependent poly(Phe) synthesis but the severe inhibition of Pct on poly(A)-dependent poly(Lys). In conclusion, these results suggest that Pct should not be referred to as an initiation inhibitor, but in fact as an early elongation or translocation inhibitor.

Since the binding site of Pct maintains the C795 and G693 bases in an open conformation, whereas the presence of Ede induces a closed conformation, viz. a Watson–Crick base-pair, the relationship between these two antibiotics was investigated [22]. This study could demonstrate that the inhibition by Ede of fMet-tRNA binding to 30S subunits could be relieved with increasing concentrations of Pct. Similarly, the inhibition of binding of AcPhe-tRNA to the P-site of 70S ribosomes by Ede could also be alleviated by addition of Pct. This led to the proposal that P-site tRNA binding is regulated by the conformation of the C795-G693 basepair and illustrates how studies into antibiotic action yield insight into fundamental mechanisms of ribosome function.

12.2.4
Evernimicin and Avilamycin

The orthosomycins evernimicin (Evn) and avilamycin (Avn) are oligosaccharide antibiotics that exhibit excellent activity against a broad range of Gram-positive bacteria. Evernimicin (SCH27899) was isolated from *Micromonospora carbonaceae* and was trialed as therapeutic agent by Schering-Plough under the name Ziracin. Resistance to these antibiotics has resulted from mutations in ribosomal protein L16 [30–33] and in H89 and H91 of the 23S rRNA [34–36], suggesting that both antibiotics bind the large ribosomal subunit. In agreement, chemical footprinting of Avn on the 23S rRNA identified residues A2482 in H89 and A2534 in H91 [36] whereas the same technique identified these bases, amongst others, within the same helices using Evn [35]. Furthermore, position G2470 is methylated by EmtA,

a methyltransferase – the effect of which is to confer resistance to both Avn and Evn [37] (see Table 12.2 and Fig. 12.2B). The locations of H89, H91 and L16 are in close proximity to each other in the crystal structures of the large subunit [38, 39], being located towards the base of the ribosomal stalk, some distance from the tunnel and PTF center – the "hotspots" for antibiotic interference on the 50S subunit (Figs. 12.5A and B). These are the only known antibiotics to interact with this region of the ribosome, thus explaining the previous observations that bacteria resistant to numerous other antibiotics show no cross-resistance to Evn or Avn as well as the observation that other ribosomal antibiotics do not compete with Evn for ribosome binding [40].

Interestingly, H89 has also been associated with initiation factor IF2, namely, the protection of positions A1476 and A2478 by IF2 from chemical probing when the modifying agent dimethylsulfate was used [41]. Belova et al. [35] proposed that Evn specifically inhibited IF2-dependent formation of a 70S initiation complex, but since the assay that was employed monitors only the transfer of f[^{3}H]Met to puromycin, it was not possible to determine whether Evn actually inhibits subunit association or whether association occurs, but the fMet is not in the correct orientation for transfer to puromycin. The former seems most probable given that *in vivo* brief incubation of bacterial cells with Evn reduced the amount of 70S ribosomes. In agreement with

Table 12.2 Evernimicin- and avilamycin-resistant mutations in L16 and 23S rRNA

Antibiotic	Ribosomal component	Mutation position	Detection[a]	Reference
Evn	L16	R51H, I52T, R56H	Spontaneous	33
Evn	L16	I52S, I52T, I52N, R51C	Spontaneous, engineered	31
Evn	L16	R51C, R51H	Spontaneous	32
Evn/Avn	L16	R56H, R56H, I52T, I52S	Spontaneous	30
Evn	23S rRNA	A2469C, C2480T, G2535A, G2536C	Spontaneous	34
Evn	23S rRNA	G2535A	Spontaneous	33
Evn	23S rRNA	A2471G, A2471C, A2478C, U2479C, C2480A, C2480U, G2527A, U2528C, and G2535A	Spontaneous, Two were also engineered	35
Evn	23S rRNA	A2468, A2469, A2476, A2478, A2482 in H89 and A2534 was protected in H91	Footprinting	35
Avn	23S rRNA	G2470U, A2471G, G2472U, U2479C, C2480U	Spontaneous	36
Avn	23S rRNA	A2482 (H89) A2534 (H91)	Footprinting	36

a Although *E. coli* numbering is given for convenience, the spontaneous resistance mutations were generally detected in other organisms such as *Streptococcus pneumoniae, S. aureus and H. halobium.*

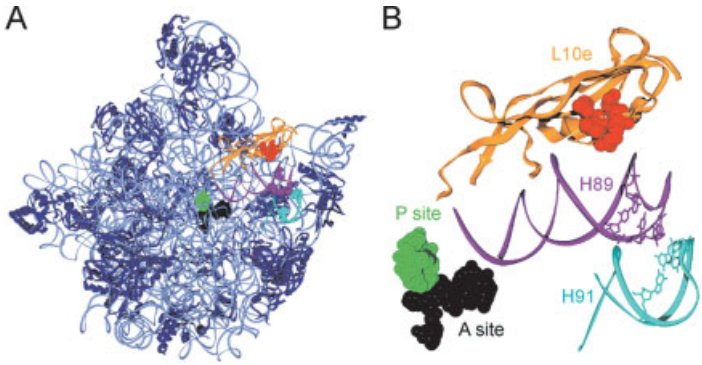

Figure 12.5 The putative binding site of Evernimicin and Avilamycin on the 50S subunit. (A) Regions associated with resistance to Evn and Avn are highlighted on the *H. marismortui* 50S subunit (PDB1KQS; [107]). Ribosomal RNA shown in ribbons with H89 (purple) and H91 (cyan) and ribosomal proteins coloured dark blue except L10e (L16 homolog) which is coloured yellow. Positions of L10e and H89/H91 associated with resistance to Evn or Avn are indicated in red spacefill. The products of the PTF reaction in the A site (dark green) and P site (light green) are provided as a reference for the PTF center. (B) Close-up of (A), showing only H89, H91, L10e and, as a positional reference, the PTF products bound at the PTF centre. Coloured as in (A), except here the bases of H89 and H91 that are associated with resistance to Evn/Avn are coloured in purple and cyan respectively.

this proposal, *in vitro* assays with Evn did not inhibit peptidyl-transferase activity in the absence of IF2 nor did Evn prevent pre-initiation complex formation [35].

It should also be noted that Evn has also been shown to inhibit specifically assembly of the 50S subunit. However, this assembly inhibition required a 50% inhibitory dose some 10 times higher than that required to inhibit protein synthesis indicating that ribosome function is the primary target of the drug [42]. There are numerous antibiotics that are much more efficient inhibitors of ribosome assembly and they are the subject of the next section.

12.2.5
Antibiotic Inhibitors of Ribosome Assembly

It is becoming clear that a large number of antibiotics that have been well characterized as protein synthesis inhibitors, also double as inhibitors of ribosomal subunit assembly (reviewed in Ref. [43]). In the past few years the list has been growing rapidly and now includes representatives of the entire MLS_B class of 50S subunit inhibitors, i.e., macrolides, lincosamides and streptogramin B compounds [42], as well as many antibiotics that target the 30S subunit, such as members of the aminoglycoside family [44]. A number of clinical relevant antibiotics fall into these categories

emphasizing the importance of understanding the dual action of these drugs to develop more effective inhibitors; examples include both 14-/15- (erythromycin and semi-synthetic derivatives azithromycin, clarithromycin, and roxithromycin) and 16-membered macrolides (tylosin and spiramycin), the ketolide antibiotics, the lincosamides lincomycin and clindamycin, the oxazolidone linezolid and also the medically important aminogylcosides (see later sections for more information on these antibiotics).

The importance of the inhibition of subunit assembly is determined by measuring the effect of each antibiotic on both protein synthesis and subunit assembly over a range of antibiotic concentrations. In almost all cases the IC_{50} for translation inhibition was precisely half the IC_{50} required for blocking subunit assembly (see Table 12.3; [43]), suggesting that the inhibitory effects on translation and subunit assembly are equivalent. The reasoning is that since subunit assembly is a prerequisite for active ribosomes, an IC_{50} for subunit assembly will reduce the number of translationally active ribosomes by half and therefore the IC_{50} for translation will be exactly half that observed for subunit assembly. The exception was evernimicin, which, as mentioned previously, required a 13-fold higher concentration to inhibit subunit assembly than that required for translation inhibition.

Furthermore, most of the antibiotics tested specifically inhibited assembly of only one ribosomal subunit, such that antibiotics that inhibited 50S subunit formation exhibited no inhibition on 30S subunit assembly and *vice versa*. Subunit inhibition also correlated with the known inhibitory action on translation of each antibiotic, for example, the macrolide erythromycin, which has been shown to obstruct the progression of the nascent chain by binding within the tunnel of the 50S subunit (see Sect. 12.3.2.4), inhibited 50S subunit formation without influencing 30S subunit formation [45]. Likewise, the aminoglycoside neomycin and a closely related derivative paramomycin (both of which induce translational misreading by binding within the decoding center of the 30S subunit; see Sect. 12.3.1.2), were shown *in vivo* to reduce 30S subunit formation without effecting 50S subunit assembly [44]. In contrast, antibiotics, such as chloramphenicol, a potent peptidyl-transferase inhibitor, were shown to inhibit formation of both ribosomal subunits in a non-specific fashion. Although this is also true of streptogramin A class (e.g. virginiamycin M and

Table 12.3 Antibiotics IC_{50} for translation and subunit assembly [43]

	Half-inhibitory concentration IC_{50} ($\mu g\ ml^{-1}$)	
Antibiotic	**Translation**	**Assembly**
Erythromycin	0.17	0.36
Azithromycin	2.5	5.0
Clarithromycin	0.075	0.15
ABT773	0.02	0.035
Telithromycin	0.04	0.08
Evernimicin	0.03	0.4
Linezolid	0.3	0.6
TAN1057A	4.5	9.0

CP36926), the streptogramin B antibiotics (e.g. pristinamycin I_A, virginiamycin S and CP37277) inhibit only 50S subunit formation – a difference not necessarily unexpected since the streptogramin A and B class are not structurally related.

Recently, experiments were undertaken to determine the mechanism of inhibition on subunit assembly [46]. Cells were treated with radiolabelled erythromycin and then the 70S ribosomes and subunits were separated from one another on a sucrose gradient and their radioactive content determined. The results revealed that erythromycin bound both the mature form of the 50S subunit as expected but also an assembly intermediate found to contain the 23S and 5S rRNAs and 18 of the 34 ribosomal proteins found in the *E. coli* 50S subunit. Importantly, the binding stoichiometry of each interaction was 1:1. Therefore, it seems likely that during an early stage in the assembly of the 50S subunit, a binding site is formed, perhaps the same or similar one to that in the mature subunit, to which erythromycin binds. Binding of erythromycin might prevent either conformational changes in the precursor particle, or the binding of additional ribosomal proteins, necessary for further assembly. This mode of inhibition is likely to be transferable to other antibiotics, especially other macrolides (and ketolides), and also to the structurally unrelated lincomycins, all of whose binding sites overlap to a large extent (see Sect. 12.3.2). Furthermore, 30S subunit assembly progresses through intermediates (see Sect. 3.1); therefore, by applying the same model for assembly inhibition, one would predict that small subunit assembly is stalled at a precursor stage, perhaps formation of the 21S particle.

12.3 Inhibitors of the Elongation Cycle

Following initiation, the ribosome is "primed" with an initiator tRNA at the P-site (fMet-tRNA in bacteria and Met-$tRNA_i$ in eukaryotes and archaea) and displays a codon at the A-site specific for one species of tRNA. (A species of tRNAs is defined by the anticodon it bears as opposed to the amino acid. This is because there are a set of tRNAs that are charged with the same amino acid although they bear distinct anticodons. See Chap. 4.1 for more information.) This is a unique situation for a ribosome since it has only a single tRNA bound, i.e., the A and E-sites are free. Binding of a tRNA to the A-site in this situation is termed A-site occupation of the initiation type (i-type). In all subsequent rounds of elongation, the ribosome will always carry two tRNAs, either an A- and P-tRNA in the PRE or a P- and E-tRNA in the POST state. Binding of a tRNA to the A-site of the latter is termed A-site binding of the elongation type (e-type). For some antibiotics, this distinction is irrelevant, for example, tetracycline inhibits both states, but for others it is not, as exemplified by the differential inhibition observed by various antibiotics including aminoglycosides, thiostrepton and viomycin [47].

The elongation cycle can be thought of as the heart of protein synthesis and as such is the prime target of the majority of antibiotics identified to date. Because of the diversity and "ingenuity" of the action of the vast array of studied antibiotics, each step of inhibition will be subdivided into distinct categories for convenience,

although it is acknowledged that some antibiotics can be classified into more than one category.

12.3.1 Antibiotic Action and A-site Occupation

The first step of the elongation cycle involves A-site occupation. Binding of tRNA to the A-site can be separated into two consecutive steps: (i) An initial step involving the binding of the ternary complex aa-tRNA•EF-Tu•GTP to the ribosome, during which only parts of the anticodon stem-loop of the incoming tRNA is in the A-site proper (discussed in more detail in Chap. 8.2), and (ii) a second step involving the hydrolysis of GTP to GDP by EF-Tu and dissociation of EF-Tu from the ribosome, which in turn releases the CCA end of the tRNA enabling it to move into position on the 50S subunit. The outcome being that the tRNA is now fully "accommodated" into the A-site.

Antibiotics inhibit or impair A-site occupation in a number of ways. Tetracycline inhibits the conversion between the first and second binding steps, i.e., prevents full accommodation of the A-site tRNA, which results in the loss of the tRNA from the A-site. In contrast, streptomycin and the aminoglycoside family of antibiotics could be said to "encourage" binding of tRNAs to the A-site, regardless of whether they are cognate for the codon being displayed there. Finally, there is a subset of antibiotics that interfere with EF-Tu function in a significantly different way; for example, the ribotoxins sarcin and ricin prevent binding of EF-Tu to the ribosome, while the antibiotic kirromycin has the exact opposite effect to prevent EF-Tu dissociation.

12.3.1.1 Tetracycline: An Inhibitor of A-site Occupation

Although tetracycline (Tet) was introduced into medicine as early as 1948, it is only recently that the inhibitory mode of action of this antibiotic has become clear. During protein synthesis, Tet is an inhibitor of the elongation cycle, where it specifically prevents binding of tRNA to the A-site. Though non-enzymatic binding (without EF-Tu) of tRNA to the A-site is totally inhibited, the first step of tRNA binding in the form of the ternary complex aa-tRNA•EF-Tu•GTP is possible. However, upon hydrolysis of GTP to GDP by EF-Tu the incoming tRNA is lost from the ribosome.

Recently, two independent crystallography groups solved the structure of the 30S subunit in complex with Tet [29, 24]. In one of the studies two binding sites were identified [29], whereas the other identified six, two of which were equivalent to those of the first study [24] (Fig. 12.6A). Since the inhibitory effect of Tet is presumed to result from binding at a single high-affinity site on the ribosome the task now is to decide which of the identified sites is the biologically relevant inhibitory site. Mounting evidence suggests that the highest occupancy site in both structures is the relevant one and will be referred to hereafter as the primary binding site (Tet-1 in Ref. [24]). In contrast, it seems probable that the contribution made by the secondary (Tet-5 in Ref. [24]) and lesser-occupied sites to inhibition of A-site

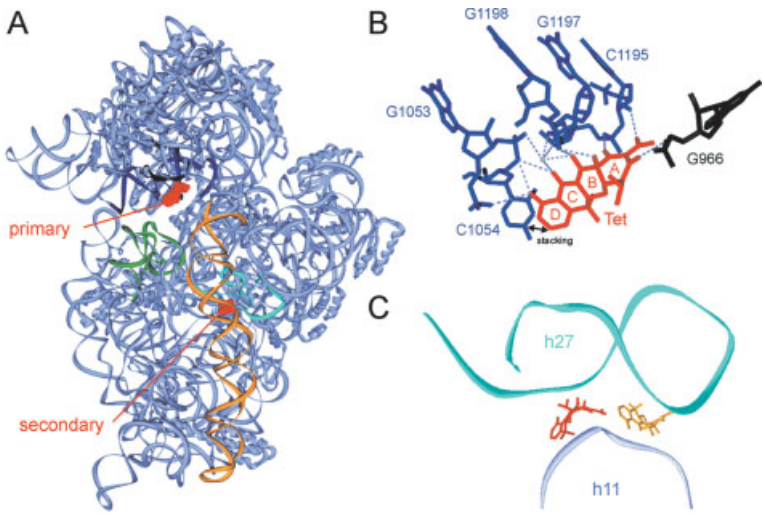

Figure 12.6 The primary and secondary tetracycline binding sites on the 30S subunit. (A) Overview of the primary and secondary tetracycline binding sites (pdb 1hnw) [29], with h34 (blue), h31 (dark green), h18 (light green) h27 (cyan) and h44 (yellow) high-lighted. (B) In the primary binding site the charged or polar face of Tet makes contact exclusively with the phosphate backbone of the 16S rRNA (positions G1053, C1054, 1195-1198 of h34 (blue) and 966 of h31 (green); note that position A965 and the base of U1196 are omitted for clarity), except for stacking interaction with the base of G1054. (C) The secondary Tet binding sites differ significantly between the two independent studies and are shown in red [29] and yellow [24] with h11 (light blue) and h27 (cyan).

binding are negligible, although they do explain the previously inexplicable and often contradictory data for Tet obtained via a variety of biochemical techniques.

In both structures, the primary binding site encompasses the irregular minor groove of h34 and the loop of h31, thus placing Tet directly in the decoding center of the A-site (Fig. 12.6A, B). From this position, Tet was proposed to interfere sterically with a tRNA bound at the A-site. Since the binding mode of the aa-tRNA when in the form of a ternary complex was notably different in orientation to that of the final accommodated state (see Sect. 12.3.1.3 for more details), this explains why the initial binding step of the ternary complex was not inhibited by Tet. Therefore, it is conceivable that upon release of the aa-tRNA from the ternary complex (concomitant with GTP hydrolysis and EF-Tu dissociation from the ribosome) the aa-tRNA falls off the ribosome, since it is only bound weakly to the ribosome through codon–anticodon interactions. The position of Tet in the primary binding site sterically prohibits the accommodation step causing the aa-tRNA to fall-off of the ribosome. This also explains why non-enzymatic binding is inhibited directly.

Moreover, the primary binding site best fulfils the plethora of biochemical data supporting it as the biological inhibitory one:

1. In the primary Tet binding site some interactions between Tet and the 16S rRNA are mediated through a bound magnesium ion (Fig. 12.6B) which may explain the magnesium dependence that has been observed with Tet inhibition [48].
2. Tet interacts with the rRNA using the charged face of the molecule whereas the more hydrophobic face protrudes into the intersubunit space (Fig. 12.6B). Consistently, substitutions generated along the hydrophobic face are generally tolerated (with the exception of the 4-dimethylamino group), while substitutions along the charged face result in loss of antibacterial activity [49].
3. While Tet derivatives that bind the ribosome and inhibit protein synthesis always enhance the DMS reactivity of bases associated with the primary site (for example, C1054 and U1052 in the 16S rRNA), only a subset protects bases associated with the secondary sites (A892) [50].
4. Single-site mutations that confer resistance to Tet are in close proximity to the primary binding site, such as the 16S rRNA mutations discovered in *Helicobacter pylori* and *Propionibacterium acnes* [51-53].
5. The ribosome protection protein Tet(O) binds to the ribosome in the vicinity of the primary binding site and confers resistance to Tet by chasing Tet specifically from this site [54] (this is discussed in more detail in Sect. 12.5.6).

It should be noted that the position of the secondary binding site is often regarded as the other most probable candidate for the inhibitory action of Tet because of its position in the so-called switch region of the ribosome (discussed in more detail in Sect. 12.3.1.2). This region was initially thought to be important for translational fidelity [55], but similar experiments with yeast ribosomes could not confirm this conclusion [56]. In any case, for the reasons mentioned above, its contribution to antimicrobial activity is likely to be less significant. In addition, it is noteworthy that the binding positions of the secondary sites, although being similar between both studies, are upon closer inspection notably different (Fig. 12.6C).

With regard to the broad spectrum of action of Tet, i.e., the observed inhibition of *in vitro* translation across all kingdoms, there is agreement with the interaction of Tet on the 30S, at least for the primary binding site, since the interactions of the Tet molecule are almost entirely composed of interactions with the sugar-phosphate backbone of the rRNA. The single interaction with the base of a nucleotide is via stacking interactions, and therefore does not discriminate between the type of base (Fig. 12.6B). As a corollary, the base mutations that give rise to Tet resistance are usually not associated with the strand containing the stacked bases, but the opposite strand and therefore resistance clearly results from conformational changes that disturb the Tet binding pocket. Other mechanisms that give rise to Tet resistance are reviewed in Ref. [57] and discussed in more detail in Sect. 12.5.6. In spite of its universal inhibition of ribosomes from all organisms, its wide use in medicine is due to the fact that the drug penetrates bacterial cell walls easily in contrast with those of eukaryotic cells.

The increasing incidence of bacterial resistance to the Tet group of antibiotics has led to a decline in their medical usage, which, in turn, has led to a new drive to find novel Tet derivatives. Although attempts were well underway since the discovery of chlortetracycline (reviewed in Ref. [49]), only the recently developed third-generation glycylcyclines look to fulfill their promise (reviewed in Ref. [58]). The glycylcyclines are derivatives of minocycline (7-demethylamino-6-demethyl-6-deoxy-tetracycline) and contain various substitutions at position 9 of the molecule (see Appendix B1 for structure comparisons). Of particular interest are DMG-MINO (9-(*N,N*-dimethylglycylamido)-minocycline), DMG-doxycycline, DMG-DMDOT (9-(*N,N*-dimethylglycylamido)-6-demethyl-6-deoxytetracycline), all of which retained antimicrobial activity and were even effective against some bacterial strains bearing *tet* resistance genes. Reports showed that these derivatives bound more effectively to the primary binding site than Tet, resulting in a 10-fold increase in potency for inhibition [59, 60], perhaps explaining why the ribosomal protection proteins are ineffective against these drugs. Recent interest has focused on one particular derivative, tigecycline or GAR-936 (also called TBG-MINO or 9-(*t*-butylglycylamido-minocycline)), which is currently undergoing Phase II clinical trials. In a recent study, strains resistant to both DMG-MINO and DMD-DOT were discovered (all with mutations in genes encoding Tet efflux proteins). These strains were susceptible to tigecycline; however, screening for resistant mutants uncovered strains with mutant efflux proteins conferring up to 4-fold higher resistance to tigecycline [61].

12.3.1.2 **Antibiotics Affecting the Fidelity of Translation**

The ribosome misreads 1 in ~3000 codons [62]. This effectively means that for every 3000 correct amino acids introduced into nascent polypeptides only one single erroneous amino acid is incorporated. This intrinsically low rate of misincorporation ensures that almost every protein produced by the ribosome is functionally active. The mechanism by which the ribosome successfully accomplishes this feat of translational fidelity has been solved at atomic resolution (see Sect. 8.2). In short, the ribosome monitors the stereochemical interactions between the A-site codon of the mRNA and the anticodon of the tRNA, to distinguish correct (cognate) from incorrect (near- or non-cognate) codon–anticodon interactions.

The aminoglycosides, i.e., streptomycin and the gentamycin, kanamycin, and neomycin families, interfere primarily with A-site occupation of the e-type, but not with that of the i-type [47]. These antibiotics commonly stimulate misreading, resulting in the incorporation of an incorrect amino acid. The increased misincorporation (=1:100) is not responsible for the bactericidal effect *per se*. (Note that a drug is bactericidal if it kills the cells rather than the usual blocking of growth, which is termed a bacteriostatic effect.) This is indicated by the fact that some mutants of the ribosomal protein S4 impair the accuracy of protein synthesis to a similar extent without affecting cell viability. Instead, the bactericidal effect is probably due to the blockage of A-site occupation of the e-type (both P and E-sites are occupied, see Fig. 12.1), i.e., the transition from the POST to the PRE state of the ribosome is blocked. Neomycin and hygromycin additionally impede the movement in the reverse direction

(from PRE to POST), viz. the translocation reaction. Similarly, blockage of the transition between the PRE and POST states in either direction has also been observed with the translocation inhibitors thiostrepton and viomycin [47].

Streptomycin

Streptomycin (Stp) is one of the most extensively investigated antibiotics known to directly interact with the ribosome. Stp is structurally related to the aminoglycoside family of antibiotics and exhibits the same classical hallmark, i.e., it induces translational misreading. Despite these common features, streptomycin binds to a distinct site on the ribosome and therefore mediates its inhibitory and misreading effects by an unrelated mechanism. For this reason streptomycin is treated separately from the other aminoglycosides. The amount of biochemical and structural data relating to this antibiotic that have accumulated over the past 50 years of study is immense, yet the mechanism of inhibition remains to be completely deciphered.

Stp has been co-crystallized in a complex with the 30S subunit of *T. thermophilus* [63]. In excellent agreement with much of the biochemical data (discussed in detail in Ref. [64]) Stp has a single binding site on the 30S subunit that connects helices from all four different domains of the 16S rRNA, namely h1 (nts 13), h18 (526), h27 (915) and h44 (1490) and makes interactions with ribosomal protein S12 (Fig. 12.7). Interestingly, streptomycin interacts only with the sugar-phosphate backbone of the 16S rRNA, i.e., there are no base-specific interactions. A number of the mutations in the ribosomal protein S12 that confer resistance to, and in some cases even dependence on, Stp map within the loop of S12 that directly contacts the molecule (see Table 12.6, with the exception of K53 which contacts h44). Of these mutations, only position K42 directly interacts with Stp, forming a hydrogen-bond with ring I, explaining why mutation of this residue to Arg (R) or Gln (Q) confers resistance. Mutations in other ribosomal proteins, mainly S4 and S5, were found to reverse the Stp-dependent phenotype of the S12 mutations [65]. Ribosomes containing one of the S12 mutations are hyperaccurate in tRNA selection (with the exception of the K42R resistance mutant, which does not alter translation accuracy), i.e., they restrict errors. In contrast, the S4 or S5 mutants are characterized as error-prone or ribosomal ambiguity mutants (*ram*). The same interplay in controlling accuracy is also evident when the yeast *Saccharomyces cerevisiae* harbors the analogous mutations in the equivalent proteins. It follows that the accuracy balance exerted by S12 versus S4 and S5 has been conserved during 2 billion years of evolution underlining its importance for all ribosomes.

The first real insights into the action of, and resistance to, Stp were concurrent with a better understanding of the ribosomal changes associated with tRNA selection. Comparison of 30S subunit crystal structures bound with codon and anticodon, in one case cognate to the codon and in the other, near-cognate, led to the proposal that selection of the correct or cognate tRNA by the ribosome requires a transition from an open to a closed form [66] (discussed in more detail in Chap. 8.2). Stp binding stabilizes the closed form and, by doing so, explains the lower translational fidelity. Transition into the closed form involves (i) disruption of

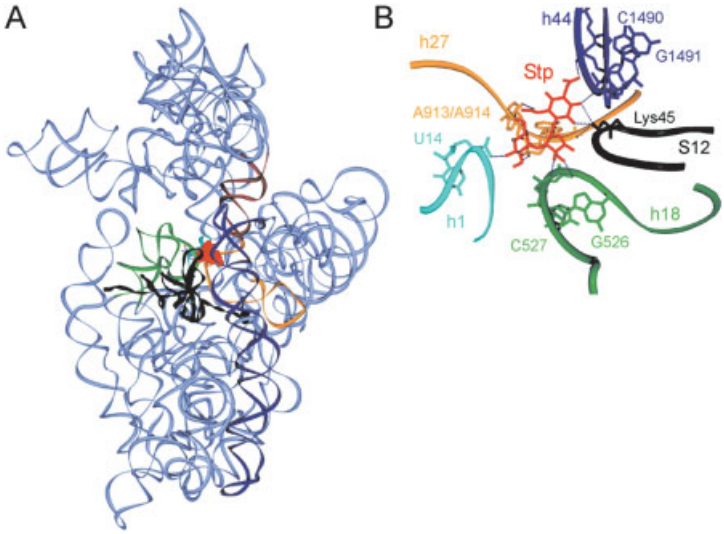

Figure 12.7 The streptomycin binding site on the 30S subunit. (A) Overview Streptomycin binding site (pdb 1FJG)[63] with streptomycin in red space-fill. The 16S rRNA is in ribbons with h1 (cyan), 530 loop or h18 (green), h27 (yellow), h28 (magenta) and h44 (dark blue) and ribosomal protein S12 (dark green) illustrated. (B) Detailed view of the streptomycin binding site. Streptomycin (red) interacts exclusively with sugar-phosphate backbone of the 16S rRNA and in doing so locks together all four of the 16S rRNA domains, namely, the 5′domain (U14 in h1), the central domain (G526 and C527 in the 530 loop), 3′ major domain (A913 and A914 in h27/h28) and 3′ minor domain (C1490 and G1491 of h44). Lysine 45 of S12 interacts with ring I of streptomycin and also the phosphate oxygen of A913. All colours are as in (A).

multiple interactions at the interface between S4 and S5 and (ii) establishment of salt-bridge interactions between S12 and either h44 or h27 of the rRNA. Consistently, (i) mutations in S4 and S5 that promote formation of the *ram* state would also lead to disruptions at this interface, suggesting that the observed error-prone phenotype stems from partially inducing the closed form and (ii) mutations in S12 that block salt-bridge formation may destabilize the closed form and thus confer resistance (or in some cases even dependence on the drug). The antagonistic effects of the S4/S5 *ram* mutants to destabilize the closed form, and the S12 streptomycin-resistant mutants to stabilize it, rationalizes the compensatory effects observed on translational fidelity.

Distinct from the open and closed forms, the ribosome has also been proposed to exist in two distinct states, the *ram* state, which as mentioned above is stabilized by Stp or established by mutations in S4 or S5, and the restrictive state as seen in S12 mutants. The *ram* state is characterized functionally by a large decoding error caused by a high affinity for aa-tRNAs, and was thought also to be achieved by base-pairing of the bases 885–887 with 912–910 in h27 [55]. If the base-pairing in the "switch region" is shifted by three nucleotides so that 912–910 now base-pairs to

888–890, the ribosome was believed to reside in a restrictive state [55]. However, this latter state has not been observed in any of the 30S crystal structures determined to date; in particular, it was not observed in either the closed or open forms, both of which had the 885–887/912–910 base-pairing combination. Furthermore, the importance of this proposed switching mechanism involving universally conserved bases is questionable, since it was shown not to play a role in yeast [56].

Aminoglycosides (2-deoxystreptamines)

Aminoglycosides can be divided into two categories based simply on whether they contain a 2-deoxystreptamine (2-DOS) group or not. Aminoglycosides that target the ribosome predominantly fall into the former class and can be further sub-classified depending on the substitution pattern of the 2-DOS ring, namely, those having sugar rings at position 4 (as for apramycin), both 4 and 5 positions (such as the neomycins (neo), paramomycins (Par) and ribostamycins) or 4,6 di-substituted (for, e.g., gentamycin, kanamycin (Kan) and tobramycin) as seen in the Appendix C1. The amino groups, which are protonated at neutral pH, make them positively charged molecules with high affinity to RNA – a property that was at one time exploited to recover RNA molecules from solution by centrifugation.

Paromomycin (Par) has been solved in complex with the complete 30S subunit [66–68] and also at higher resolution using short rRNA fragments mimicking their binding site on the ribosome [69–72]. The latter technique has also been successfully used to solve the structures of the binding site with a number of 4,6-disubstituted aminoglycosides (reviewed in Ref. [73]), namely, gentamycin C1a [71, 74] and the closely related Geneticin (also called G418 or gentamycin G; [75]) as well as tobramycin [76].

These structures show that the aminoglycoside family of antibiotics target an internal loop in h44 within a region referred to as the decoding site (A-site on 30S, see Fig. 12.8). Binding of aminoglycosides induces conformational changes in the ribosome, first evident from the altered reactivity to modifying agents of nucleotides A1408 and G1494 within this region [23]. The aminoglycoside-bound conformation has a higher affinity for the codon–anticodon complex, which increases the selection of near-cognate tRNAs [77], thereby explaining the decrease in translational fidelity in the presence of this class of antibiotics, as first observed in the 1960s (reviewed in Ref. [28]).

In detail, binding of Par within the decoding center induces the universally conserved residues A1492 and A1493 (green) to flip out of h44 (Figs. 12.8A and B), in a fashion reminiscent to that observed during aa-tRNA binding to the A-site [68]. This conformational change results from the insertion of one (ring I) of the four rings of Par into h44. By doing so, ring I mimics a nucleotide base, stacking against G1491 and forming a hydrogen-bond from the 6′-OH of ring I with the N1 position of A1408. The stability of this conformation is strengthened further by hydrogen-bonding between ring I and the backbone of the flipped out A1493.

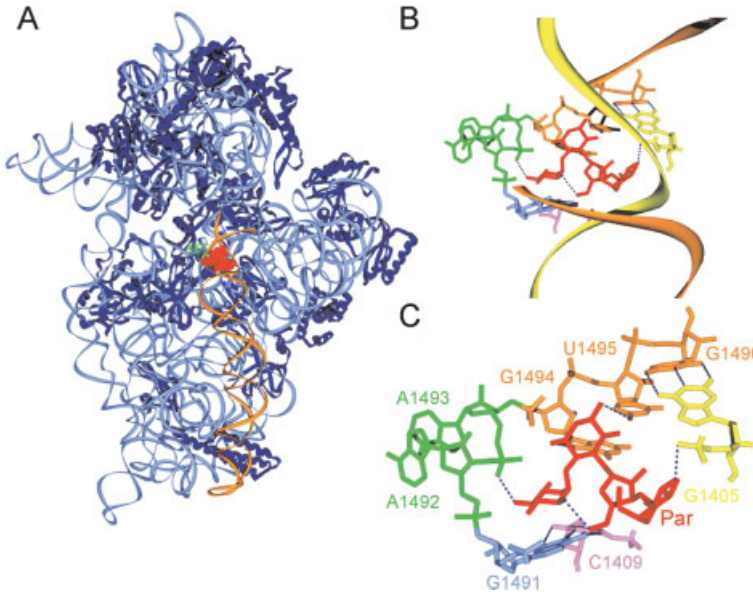

Figure 12.8 Overview of the aminoglycoside paromomycin binding site on the *T. thermophilus* 30S subunit (pdb 1ibk; [68]). (A) Ribbons representation of 16S rRNA (light blue) and ribosomal proteins (dark blue) with h44 high-lighted in yellow and the flipped out A1492 and A1493 in green. Paromomycin is shown in red spacefill representation bound at the top of helix 44. (B) Close-up view of paromomycin site binding site within h44. The different strands of h44 are coloured yellow (1400-1410) and gold (1490-1496) and paromomycin is red. Note the ribbon representation is broken on one strand between 1491-1494. (C) Close-up view of the bases associated with the paromomycin binding site. The flipped out bases of A1492 and A1493 (green), the G1491-C1409 base-pair that forms the shelf upon which ring I sits (pale blue and pink respectively) as well as U1405 (yellow) and G1494, U1495 and G1496 (orange). Hydrogen bond interactions are indicated with a dashed line, for example, in the Watson-Crick 1405-1496 base pair. Paromomycin is coloured red.

As discussed in Chap. 8.2, the formation of correct codon–anticodon interactions is monitored by the formation of A-minor interactions between A1492 and A1493 with the codon–anticodon helix. Presumably, the energy required to flip out A1492 and A1493 during decoding is compensated for by interactions established with the codon–anticodon helix, thus stabilizing this conformation [68]. In the presence of near-cognate tRNA, the prediction is that these compensatory interactions are insufficient to stabilize the flipping out of A1492 and A1493 and, thus, A-site accommodation does not occur. However, in the presence of Par, the uncompensated losses of energy are absorbed by Par that has already induced A1492 and A1493 to

flip out and has stabilized them in this open conformation. The outcome being that a near-cognate tRNA becomes fully accommodated into the A-site and thus results in mis-incorporation of an amino acid (reviewed in Ref. [78] and also discussed in Sect. 8.2.3).

Comparison of the structures for the aminoglycosides complexed with the 30S subunit and with the decoding site rRNA fragment reveal their striking similarity, especially with regard to the position in the A-site of the common neamine core (rings I and II) of the 4,5- and 4,6-disubstituted varieties. This latter point is consistent with the conclusion that the neamine core is sufficient for A-site binding [15, 79]. Furthermore, despite differences in the specific contacts between the aminoglycoside subclasses and the rRNA – resulting from both the different position of substituted ring III and also the different substitutions at each position within the rings themselves – the number of contacts remain equivalent, for example, direct hydrogen-bonds from ring III in one subclass are replaced by water bridges in the other [76]. Similarly, Par forms hydrogen-bonds with the 3′- and 4′-OH from ring I with G1491, whereas the gentamycin C class have methyl groups in this position; thus the hydrogen-bonds are replaced by hydrophobic interactions [74]. This explains the similar minimal inhibitory concentrations (MIC) between the different subclasses, for example, 2.5, 5, 10 and 40 μg ml^{-1} for tobramycin, geneticin, Par/ribostamycin and neamine, respectively. However, the affinity of aminoglycosides for the A site decreases significantly with the absence of rings III and IV, thus explaining the higher MIC of neamine with respect to the other aminoglycosides. As well as providing additional contacts with the rRNA, the presence of the additional rings III and IV contributes to a stabilization in the positioning of rings I and II.

All aminoglycosides that bind to the decoding center have a hydrogen-bond donor at the 6′ position on ring I. The 1408 position is an adenosine in all bacterial sequences whereas it is usually guanosine in eukaryotic sequences. This has implications for the specificity of aminoglycosides since mutations of A1408 to G confer high-level resistance to all of the aminoglycosides except those with a 6′ OH. Structural studies suggest that a G1408–A1493 base-pair would disrupt the binding site for these aminoglycosides and the 6′ amino group would be unable to hydrogen-bond the phosphate backbone at A1493 [80, 81]. Organisms that produce aminoglycosides protect themselves by having methylases that specifically modify either the drug (see Sect. 12.5.5) or the 16S rRNA at nucleotides G1405(N7) (Kan and gentamycin-resistant but not Par or neo) or A1408(N1) (Kan, apramycin and istamycin-resistant). Methylation of G1405 would be predicted to prevent hydrogen-bonding with ring III of Kan or gentamycin (whereas no contacts between Par and the base of G1405 are observed), whereas methylation of A1408 prevents formation of the A1408–A1493 base-pair that is essential for aminoglycoside binding. Similarly, the base-pair between C1409 and G1491 is also important for aminoglycoside binding: This base-pair forms a “shelf” in the aminoglycoside-binding pocket, upon which ring I makes stacking interactions with the base moiety of G1491. Disruption of this base-pair, for example by the mutation G1491C (or G1491U), leads to neomycin resistance in *E. coli*. Higher eukaryotes have a mispair at 1409–1491 positions,

which together with G1408, accounts for the 10-fold lower affinity of aminoglycosides for eukaryotic ribosomes. However, it should be noted that breaking the C1409-G1491 base-pair is not always sufficient in bacteria to attain a significant level of resistance to Par, nor to other members of the neomycin family. Furthermore, the G1491U mutation (in contrast with the G1491C mutation) confers resistance only in strains that contain additionally the streptomycin-resistant S12 allele. On the other hand, the 16S rRNA mutations G1491U or G1491C in strains carrying a mutant S12, influence the interaction of the ribosomes with streptomycin in a more complex way. The combination of the 16S rRNA mutations with highly restrictive S12 mutations produces a streptomycin-dependent phenotype (the strain can grow only in the presence of the drug), whereas, when combined with weak or non-restrictive streptomycin-resistant S12 mutations, the streptomycin sensitivity is partially restored. The interplay of mutations in both S12 and helix h44 can be easily envisioned if one considers the binding site of streptomycin.

One interesting observation when comparing the 4,5- and 4,6-disubstituted aminoglycosides is that there are no members of the latter family that contain a four-ring system. In light of structures for representatives of each family bound to the decoding center, the reason for this is that the 4,6-disubstitution generates a rather linear molecule which when extended by an additional ring would be difficult to accommodate in the binding site due to space restrictions [74]. Despite this restriction, the 4,6-disubstituted family of aminoglycosides are clinically preferred, i.e., the predominantly used aminoglycosides are gentamycin (Garamycin® introduced in the mid-1960 s by Schering-Plough) and two kanamycin derivatives, tobramycin (Nebcin® marketed Eli Lilly and Company) and amikacin (marketed under the name Amikin® by Bristol-Myers Squibb). This may in part relate to the fact that ring III of this family makes additional base-specific contacts with the A-site which are not present in the neomycin family [74]. Furthermore, position 1 of ring II of amikacin bears a bulky chain that blocks resistance enzymes from modifying this ring, while at the same time still allowing hydrogen-bonding with O4 of U1495. Similarly, the absence of 3′- and 4′-OH groups on tobramycin and certain gentamycins also protect the drug from inactivation since these groups are also targets for resistance enzymes.

The binding site for the aminoglycoside Hygromycin B has been determined on the 30S subunit [29]. Although Hygromycin B also binds within the decoding center, making exclusively contacts with h44, the location is slightly displaced towards the top of h44 when compared with the position of, for example, paromomycin. The binding of Hygromycin B is very sequence-specific since all interactions are with the bases of the rRNA, rather than the backbone, however, no conformational changes were observed within the rRNA upon binding of the drug [29]. Hygromycin B has been demonstrated to be a powerful translocation inhibitor [47]. Since the top of h44 is thought to move with the A- and P-site tRNAs during the translocation reaction (see Chap. 8), the inhibition of translocation probably results from the reduced flexibility arising from drug binding within this region [29].

12.3.1.3 Inhibitors of EF-Tu-mediated Reactions

There are three basic mechanisms by which antibiotics can disrupt EF-Tu function:

1. Preventing the release or dissociation of EF-Tu from the ribosome without necessarily affecting the GTPase activity, as exemplified by kirromycin and enacyloxin IIa.
2. Blocking EF-Tu from forming the ternary complex, as evident for GE2270A and pulvomycin.
3. Disrupting the capability of ribosomes to bind the aa-tRNA•EF-Tu•GTP ternary complex, as exemplified by the ribotoxin family of proteins, such as the well-known α-sarcin and ricin.

Point 1 is well reviewed in Refs. [82, 83], whereas points 2 and 3 are discussed thoroughly in a recent review by Hilgenfeld and co-workers [84].

The Kirromycins Trap EF-Tu on the Ribosome

Initial binding of the ternary complex aa-tRNA•EF-Tu•GTP to the A-site results in EF-Tu-dependent GTP hydrolysis. Cleavage of GTP causes EF-Tu to adopt the low-affinity GDP conformation that dissociates from the ribosome – analogous with the action of typical G-proteins. Kirromycin and aurodox (*N*-methyl kirromycin) are members of a large family of agents produced by the actinomycetes (see Appendix D1 for structures). The kirromycins stall the ternary complex on the ribosome, not by preventing hydrolysis of GTP to GDP by EF-Tu, but by preventing the conformational changes in EF-Tu that are associated with GTP hydrolysis. In effect, kirromycins lock EF-Tu in a high-affinity state, which prevents both release of the aa-tRNA from EF-Tu and dissociation of EF-Tu from the ribosome. This made the kirromycin-stalled ternary complex-bound ribosomes ideal for analysis using cryo-electron microscopy, which provided the first direct visualization of this state [85]. The recent more refined reconstructions reveal that kirromycin captures the ternary complex during the initial stages of A-site binding; in this situation the anticodon of the tRNA is "kinked" to enable it to undergo codon–anticodon interactions and simultaneously maintain interaction between the acceptor stem and EF-Tu [86]. Correct codon–anticodon interaction is proposed to trigger hydrolysis of GTP by EF-Tu leading to dissociation of EF-Tu from the ribosome, which in turn enables the aa-tRNA to move into the A-site on the 50S subunit, become fully "accommodated" and to partake in peptide-bond formation. The corollary being that in the kirromycin-stalled complex, the acceptor stem and aminoacyl moiety of the aa-tRNA, by remaining bound to EF-Tu, are unable to move into the PTF center and thus progression of the elongation cycle is prevented since no subsequent peptide-bond formation is possible.

Since the structures for EF-Tu in both the GTP (actually with the non-hydrolyzable GTP analog, GDPNP) and GDP form have been solved to high resolution, the conformational rearrangements that are undertaken as a results of GTP hydrolysis are well understood (reviewed in Refs. [87, 88]). Briefly, following GTP hydrolysis,

domain I (the GTP binding domain) of EF-Tu undergoes a conformational change and is rotated relative to domains II and III by up to 40 Å (cf. Figs. 12.9A and B). Comparison of these structures with the recent structure of *T. thermophilus* EF-Tu•GDP•aurodox [89] confirms the resemblance of this latter structure with the GTP conformation (cf. Figs. 12.9A and C). In this structure, aurodox is wedged between domains I and III making almost exclusively hydrophobic interactions. By binding within this region, kirromycin may lock domains I and III together thereby preventing allosteric switching.

This location is in agreement with the numerous kirromycin-resistant mutations that map to amino acids clustering at the interface between domains I and III in the

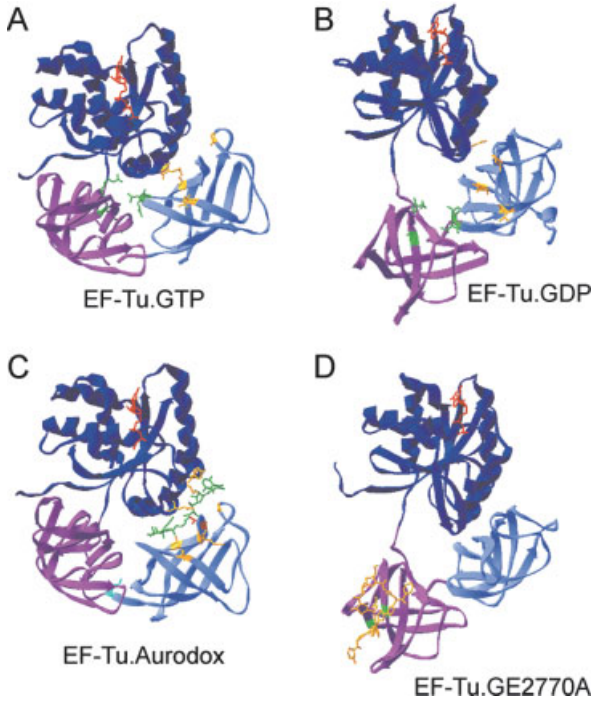

Figure 12.9 The structures of aurodox and GE2770A bound to EF-Tu. (A) EF-Tu•GDPNP (PDB1EXM; [88]), (B) EF-Tu•GDP (PDB1D2E; [87]), (C) EF-Tu•GDP•Aurodox (PDB1HA3; [89]) (D) EF-Tu•GDP•GE2770A (PDB1D8T; [94]). In A and B, the residues conferring resistance to Enacyloxin IIa and pulvomycin are coloured yellow and green, respectively. In C and D, the antibiotics aurodox and GE2770A are coloured green and yellow, respectively. In C, substitutions at residues giving rise to kirromycin resistance are coloured yellow. Position I298 and T382, which when deleted or phosphorylated (respectively) confer resistance to kirromycin are coloured cyan and red, respectively. In Figure D, sites of mutations giving rise to GE2770A are indicated in green. In Figures A-D, domains I, II and III are coloured dark blue, magenta and light blue, respectively, and the guanine nucleotide is always red.

GTP form (but not the GDP form) (see Table 12.4 and as indicated in Fig. 12.9C). Resistance is conferred through two distinct mechanisms:

1. Obstruction of the binding of kirromycin to EF-Tu•GTP by disrupting the kirromycin-binding site.
2. Promoting dissociation of kirromycin from the ternary complex following GTP hydrolysis since kirromycin has a lower affinity for EF-Tu•GDP. This protection mechanism implies that some mutants permit sufficient conformational change within EF-Tu concomitant to GTP hydrolysis despite the presence of kirromycin.

Kirromycin resistance is a recessive phenotype and therefore sensitivity to kirromycin is dominant. Moreover, many bacteria, including *E. coli*, contain two genes encoding EF-Tu (*tufA* and *tufB*). In these particular cases, resistance is dependent on an alteration in both genes. Alteration of only one of the genes will not confer resistance to kirromycin [90], since a ribosome blocked by a sensitive EF-Tu prevents translation for the subsequent ribosomes of the polysome.

Enacyloxin IIa is a linear polyenic acid similar to kirromycin (Appendix D1) isolated from *Fratueria* W-315 (i.e., not from the actinomycetes as all other EF-Tu-binding inhibitory antibiotics) and is active against Gram-positive and Gram-negative bacteria [91, 92]. It is easy to envisage enacyloxin IIa operating through a similar

Table 12.4 Mutations in EF-Tu giving rise to antibiotic resistance

Antibiotic	Mutation position[a]	EF-Tu domain	Reference
Kirromycin	L120Q,	I	240–242 and references therein.
	Q124R[b], E, K, N	I	
	Y160N, D, C	I	
	Δ298	II–III linker	
	G316D[b]	III	
	Q329H,	III	
	A375T, N, V, S	III	
	E378K	III	
Kirromycin	T382- phosphorylation	III	243
Enacyloxin IIa	Q124K,	I	93
	G316, Q329, A375	III	
GE2270A	G257A, G275A, S	II	244
Pulvomycin	R230C, R233S,	II	245, 96
	R333C, T334A	III	
	R230V-R233F	II; III	

a *E. coli* numbering is given although resistance mutants were not necessarily identified in *E. coli*.

b Kirromycin-resistant eukaryotic and archaebacterial EF-1 (the EF-Tu homolog) have substitution and deletion of the positions equivalent to Q124T and ΔG316, respectively [246].

mechanism to kirromycin, since enacyloxin is structurally similar and the mutations that give rise to enacyloxin resistance were originally identified as kirromycin-resistant mutations (indicated in Figs. 12.9A and B). This suggests that they have, at least to some extent, overlapping binding sites on EF-Tu. However, there are some differences with the kirromycins, for example, the enacyloxin IIa-bound EF-Tu•GDP complex has an even higher affinity for aa-tRNA than kirromycin and enacyloxin IIa does not enhance the GTPase activity of EF-Tu in the way kirromycin does. Furthermore, subtle substitution changes at sites in EF-Tu can affect resistance to kirromycin and enacyloxin differently, for example, A375V confers resistance to kirromycin but not enacyloxin whereas A375T confers resistance to both [93]. This raises doubt as to whether Enacyloxin IIa should simply be classified along with kirromycin or whether it should be differentiated. Structural studies with the enacyloxin-bound EF-Tu complexes should resolve this issue.

Inhibition of Ternary Complex Formation: Pulvomycin and GE2270A

Both pulvomycin and GE2270A (also referred to as MDL 62, 879) prevent the binding of the aa-tRNA to EF-Tu, i.e., they prevent ternary complex formation; however it appears likely that they operate through dissimilar mechanisms, although this remains to be verified. First, pulvomycin and GE2270A are structurally unrelated. While pulvomycin bears some resemblance to the kirromycins, GE2770A is a member of the cyclic thiazolyl peptide family (Appendix D1). In fact, GE2770A is more closely related in structural terms to the thiostreptons and micrococcins, which are also inhibitors of protein synthesis, but act by binding directly to the ribosome (see Sect. 12.3.3.1). Recently, the crystal structure of EF-Tu•GDP•GE2770A was solved to 2.35 Å resolution [94]. GE2770A was located in a cleft of domain II (Fig. 12.9D), where ionic interactions with R223 and E259 account for the strong affinity of this antibiotic. In agreement, mutations at these two residues are associated with resistance to this antibiotic (Table 12.4 and as colored green in Fig. 12.9D) – however, it should be noted that these residues are not invariant throughout the prokaryotes suggesting that some organisms may be naturally resistant (a good example being the producer of GE2770A, *Planobispora rosea*). A comparison of the aforementioned structure with that for binary complex EF-Tu•GTP and the ternary complex EF-Tu•GTP•tRNA suggested that the binding position of GE2770A would sterically clash with that of the amino-acyl moiety of the aa-tRNA. This in itself explains the inhibitory action of GE2770A to prevent ternary complex formation, but in addition, the binding position of GE2770A at the interface of domain II would prevent tight association with domain I, an interaction necessary to adopt fully the GTP conformation. Therefore, GE2770A can be supposed as having a dual action in preventing ternary complex formation.

In contrast with GE2770A, the action of pulvomycin (Appendix D1) is not so well understood. Although pulvomycin, like GE2770A, inhibits ternary complex formation, the locations of the resistance mutations are distinct from those of GE2770A (Table 12.4), suggesting that the inhibitory mechanism also differs. The location of the pulvomycin-resistant mutations is at the junction between domains II and III

(as indicated in Figs. 12.9A and B). Since pulvomycin (as GE2770A) does not compete with kirromycin for binding to EF-Tu [95], this suggests that if pulvomycin does interact with domain II, it is probably not at the I–II interface. Domain III of EF-Tu has been shown to be necessary for pulvomycin binding, leading to the speculation that the binding site of pulvomycin lies at the domain II–III interface [84]. A striking difference between pulvomycin and GE2770A relates to their resistance phenotype; pulvomycin sensitivity was found to be dominant to resistance [96], whereas in contrast GE2770A resistance was dominant over sensitivity [97, 98]. This suggests that in the case of pulvomycin an additional mechanism must be operating other than simply limiting the availability of active ternary complex.

The ribotoxins: α-sarcin and ricin A

Ribosome-inactivating proteins (RIPs) are ribotoxins produced by bacteria, fungi, and plants to damage the ribosomes of other organisms, either prokaryotic or eukaryotic. These ubiquitous proteins can be grouped, based on their method of inactivation, into either the α-sarcin-like fungal ribonucleases (RNases) or the bacterial and plant RIP family of glycosidases, for which ricin is perhaps the best known member. The action of α-sarcin or ricin A on *E. coli* ribosomes results in a direct loss in binding of both elongation factors. Although EF-Tu-dependent A-site occupation and EF-G-catalyzed translocation are blocked, all other functions of the ribosome including non-enzymatic A-site binding and spontaneous translocation remain unaffected [99]. The target of the RIPs is a 12-base loop (termed the sarcin-ricin loop (SRL)), a constituent of domain VI of large subunit ribosomal RNA, and contains the longest stretch of universally conserved nucleotides in the cell (Fig. 12.2B). The SRL is a continuous irregular helix with a bulged G2655, which distorts the backbone creating a characteristic S-shape. The helix is closed by a GAGA tetraloop, of which the two bases A2660 and G2661 are 'looped out' and accessible for possible interactions with EFs or RIPs.

The cytotoxic protein α-sarcin is produced by the *Aspergillus* species and inhibits protein biosynthesis by cleavage of the SRL. The high specificity and effectiveness of this single cut is illustrated by the observation that fragmentation of the rRNA by introducing up to 10 randomly distributed breaks does not affect protein synthesis *in vitro*, but the α-sarcin specific cleavage at the 3′ side of G2661 in 23S rRNA (or G4326 in the rat 28S rRNA) completely abolishes protein synthesis [99, 100]. The extreme conservation probably explains the observation that α-sarcin is active against ribosomes across all kingdoms. Although this is also true for glycosidase family of ribotoxins, for example, gypsophilin (from *Gypsophilia elegans*) acts on both prokaryotic and eukaryotic ribosomes [101], there are a number that effectively target only the SRL of eukaryotes, for example, pepocin is 10000-fold less effective against *E. coli* as against mammalian ribosomes [102]. RIPs from higher plants can be further divided into two distinct categories based on their structures; the type I RIPs composed of a single protein chain of ~30 kDa and the larger type II RIPs, which are composed of two unequal chains, an A chain homologous to the type I RIP and a B chain that binds to the A chain and facilitates its cellular uptake. The A

chain of the type II ribotoxin ricin depurinates (depurination involves hydrolysis of the N-glycosidic linkage between the ribose and sugar resulting in the removal of a purine base, which in this case is adenine) only eukaryotic ribosomes at A4324 of the 28S rRNA (which corresponds to *E. coli* A2660). Only the naked 23S rRNA of *E. coli,* but not the complete ribosome, is a substrate for ricin A, suggesting that the ricin-binding site on the mature *E. coli* ribosomes is not exposed in the same manner as that for eukaryotic ribosomes. Recently, this was elegantly confirmed using hybrid ribosomes constructed from *E. coli* ribosomes where the pentameric L10•(L7/L12)$_4$ complex and L11 were substituted for the rat counterparts (P0•(P1/P2) and eL12, respectively). Pepocin, which normally acts only on eukaryotic ribosomes, was demonstrated to act on the *E. coli* hybrid ribosomes but only in the presence of both P0•(P1/P2)$_2$ and eL12 [103]. Similarly, the binding of L10•(L7/L12)$_4$ complex and L11 to *E. coli* ribosomes was necessary for susceptibility to gypsophilin. This suggests that the binding of these specific ribosomal proteins dictates the conformational state of the SRL and its accessibility to the RIPs.

12.3.2
Inhibitors of Peptide-bond Formation and Nascent Chain Progression

The central enzymatic function of the ribosome is peptidyl transferase (PTF), which is the domain of the large ribosomal subunit. The recent structures of the 50S subunit, alone and in complex with various ligands and antibiotics, has led to rapid improvement in our understanding of the PTF reaction itself (see Chap. 8.3 for more details), but also the mechanism of action of the multitude of antibiotics that target this region. The PTF center of the ribosome is composed entirely of rRNA, made up mostly of residues from the PTF ring of domain V of the 23S rRNA (Fig. 12.2B). This active center and the associated region of tunnel extending from it comprise the target for the majority of large subunit binding antibiotics that have been structurally characterized to date. For this reason, the predominant interactions are made with rRNA, relegating ribosomal proteins almost exclusively to indirect role in antibiotic interactions. Despite this, numerous ribosomal proteins have been associated with antibiotic resistance (summarized in Table 12.6). A special feature of about two-thirds of the ribosomal proteins is the presence of a globular domain, usually located at the solvent surface of the ribosome, and long finger-like extensions that weave their way through the rRNA into the core of the ribosome. These protein extensions are thought to act like "glue" and provide a scaffold for the rRNA. For this reason, mutations in ribosomal proteins that confer resistance to particular antibiotics, despite making no direct contact, probably do so by altering the architecture of the rRNA and therefore the antibiotic binding site.

12.3.2.1 **Puromycin and Blasticidin S mimic the CCA end of tRNAs**

Puromycin (Puro) is a structural analog of the 3′-end of aminoacyl-tRNA, except that the aminoacyl residue is linked to the ribose via an amide bridge rather than an

ester bond (Fig. 12.10A). Puro binds to the A-site region of the PTF center. Following A-site binding, peptidyl transfer links the peptidyl residue covalently to the drug. The peptidyl-Puro then dissociates from the ribosome since it has a low affinity being bound at the A-site only via the 3′-terminal adenine. Furthermore, should the peptidyl-Puro arrive at the P-site, by rebinding, no further peptidyl transfer could ensue as the amide bridge cannot be cleaved by the ribosome. Thus, Puro is effectively terminating peptide chain elongation by exploiting the ribosomal PTF activity. Peptide-bond formation of Puro with peptidyl-tRNA, peptidyl-tRNA analogs or 3′-terminal fragments of these tRNAs, are important tools for studying the PTF reaction. In fact, the classical definitions of A- and P-sites are based on the inability or ability, respectively, of peptidyl-tRNA or its analog *N*-acetyl-Phe-tRNA (AcPhe-tRNA) to react with Puro.

The binding site of Puro was first visualized at high resolution in the 3.3 Å structure of the *H. marismortui* 50S subunit bound with the Yarus inhibitor [104], an analog of the peptide-bond intermediate formed by linkage of CCdA to Puro via a phosphoramide group [105](see Chap. 8.3). In this structure, the Puro component of the Yarus inhibitor occupies the A-site position: a type-I A-minor interaction between the adenosine base (termed A76 since its position mimics the terminal adenosine (A76) of a tRNA) and the G2583–U2506 base-pair as well as an additional H-bond interaction between the 2′-OH of A76 with U2585 and stacking of A76 with U2558 (Fig. 12.10B). Subsequently, similar positions for puromycin were observed as the substrate in the A- and P-sites namely CC-pcb (CC-Puro-caprioic acid-biotin) [106] and as the post-peptide-bond formation product at the P-site of the *H. marismortui* 50S (Fig. 12.10C) [107], as well as, ACC-Puro with the *D. radiodurans* 50S subunit [108]. Interestingly, CCA-Pcb bound to both A- and P-sites suggesting that it had equal affinity for both sites, but in the presence of sparsomycin, was only present in the P-site [106]. In contrast, CACCA-Leu and CACCA-LeuAc (α-amino group is blocked by an acetyl residue) show a perfect specificity for A and P-site regions of the PTF center, respectively [109].

Unlike puromycin, which mimics an aminoacylated-terminal adenosine (A76) of a tRNA, blasticidin S has a structure resembling either of the preceding cytosines (C74 or C75) of the tRNA. Specifically, blasticidin S is composed of a cytosine base and a pyranose sugar with an N-methylguanidine tail (Appendix E1). Although few studies have addressed the mechanism of blasticidin S, it has been reported to inhibit the PTF reaction of both bacterial 70S and eukaryotic 80S ribosomes [110, 111].

The structure of blasticidin S soaked *H. marismortui* 50S subunits was reported at 3 Å resolution [112]. Two molecules of blasticidin S were identified, both bound at the PTF center, where they are positioned so as to mimic C74 and C75 of a tRNA at the P-site by making interactions with P loop residues. In the higher occupancy site, the cytosine base of blasticidin S makes Watson–Crick (WC) base-pairs with G2251, whereas in the lower affinity site the cytosine of the second molecule of blasticidin S forms WC interactions with G2252. Binding to the higher affinity site is further stabilized by stacking of the *N*-methylguanidine tail onto the base of A2439 as well

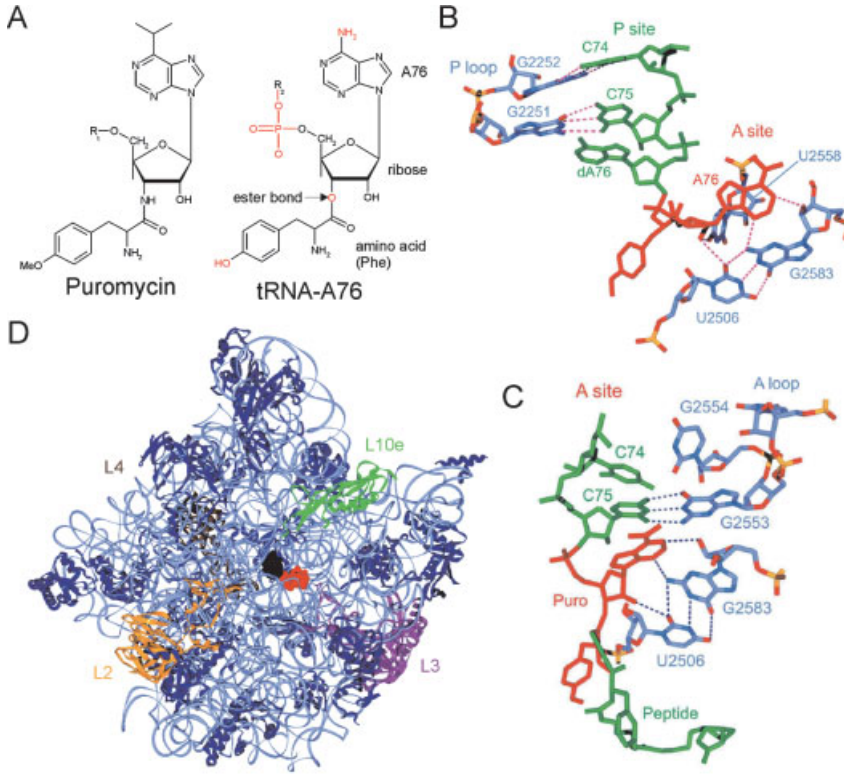

Figure 12.10 Puromycin binds at the peptidyl-transferase center of the 50S subunit. (A) Comparison of structures of puromycin with the terminal adenine (A76) aminoacylated with phenylalanine. Differences between puromycin and the physiological tRNA substrate are indicated in red on the tRNA. Puromycin bound to the *H. marismortui* 50S ribosomal subunit in the form of (B) the Yarus inhibitor (pdb 1FFZ)[104] and (C) the products following peptide bond formation (pdb 1KQS)[107]. The puromycin part of each of the respective compounds is coloured red. Selected rRNA residues of domain V of the 23S rRNA are colored light blue, including the A- and P-loop bases that participate in A and P site CCA end fixation (*E. coli* numbering). In (B) the A site C74 and C75 mimics have been omitted for clarity, likewise in (C) for the P site product. Dashes indicate hydrogen bonding and rRNA nucleotides use the following color scheme: Oxygen, red; phosphorus, yellow; nitrogen, blue; carbon, dark blue. (D) Overview of where the PTC is on the ribosome using the A site and P site products shown in red and green respectively. Ribosomal Protiens L4 (purple) L10e (green) L16 in bacteria L2 (yellow), and L3 (crimson) have long extenstions that reach towards the PTC.

as hydrogen-bonding interactions with the phosphates of both A2439 and A2600. The removal of or alterations in the tail markedly decreases the effectiveness of blasticidin S on translation [113], suggesting these interactions are important for drug binding. Residue 2439 has also been identified as being protected by blasticidin S from chemical probing [114] and mutation of the neighboring base U2438 to C confers resistance to blasticidin S in the archaeabacterium *H. halobium* [115].

12.3.2.2 **Sparsomycin Prevents A-site Binding and Stimulates P-site Binding**

Sparsomycin (Spm), a modified uracil antibiotic produced by *Streptomyces sparsogenes*, has long been known as a potent inhibitor of PTF activity in all organisms studied (reviewed in [28]). Specifically, Spm has been shown to interfere with binding of tRNA (and CCA-end fragments) to the A-site, while enhancing the affinity of peptidyl-tRNAs (especially N-acetylated aa-tRNAs and aa-ACC end fragments) for the P-site. Despite this early biochemical characterization, the binding site for Spm has remained elusive since Spm did not produce clear footprints on the rRNA [116, 117] nor could resistant mutants be isolated in *E. coli*. However, the subsequent isolation of Spm-resistant mutations was successfully achieved in several archaeal species indicating that the PTF center was the likely site of drug interaction: In *H. halobium,* mutation of C2518U and to a lesser extent C2471 and U2519 (C2499, C2452 and U2500 in *E. coli*, respectively) conferred resistance to Spm [117], as did loss in methylation (probably at the N3 position) of U2603 in *H. salinarium* (U2584 in *E. coli*) [118]. These residues are to be found in the PTF ring of domain V of the 23S rRNA (Fig. 12.2B). Consistently, Spm competes for binding with the PTF inhibitors chloramphenicol and lincomycin [119] and has been crosslinked to residue A2602 [120].

The high-resolution structures of Spm bound to the 50S subunit of both *H. marismortui* (H50S) [112, 106] and *D. radiodurans* (D50S) [108] have revealed why the footprinting techniques had been so unsuccessful: in the H50S complexes, density for Spm was only observed when a P-site substrate was included in the co-crystallization experiment [112], whereas, in the D50S, although density for Spm was observed in the absence of a P-site ligand, the sole interaction with the ribosome was through a stacking interaction between the modified uracil ring of Spm and the base of A2602. This stacking interaction is also observed in both H50S and D50S complexes, where P-site ligands are included, however, despite this similarity, the orientation of A2602 and Spm itself differed significantly.

In the D50S-Spm structure with a tRNA acceptor-stem mimic (ASM), the presence of Spm has pushed the helical region of the ASM towards the P-site, but the CCA-end of the ASM still maintains interactions with the A loop, thus placing it in the A-site. In contrast, the H50S-Spm structure with the tRNA mimic, CCA-phe-cap-biotin (CCA-pcb), the mimic is clearly bound at the P-site. Furthermore, in this latter structure, the extensive interactions made with Spm explain how the presence of a P-site substrate significantly enhances Spm binding and *vice versa:* the uracil ring of

Spm is sandwiched between the P-site substrate and A2602, the N3 position of the uracil makes a hydrogen-bond with the phosphate group of C75, the exocyclic methyl group of the uracil forms van der Waals contacts with C75 and A76 and the C3-keto group of uracil is co-ordinated through a bound Mg ion with two phosphate-oxygen atoms of the P-site substrate (Fig. 12.11). In addition, the sulphurous tail of Spm contributes to the binding affinity by inserting into the A-site, where it would be predicted to inhibit binding of A-site ligands, thus explaining the observed competition with drugs such as chloramphenicol and puromycin. Therefore, the inhibitory action of Spm is likely to be due to blocking the binding of the A-site ligand in a fashion that is dependent on the presence of a P-site ligand necessary to stabilize Spm binding. Ribosomes that are in a PRE state, i.e., having both A- and P-sites occupied, are not protected from the action of Spm, since under these conditions Spm induces translocation of the A and P substrates [121], relegating the situation to a peptidyl-tRNA at the P-site and an A-site blocked by Spm. It is worth mentioning that the base in the PTF center that Spm stacks upon, A2602, is at the center of the rotational symmetry of the PTF center, where it has been proposed to play a role in guiding the CCA ends from the A- to P-site during translocation [122].

12.3.2.3 **Antibiotic Overlap in the PTF Center: chloramphenicol, Anisomycin and the Lincosamides**

Chloramphenicol (Cam; Appendix E1) inhibits several kinds of PTF assays. However, it does not interfere with, but rather stimulates, tRNA fragment binding to the

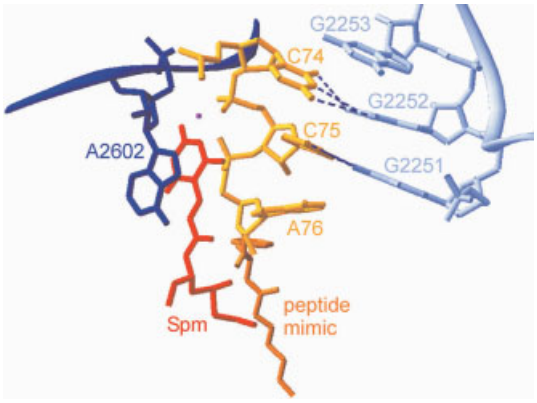

Figure 12.11 Sparsomycin binding is stabilized by interaction with the P site substrate. Spm (red) bound within the PTF center of the *H. marismortui* 50S subunit in the presence of P site substrate (CCA-pcb, yellow) [112, 106]. The uracil of Spm can be seen to make stacking interactions with the base of A2602 (blue) of the 23S rRNA. The P site substrate interacts with the residues G2251 and G2252 of the P loop (23S rRNA) by making hydrogen bond interactions (dashed blue lines) from the positions mimicking C75 and C74 of a bound tRNA.
Note additional interactions between Spm and P site substrate can be coordinated through the bound Mg ion (purple).

P-site of the PTF center [109], and competes with the binding of tRNA fragments to the A-site and with puromycin [123]. In intact bacteria, Cam "freezes" the polysome profile, suggesting that the drug inhibits the PTF reaction by disturbing the binding of the CCA 3′-end at the A-site within the catalytic center but without weakening tRNA binding *per se*. Curiously, the degree of inhibition depends on the character of the peptidyl residue or the A-site substrate, for example, AcPhe-puromycin formation is blocked, as well as Gly-Phe-puromycin formation, but the formation of AcPhe-Phe, AcPhe-Phe-puromycin or Leu-Phe-puromycin is not [124–126]. On this evidence it was argued that aromatic amino acids can displace Cam during peptide-bond formation by competing with the phenyl group of the drug.

The ribosome-binding site of Cam was determined to 3.5 Å by soaking 50S crystals of *D. radiodurans* in a solution containing 100 µM Cam and shown to involve interaction with seven nucleotides within the PTF center [127] (Fig. 12.12). Many of these interactions were indirect being mediated through two putative Mg^{2+} ions. Functionally important moieties for the antibiotic action of Cam constitute these interactions suggesting the presence of ions is of utmost importance for antibiotic binding and therefore PTF inhibition. The position of the dichloroacetamido tail of

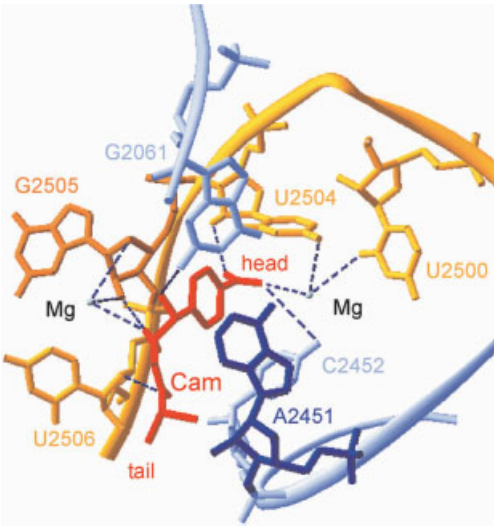

Figure 12.12 Chloramphenicol binding within the A site of the peptidyl-transferase center of the *D. radiodurans* 50S subunit (pdb 1k01) [127]. Chloramphenicol (Cam, red) interacts with 7 nucleotides within the PTF center, three through interactions with the head and four through the tail. Hydrogen bond interactions (blue dashed lines) between the p-NO_2 group of the head with U2500, U2504 and C2452 are evident as well as from the tail with G2061, G2505 and U2506. Some of these interactions are direct whereas others are stabilized through either of the two Mg ions present in the binding site.

Cam within the PTF center is located such that it extends towards, and may even displace, the CCA end of the A-site tRNA. This is in agreement with the observation that tRNAs can bind in the presence of Cam but they cannot undergo peptide-bond formation. Furthermore, the major overlap between Cam and an A-tRNA encompasses predominantly the amino acid moiety, lending credence to the idea that Cam operates predominantly by displacing the aminoacyl residue of the A-site tRNA and thus probably displaces the CCA end as an indirect result of this.

Cam protects bases A2059, *A2062*, A2070, A2451, *G2505*, *U2506* and enhances the reactivity of A2058 [128, 114]. Interactions with three of these residues (italicized) are made by Cam and A2451 is within 3.0 Å, whereas the other three (A2070, A2058 and A2059) are located over 10 Å away. Mutations that confer resistance to Cam map near to the sites of protection at positions 2057, 2451, *2452*, 2447, *2503* and *2504*, whereas the mutations *G2505C* and G2583U or C (but not G2583A) cause hypersensitivity towards Cam in an *in vitro* translation system [129]. The discrepancy between the Cam-binding site at the A-site and the protections (and some modest resistance mutations) located within the tunnel region, can be best explained by a second lower affinity binding site for Cam. Indeed, the structure of Cam bound to the *H. marismortui* 50S subunit identified a site distinct from that found in *D. radiodurans* located within the tunnel, overlapping the binding site of the macrolide class of antibiotics [112]. This is not totally unexpected since most archaea exhibit a natural resistance to Cam (probably due to sequence differences within the region of the D50S Cam site) and thus unusually high concentrations of Cam (20 mM) were necessary to bind Cam to this lower affinity site. This suggests that eubacterial ribosomes may also bind a second molecule of Cam at this lower affinity secondary site, which would correlate nicely with the previously contradictory biochemical data. It should be noted that the primary binding site is sufficient to account for the inhibitory action of Cam and also that in eukaryotes, Cam is not even taken up by the cells, although cycloheximide functions in a very similar fashion.

Cam has been crosslinked to ribosomal proteins L16 and L27 [130], extensions of both proteins approach the PTF center, although not close enough in the case of L16 for any direct contact with Cam in either the primary or secondary site. Therefore, the conclusion from reconstitution studies that L16 constitutes a component of the Cam-binding site [131], probably reflects instead alterations in the PTF center, due to the proteins absence, that perturb Cam binding. Unfortunately, the N-terminal of L27 in the D50S structure is relatively disordered and there is no counterpart in the H50S structure. The N-terminal residues of L27 have been crosslinked to the acceptor stem of a P-site-bound tRNA leading to the proposal that it may play a role in positioning the acceptor ends of the tRNA within the PTF center – this could place L27 in direct contact with the primary Cam-binding site.

In contrast with Cam, the anisomycin and lincosamide classes of antibiotics have been reported to interfere with binding of ribosomal ligands at both the A- and P-sites. Anisomycin acts exclusively against eukaryotic cells, whereas lincosamides specifically inhibit bacterial protein synthesis (reviewed in Ref. [28]). Structurally, anisomycin shares similarity with both puromycin and chloramphenicol; therefore, it

was not surprising that it was found to be bound at the A-site of the PTF center in the *H. marismortui* 50S subunit [112]. The aromatic methoxyl-phenyl ring of anisomycin inserts into a pocket created by A2451–A2452, where it makes stacking interactions with the latter. The N3 of the pyrrolidine sugar also forms a hydrogen-bond with A2452 and the hydroxyl group of this sugar, hydrogen-bonds with the O1P of 2504, and is co-ordinated by a potassium ion that is chelated between positions 2061, 2447 and 2501 of the 23S rRNA. The outcome is that anisomycin binds in a position that overlaps extensively with puromycin or an A-site-bound tRNA, except that anisomycin approaches the binding site from the opposite side. This means that it is predominantly the aromatic ring and methoxy sidechain that superimposes with the position of the amino acyl moiety (tyrosine-like moiety in the case of puromycin), whereas the pyrrolidine ring and tail have no counterpart, being located on the side opposite to the A-site ligand. What is surprising about the binding position of anisomycin is that no part of the molecule encroaches the position of the P-site. This suggests that anisomycin interferes with P-site binding indirectly, perhaps by inducing conformational changes within the PTF center. In fact, modest conformational changes are observed within the PTF center, but not with bases that directly interact with the CCA end of a P-site bound ligand.

Two commonly discussed lincosamides are lincomycin, naturally produced by several species of actinomycetes (such as *Streptomyces lincolnensis*, *espinosus* and *Actinomyces roseolus*), and clindamycin, a semi-synthetic derivative of lincomycin (Appendix E1). Although they exhibit similar affinities for the ribosome (5 and 8 μM respectively), clindamycin is generally a more effective inhibitor (probably due to better cellular uptake) and is used clinically, for example, as part of combination therapy, with pyrimethamine and folinic acid, as treatment against toxoplasmosis. The dual-site interference of lincosamides is evident from the inhibition by lincomycin of the transfer of fMet or AcPhe to Puro as well as preventing the binding of small tRNA 3′-end mimics, namely, CACCA-Leu to the A-site and CACCA-AcLeu to the P-site (see Ref. [132] and references therein). Furthermore, lincomycin has been shown to compete for binding with both erythromycin and Cam [28]. This latter point is consistent with observation that a number of strains exhibiting resistance to macrolides also protect the ribosomes from the action of lincomycin and streptogramin Bs (the so-called MLS_B resistance, reviewed in Ref. [133]).

In agreement with most of the biochemical data, the binding site determined for clindamycin spans between both A and P-sites at the PTF center, with the sugar moiety extending towards the tunnel and the prolyl moiety encroaching on the A and P-sites [127]. The majority of the interactions involve hydrogen-bonds from hydroxyl groups on the sugar moiety with nucleotides within the PTF center, specifically, to bases of A2058, A2059 and C2611 (U2590 in *D. radiodurans*), the phosphate of G2505 and the ribose of A2503 (Fig. 12.13). Bases A2058, A2059 and G2505 (as well as A2451) are strongly protected from chemical modification in the presence of clindamycin [134]. The same pattern of protection was found in the presence of lincomycin except that the protection of A2059 was absent (Fig. 12.2B). This suggests that there is some difference in the binding positions, although this is somewhat surprising since the structural differences between the two lincosamides occur at the C7

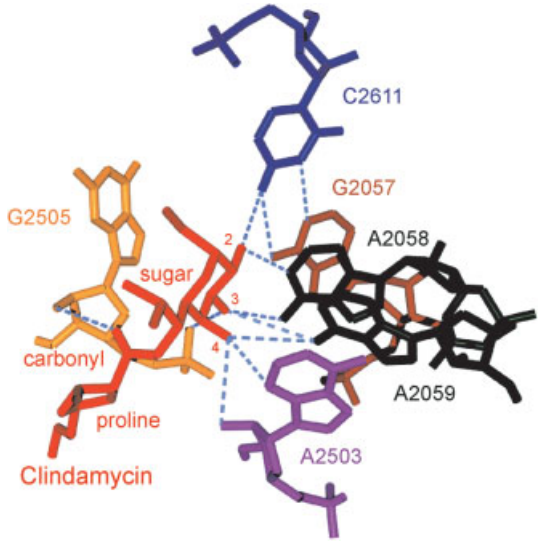

Figure 12.13 Interaction of clindamycin with the peptidyl-transferase center of the *D. radiodurans* 50S subunit (pdb1jzx; [127]). The majority of the interactions are with the OH groups of the sugar moiety of clindamycin (red) and consist of interactions between 2 OH and the base at position C2611 (blue), which is also base-paired with G2057 (brown). The bases of A2058 and A2059 (green) interact with 2, 3 and 4 OH groups. The sugar of A2503 (magenta) with 4 OH and the sugar and phosphate at position G2505 (yellow) with the carbonyl group and 3OH respectively.

position – a position that is expected to make a less significant contribution to the binding of the drug to the ribosome. The base specificity of the interaction with A2058 and A2059 correlates with the fact that mutations at these positions [135] and dimethylation of the N6 position of A2058 (which would prevent hydrogen-bonds with the 2-OH and 3-OH groups of the sugar moiety of the drug) confer resistance to clindamycin (in fact, to members of the MLS_B antibiotics in general). At the other end of the molecule, the proline group of clindamycin overlaps in position with that of phenyl group of Cam, in line with the A-site nature of clindamycin inhibition (Fig. 12.13). The 8′ carbon extending from the proline moiety of clindamycin comes within 2.5 Å of the N3 of C2452 and thus in close proximity to a P-site-bound tRNA (and A2451, thus accounting for the aforementioned protection). Thus, the binding position of clindamycin traverses both A- and P-sites and would be expected to disturb the positioning of substrates at both sites.

12.3.2.4 **Blocking the Progression of the Nascent Chain by the Macrolide Antibiotics**

Macrolides represent a large class of therapeutically useful antibiotics that have been extensively studied since the 1950s when the first member, erythromycin, was discovered and introduced clinically. Since then macrolide inhibition of ribosome

function has been the topic of many reviews (Refs. [7, 28, 111, 136–138], to name but a few). Macrolides are polyketide compounds synthesised by the actinomycetes and can be classified structurally into groups in a variety of different ways, the easiest being on the basis of the size of their lactone ring, which can vary significantly from as small as 8–12 ring members (methylmycin) to as large as 20 (rapamycin), but here we will consider mainly those of the between 14 and 16: for example, those with 14 (erythromycin, cethromycin, telithromycin and troleandomycin), 15 (azithromycin) or 16 (tylosin, spiramycin, and carbomycin A) atoms. Alternatively (or additionally), macrolides can be distinguished based on the number, position, size and type of sugar sidechains extending from the lactone ring, for example, erythromycin and azithromycin have single C3-cladinose and C5-desosamine sugar moieties, while the larger macrolide spiramycin has C5-mycaminose–mycarose disaccharide and tylosin, an additional C14-mycinose (see Fig. 12.14D and Appendices E2 and E3 for more details). Classification can also be applied using an evolutionary viewpoint since numerous attempts have been made, and are constantly being pursued, to develop more potent macrolide inhibitors. This has led to the discovery of the second-generation erythromycin derivatives, roxithromycin and clarithromycin, which exhibited a broader spectrum of activity. The emergence of bacterial strains resistant to both first- and second-generation macrolides has resulted in the recent introduction of the third-generation ketolide antibiotics.

Early studies suggested that macrolides have a single binding site on the 50S subunit (K_D in the range of 10–100 nM). The binding site was found to be vacant on free or initiating ribosomes, but unavailable in actively elongating ribosomes. The observation that most macrolides had no effect on the ribosomal PTF activity, coupled with the observed accumulation of short oligo-peptidyl-tRNAs in the presence of certain macrolides, led to the suggestion that the action of macrolide inhibition was to block the path of the nascent chain through the exit tunnel. In fact, a distinction can also be made functionally between particular macrolides: macrolides with extensive sidechains extending from position C5 have been shown to inhibit PTF activity, such as carbomycin (100% inhibition), spiramycin (85%) and tylosin (~60%), whereas those with shorter sidechains, such as erythromycin, do not [139].

Two regions of the 23S rRNA, the central loop of domain V and H35 of domain II (Fig. 12.2B), as well as two ribosomal proteins, L4 and L22, have been implicated with macrolide activity. Specifically, footprinting studies demonstrated that erythromycin protected A2058 and A2059 in domain V from chemical modification [128] and enhanced the reactivity of A752 in H35 of domain II [140, 141]. Methylation of A2058, as well as mutations at this and neighboring positions (2057, 2059, 2062 and 2611) confer resistance to macrolides, as do mutations in ribosomal proteins L4 and L22 (see Table 12.6).

The past 2 years has seen a plethora of publications reporting the structures of the 50S subunit in complex with many antibiotics, especially within the macrolide family (see Table 12.1): from the Yonath and Franceschi groups, the D50S subunit has been solved in complex with erythromycin, the second-generation derivatives clarithromycin, roxithromycin [127] and troleandomycin [142], the third-generation

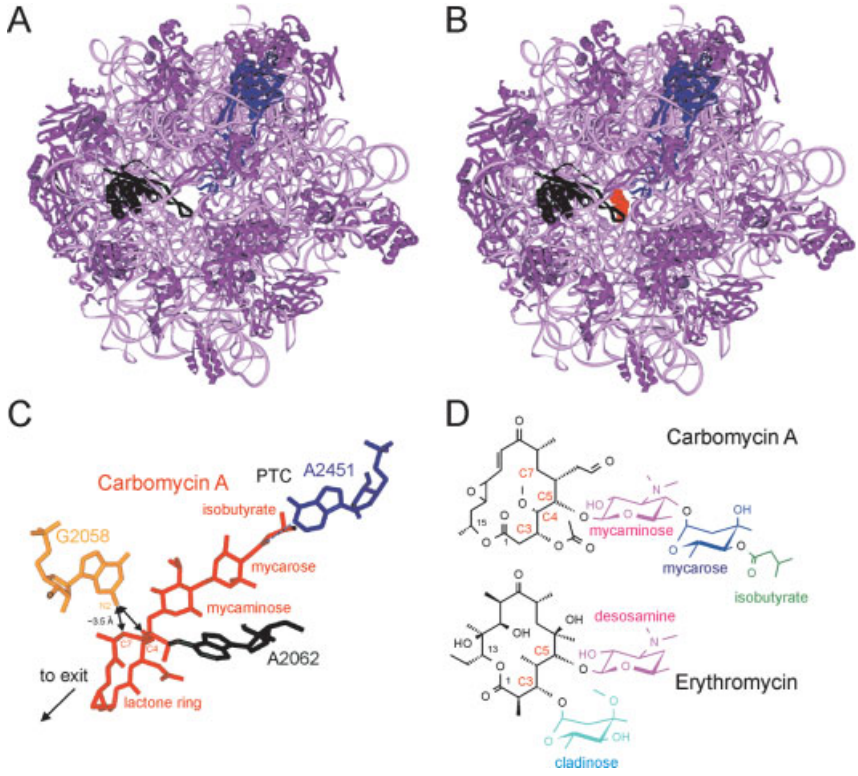

Figure 12.14 Macrolides bind within the tunnel of the 50S subunit. View from the base of the 50S subunit looking up the tunnel towards the PTC in the absence (A) and presence (B) of the macrolide carbomycin (red spacefill in (B)). The rRNA (pink) and ribosomal proteins (magenta) are in ribbons, with ribosomal protein L4 (blue) and L22 (green), whose long extensions reach into the tunnel of the 50S subunit, are highlighted. (C) The C5-sidechain of carbomycin (red) reaches into the PTC and approaches A2451 (very close to the site of peptide bond formation as discussed in Chapter 8.3). Also indicated are 23S rRNA residues A2062 (green), the N6 of which forms a covalent bond with the acetaldehyde group at the C6 position of the lactone ring of carbomycin, and G2058 (yellow), the N2 of which is in van der Waals distance with the C4 and C7 positions of the lactone ring preventing hydrogen bond foramation with the mycaminose C5 sugar position. (D) Comparison of chemical structures of carbomycin A and erythromycin, illustrating the sugar sidechains at the C3 and C5 position and the aldehyde of carbomycin at the C6 position.

ketolide antibiotics, cethromycin (more commonly known as ABT-773) [143], telithromycin (HMR-3647) [144], as well as the azalide azithromycin [143]. Steitz and coworkers [145] have reported H50S complexes with four different macrolides: azithromycin, spiramycin, carbomycin A and tylosin. This wealth of structural information enables us to attain a new level of understanding into the action of these antibiotics and reinterpret the accumulated treasure trove of biochemical and genetic data.

Consistent with the idea that the macrolide class of antibiotics inhibit progression of the nascent chain, the binding site of all the macrolide antibiotics determined to date was found to be within a distinct region of the tunnel, located adjacent to the PTF center. It is immediately apparent that in this position the tunnel lumen is significantly narrowed, being reduced in diameter from ~15 Å to almost 6–8 Å, such that the nascent chain cannot pass by (Figs. 12.14A and B). The binding site and interactions between different macrolides and ribosomal components exhibit extensive similarities, even when comparisons between the H50S and D50S structures are made (although minor but significant differences do exist and will be discussed later).

The general location is in agreement between each study to the extent that the common features of the binding site constitute primarily interactions of the lactone ring, as well as the sugar moiety attached to position C5, with the central portion of domain V. Residues in domain V that had been previously implicated in macrolide-binding make extensive interactions with the C5 sugars, including hydrogen-bonding and hydrophobic interactions with G2057, A2058, A2059 and G2505. They also provide an explanation as to why methylation, especially dimethylation at the N6 position of A2058, as well as the mutation A2058G, confer resistance to macrolides: modification of the N6 position would result in steric clashes between the methyl groups and the first C5 sugar (desosamine/mycaminose position), whereas replacing adenine with guanine at this position removes the hydrogen-bonding potential with the 2′-OH of this sugar. The importance that the sugar moieties make to the overall binding affinity of the macrolides is reflected by their sizeable contribution (between one-half to two-thirds) to the interaction surface with the ribosome [145]. Macrolides with an additional mycarose sugar attached to the mycaminose, such as carbomycin, spiramycin and tylosin, make an extra hydrogen-bond from the hydroxyl at position 3 with the ribose of G2505. Surprisingly, these larger macrolides also have a C6-ethyl-aldehyde, which forms a covalent carbinolamine bond with the N6 of base A2062 [145]. Tylosin and spiramyin have two further sugar sidechains that make additional contacts: tylosin has a mycinose sugar at the C14 position, which interacts with domain II establishing a hydrogen-bond between the N6 of A748 and 2′-OH of the sugar as well as contacting ribosomal protein L22. Methylation of A748, which confers resistance to tylosin would be predicted to disrupt this hydrogen-bond. In contrast, spiramycin contains a forosamine sugar, glycosidically linked to the C9 position that, despite being poorly resolved, clearly approaches L4 [145].

The orientation of the macrolides within the tunnel is such that the C5 position faces towards the PTF center. Thus, macrolides that bear longer C5 extensions restrict the length of the oligopeptide more than macrolides with shorter sidechains. Macrolides with C5 monosaccharides, such as erythromycin, have been observed to prevent progression of the nascent chain beyond a length of up to 6–8 amino acids [146], whereas macrolides with C5 disaccharides permit only dipeptide formation. The extreme case is carbomycin A, which has an additional isobutyrate extension on the C5 amino sugar enabling it to reach into the A-site of the PTF center,

where contacts with bases A2451 and A2452 are made (Fig. 12.14C). This explains why this drug is such a strong inhibitor of PTF activity and confirms the carbomycin/tylosin-specific protection of U2506 from chemical modification [139], the backbone of which is within 4–5 Å of the isobutyrate extension.

The removal of the desosamine sugar at the C5 position totally abolishes the effectiveness of these compounds, for example, although rapamycin still binds to the ribosome its exhibits little or no inhibitory activity for bacterial translation. In contrast, the importance of the cladinose sugar attached to the C3 position of the lactone ring seems to be less clear. The simplest ketolide (RU 56006), a derivative of erythromycin where a ketone group replaces the C3 cladinose (the basis for the name ketolide), reduces drug binding 70-fold (a change in K_D from 0.014 μM (erythromycin) to 0.980 μM; [147, 140]), suggesting this position influences the binding affinity of the drug. In the D50S-azithromycin structure, a hydrogen-bond from the cladinose is formed with the N4 of U2586 [143], however, this is not observed in the D50S-erythromycin or H50S-azithromycin structures, where the cladinose sugar seems to make a comparatively low contribution to binding and, although G2505 comes within 3–6 Å of the single hydroxyl group (4′-OH) of the cladinose sugar, it cannot make hydrogen-bond interactions. This latter point is at least consistent with the fact that this hydroxyl group has been shown to be dispensable for anti-microbial activity [148]. In contrast, the broader spectrum of activity of the ketolides, despite the absence of the C3-cladinose, seems to be related to the presence of their additional sidechains and modifications, for example, the ketolides ABT-773 and telithromycin have a cyclic carbamate inserted at the C11–C12 position of the lactone ring and an alkyl–aryl sidechain attached to the C6–O position or to the carbamate, respectively. In the D50S-ABT-773 structure, the N2 of the carbamate forms a hydrogen-bond with O4 of U2609, whereas the N3 of the quinolylallyl can hydrogen-bond with the O2′ of U790 of domain II of the 23S rRNA. Since telithromycin has the alkyl–aryl side chain attached to the N2 of the carbamate, the analogous hydrogen-bond with U2609 cannot be formed; however, the sidechain itself also makes contacts with domain II of the rRNA. The position of attachment and the longer aryl-linker allows it to penetrate deeper into the tunnel, binding in a cleft composed of positions 789–791 and A764 of domain II. These additional interactions might explain why the ketolides have ~10-fold higher affinity for the ribosome than macrolides [140]. Significant interaction between ketolides and domain II is supported by the strong protection of A752 from chemical modification by ketolides, such as telithromycin, as well as mutations at position U754A in H35 that confer resistance to telithromycin [147, 145, 141]. However, these residues are not directly involved in ketolide binding; thus their influence must be exerted through conformational changes in the loop connecting H35a and H32 [143].

Despite the observation that mutations in L4 and L22 confer resistance to erythromycin, no direct interactions between erythromycin and any part of these proteins was evident, suggesting that resistance is conferred indirectly by inducing conformational changes within the rRNA. This is easy to envisage since the β-hairpin structures extending from L4 and L22 interact intimately with the rRNA associated

with the macrolide-binding site. This observation was not altogether surprising, since it had been reported that these mutations perturbed the 23S rRNA in the vicinity of the macrolide-binding site [149]. Although interaction between sidechains of other macrolide antibiotics and these ribosomal proteins has been observed, for example, the C9–forasamine sugar of spiramycin and L4, the C14 mycinose sugar of tylosin with L22 [145] and the second (see following) azithromycin-binding site with both L4 and L22 [143], the sites of interaction are distinct from those where the mutations arise. Perhaps the most intriguing interaction is made by troleandomycin, the binding position of which is displaced deeper in the tunnel, where it may transiently interact with L22 to induce the β-hairpin of L22, which normally lies flat against the tunnel wall, to swing out across the tunnel [142]. The implication is that this conformational change provides insight into a ribosomal gating mechanism, whereby specific sequences within the nascent chain are recognized within the tunnel to regulate their translation (reviewed in Ref. [150]).

Since the azalide azithromycin has been solved in complex with both the D50S [143] and H50S subunits [145], this provides us with the opportunity to compare directly their interactions. An immediately apparent difference is that two binding sites were found in the D50S structure, one that is equivalent to the position determined for all the other macrolide antibiotics and a second site located deeper in the tunnel, directly following the first. This second binding site is likely to be specific for *D. radiodurans*, since the interactions involve residues specific to this species; however, it nicely illustrates how small sequence deviations can subtly alter the rRNA architecture, which in turn can markedly influence the potential for antibiotic interaction. This is also evident when making a comparison between the first binding site of the D50S structure with the H50S-azithromycin-binding position: comparing the conformation of the macrolides themselves reveals no significant difference in the orientation of the C3 cladinose sugar with respect to one another. However, the orientation of the lactone ring is significantly displaced, particularly on the C9–C14 side, which faces the solvent. This may in part result from the additional azithromycin-binding site in the D50S structure, since there is direct interaction between the two molecules, via a hydrogen-bond between the desosamine sugar and the O1 in the lactone ring of the first binding site [143]. On the whole, it seems that small but distinct changes within the 23S rRNA seem to be responsible for altered lactone ring orientation; however, at a few positions more significant differences are observed, for example, the orientation of bases 2586 and 2609 are sufficiently different to preclude even similar binding modes for the lactone ring. It is interesting to note that although both *H. marismortui* and *D. radiodurans* 23S rRNAs have pyrimidines at these positions they differ in whether they have cytosine or uracil. Furthermore, the exchange of purines is seen at position 2058, which is adenine in all bacterial species (D50S) and guanine in most archaea (H50S) and eukaryotes. Replacing adenine with guanine at 2058 eliminates the potential for H-bonding with the C5-sugar and may disturb the orientation of the antibiotic, thus explaining the natural resistance of *H. marismortui* to this class of antibiotics. That the A2058G substitution in *E. coli* ribosomes reduced the binding of erythromycin by almost four orders of magnitude

[147] could explain why even at high antibiotic concentrations (1–10 mM) no binding of erythromycin was observed when soaking the H50S crystals [145], whereas more physiological concentrations (10–100 μM) were sufficient for the D50S complexes [143, 127]. However, when comparing the position of the lactone ring of the azithromycin structures (and the larger 16-membered ring macrolides) with those of the smaller 14-membered ones, even more marked differences are observable. In the latter structures, the lactone ring adopts a more compact "folded-in" structure, whereas the former exhibited an extended or "folded-out" conformation [145]. The upshot being that the lactone ring of the smaller macrolides is almost perpendicular to that observed for the larger ones and in fact results in a larger constriction of the tunnel [143]. It would be interesting to see whether this is a general feature of the 14-membered ring macrolides or whether the conformation depends on species-specific interactions: the structures of the same antibiotics in complex with different species will go some way to answering these questions.

12.3.2.5 **Streptogramins**

Streptogramins are produced as a mixture of two chemically unrelated compounds, type A and type B (Appendix E3), which act synergistically *in vivo* and *in vitro*, such that the binding of one class stimulates the binding of the other. The net result is that significantly lower concentrations of both antibiotics are needed to obtain the same level of inhibition compared with the use of each compound separately, for example, a 20-fold lower concentration of virginiamycin M and pristinamycin I_A (streptogramin A (S_A) and B (S_B), respectively) was needed when used in combination, than when used alone [43]. However, most importantly, the combination of some streptogramin A and Bs can convert a bacteriostatic effect into bactericidal lethality. This, coupled with the observation that bacteria resistant to the MLS_B class of antibiotics are still sensitive to streptogramin A inhibition, has led to the use of a streptogramin A and B mixture (in ratio of 3:7) of dalfopristin and quinupristin as a new antimicrobial agent [151] called Synercid®, marketed by the company Rhone-Poulenc Rorer.

In general, S_A antibiotics have been reported to interfere with the puromycin reaction and with P-site binding, suggesting that S_A act at both A- and P-sites. In contrast, antibiotics of the B type (S_B) do not tend to inhibit the puromycin reaction, but rather stimulate the binding of 3′-terminal fragments of aminoacyl-tRNA or N-blocked aminoacyl-tRNA to the ribosome. Binding of virginiamycin S (S_B) is inhibited by erythromycin and stimulated by virginiamycin M, the corresponding S_A. Virginiamycin S has been crosslinked to ribosomal proteins L18 and L22 and protects nucleotides A2062 and G2505 within the central loop of domain V of 23S rRNA from chemical modification. These bases are also protected by vernamycin B, another member of the S_B group, which additionally shows strong protection of A752 as well as other weaker affects. Virginiamycin M (S_A) protects A2037, A2042, G2049 and C2050 near the PTF ring (Fig. 12.2B), suggesting that binding of S_A to the ribosome induces conformational change within the PTF center [152]. In this

regard, it is interesting to note that suppression of bacterial growth persists for a prolonged period subsequent to the removal of S_A drugs [153, 154]. The implication here is that S_A binding induces a conformational change within the PTF center that is *slowly* reversible.

Conformational change within the ribosome seems to be also important for the synergistic action of S_A and S_B. The mutation A2058U in 23S rRNA causes resistance to MLS_B antibiotics and prevents binding of virginiamycin S, whereas the inhibitory action of the A-type streptogramin virginiamycin M remains unaffected. In the presence of virginiamycin M (S_A), however, the binding of virginiamycin S (S_B) to mutant ribosomes occurs with the same affinity as with wild-type ribosomes. Indeed, in some cases, following the removal of the S_A compound, the affinity of the S_B antibiotic for the ribosome is still enhanced, providing a strong argument for conformational changes in the PTF center induced by S_A binding.

A crystal structure of virginiamycin M in complex with the *H. marismortui* 50S subunit shows that this S_A does indeed bind in a position that overlaps both A- and P-sites [112], consistent with the earlier biochemical information. Specifically, the majority of the 20-membered lactone ring overlaps the P-site, whereas only the oxazole ring is inserted into the hydrophobic A-site crevice [112]. The conjugated amide group of virginiamycin M occupies the position that A2602 has in the native H50S structure, whereas the base of A2602 is rotated by 90° to end up in a position perpendicular to the tunnel wall. However, similar conformations for A2602 have also been observed in the presence of tRNA mimics, the binding sites of which do not overlap with the 'native' position of A2602. This suggests that overlap in position of the conjugated amide group of virginiamycin M with the base of A2602 is not *per se* necessary for the change in the position of this base.

Other than the rotation of A2602, little other change is observed within the PTF center, which is surprising since this does not reflect the significant conformational changes predicted from biochemical experiments. Furthermore, in these co-crystallization experiments, virginiamycin S (S_B) was also included, yet only poorly resolved electron density was observable. Despite this, the highest additional electron density was located along the opposite face of the rotated A2602, thus sandwiching between both streptogramins, possibly hinting at the basis for co-operative nature of S_A and S_B binding. It is tempting to speculate that because *H. marismortui* is naturally resistant to the MLS_B class of antibiotics (due mainly to guanine at position 2058), this may provide a reason for the weak binding of the S_B antibiotic that was observed. However, it does not explain the absence of any observable rearrangement within the PTF center, nor that in the presence of S_A, the A2058G mutations, or methylation at this position, hardly affect S_B affinity (although whether this also applies to archaeabacteria remains to be seen).

Recently, the structure of D50S in complex with both dalfopristin (S_A) and quinupristin (S_B) was determined [274]. The binding site of dalfopristin was consistent with that of virginiamycin M (S_A) in the H50S structure, and quinupristin was shown to occupy a position similar to that of the macrolide antibiotics. Analysis of this structure suggested that the synergistic binding of S_A and S_B antibiotics probably results

from their direct interaction on the ribosome, with each other, as well as indirect contact through residue A2602 [274]. In contrast to the H50S structure, significant conformational changes were observed in the PTF centre, particularly, the universally conserved residue U2585, which is displaced by dalfopristin binding and rotates 180° to establish hydrogen bonds with C2606 and G2588 of the 23S rRNA. This stable non-productive conformation provides an explanation for the bacteriocidal properties and the prolonged inhibitory effects of the S_A antibiotics.

12.3.2.6 New Classes of Translation Inhibitors; the Oxazolidinones and Novel Ribosome Inhibitors

The oxazolidinone class of antibiotics represent the first new class of drug to enter the antibiotic market in over 20 years, with the most well-characterized member being linozolid (Lin), marketed by Pharmacia under the name Zyvox® (PNU-100766; Appendix E1). The oxazolidinones act against a wide spectrum of Gram-positive and anaerobic bacteria and, of special importance, also exhibit activity against multi-drug-resistant bacteria.

There has been some confusion as to the exact binding site for this class of antibiotics. *In vitro* experiments detected crosslinks between oxazolidones and rRNA from both the small (residue A864) and the large subunit (all residues detected were within domain V near to binding site of the E-site tRNA and ribosomal protein L1) [155]. However, these positions are at odds with the multitude of oxazolidinone-resistant mutants, all of which map within the vicinity of the PTF center, i.e., far from L1 and the E-tRNA-binding site (Fig. 12.2B). This discrepancy between the biochemical and genetic data has been attributed to the tendency of the oxazolidinones to bind non-specifically *in vitro* [137]: The idea that oxazolidinones may bind a particular conformation of the ribosome led to the use of *in vivo* crosslinking experiments with an ^{125}I-labelled oxazolidinone to address this issue. Residue A2602 of the 23S rRNA and the N-terminal of ribosomal protein L27 were identified as being in proximity to the drug-binding site [156]. The specificity of the crosslink was demonstrated by addition of the non-labelled oxazolidinone eperezolid, which abolished the crosslink, or its inactive enatiomer (PNU-107112(R)), which exhibited no effect on the crosslink efficiency. Furthermore, a marked reduction in crosslinking was observed in two strains of *Staphylococcus aureus* bearing mutations (G2447U and G2576U) conferring resistance to oxazolidinones. The close proximity of A2602 to these various mutation sites not only provides support for the PTF center as the oxazolidinone-binding site but may provide some general information as to the orientation of the drug, namely that the side of ring C to which the azido group is attached should extend towards A2602, whereas the pharmacophoric oxazolidinone ring A (and attached N-acetylaminomethyl side chain) angles toward the PTF center, where the resistance mutations are located. Crosslinking to the N-terminal region of L27 is also consistent with the PTF center location, since crosslinks to L27 were also observed from other antibiotics that bind to the PTF center as well as 3′-azido-labeled aa-tRNAs (see Ref. [156] and references cited therein). Unfortunately, the

N-terminal region of L27 is disordered in the *D. radiodurans* 50S crystal structure so it remains to be seen how close this flexible extension comes to the PTC [39].

It should be noted that there seems to be a unique species-specific pattern of resistance to oxazolidinones, since there is little overlap in the reported mutation sites (Table 12.5; [137, 157]). This is probably due to slight differences within the PTC of the ribosomes, which may affect the drug-binding site and/or could simply reflect variation in the tolerance to mutations at specific sites in the PTC of the respective ribosomes. In this respect, it is interesting that the G2447U mutation in *Mycobacterium smegmatis* is lethal in *E. coli* (see Ref. [157] and references therein).

The specific binding of oxazolidinones with the 50S subunit is supported by the fact that ^{14}C-labeled eperezolid (PNU-100592(S)) bound only the 50S subunit (K_d = 20 μM), a result which was recently supported by NMR studies [158]. That the

Table 12.5 23S rRNA mutations of different organisms conferring resistance to the oxazolidinone linezolid

Organism	Mutation position[a]	Mutation creation[b]	Selected references
H. halobium	U2500C$^{>200}$	spon.	160
	U2504C^{180}	spon.	
	C2452U^{160}	spon. + engin	
	A2453G^{130}	spon.	
	A2062C^{80}	cross.	
	C2499U^{30}	cross.	
	A2453C^{15}	cross.	
E. coli JM109	G2032A	spon.	247
E. coli HN818	G2032A^{80}	spon. + engin.	247
	G2032C^{60}	engin.	
	G2032U^{40}	engin.	
	G2447U$_{\sim 20}$[c]	engin.	
M. smegmatis (rrn-)	G2447U	spon. + engin.	157
Enterococcus sp.	G2505A G2576U	spon.	248
Staphylococcus sp. / Streptococcus sp.	G2447U G2576U	spon.	275

a *E. coli* numbering is given; the minimal inhibitory concentration (MIC) is given where known (μM) as the superscripted number following the base substitution.

b Spon. and Engin. indicate whether the resistance was discovered through selecting for spontaneous-resistant mtutants or whether the mutation was engineered and then the level of resistance being determined. Lin mutants originally discovered as having resistance to another antibiotic are indicated by +.

c It should be noted that resistance was conferred in *trans* by overexpressing the 23S rRNA bearing this mutation since attempts to generate this mutation were unsuccessful suggesting it is lethal in *E. coli* [250].

binding position locates to the PTC was indicated biochemically by the competition for binding between eperezolid and chloramphenicol, lincomycin and clindamycin, but not puromycin [159]. Consistently, neither eperezolid, nor Lin, has been shown to inhibit the puromycin reaction [159, 160], although certain derivatives of Lin (PNU-176798 and DuP 791) have [157, 161, 162]. Whether this reflects differences in the drugs or the biochemical systems remains to be resolved. In any case, there is mounting evidence suggesting that the oxazolidinones exert their influence through the positioning or accommodation of initiator fMet-tRNA on the ribosome, leading to the proposal that the site of action of oxazolidinones may in fact be the initiation phase of translation [162–165]. In support of this, Colca et al. [156] also detected an oxazolidinone specific crosslink to tRNA; unfortunately, however, whether the species was the initiator-tRNA could not be determined. If this were true, then one could envisage that the PTF activity *per se* is not inhibited by the oxazolidinones, instead this inhibition is by incorrect positioning of the P-site substrate. Additionally, the oxazolidones (as well as chloramphenicol) have been shown *in vivo* to induce translational inaccuracy in the form of increased frameshifting and nonsense suppresion, which was proposed to result from perturbation of tRNA–ribosome interactions [166]. Moreover, Matassova et al. [155] detected no inhibition on any steps leading to dipeptide formation, but observed inhibition during the elongation phase, prompting the suggestion that the translocation reaction may be the site of action. In this regard, it is interesting that the residue crosslinked by the oxazolidinones, A2602, has been proposed to play a role in guiding the translocation of the CCA–end of the post-peptide-bond formation peptidyl-tRNA from the A- to P-site [108]. However, the azido crosslinking moiety that was attached to the ring C of Linezolid adds significant length to the drug making it unlikely that the drug actually comes into contact with A2602. Further work will be required to reconcile the conflicting data and determine the exact mechanism of inhibition of this clinically important class of antibiotics.

The search for novel ribosome inhibitors (NRI) has led to the recent discovery by Abbott laboratories of a series of translation inhibitors [167], structurally related to the antibacterial quinolones (Appendix E1). The quinolones are well known as DNA gyrase and topoisomerase IV inhibitors; therefore, it was surprising that small modifications in structure were sufficient to completely alter the mechanism of action of these compounds turning them into translation inhibitors. Moreoever, the specificity of action of the NRI compounds was such that both Gram-positive and Gram-negative bacteria were inhibited, including a number of common respiratory pathogens, while human cell lines remained unaffected [167]. Perhaps the most exciting observation is that the NRI compounds appear to inhibit translation using a new mechanism since NRI-resistant strains show no cross-resistance with other translation inhibitors, such as macrolides, tetracyclines, aminoglycosides or oxazolidinones. Defining the binding site of these antibiotics on the ribosome is certain to provide insights into their mechanism of inhibiton.

12.3.3 Translocation Inhibitors

12.3.3.1 Thiostrepton and Micrococcin

Thiostrepton, a modified peptide antibiotic (Appendix F1), has several effects on a number of partial reactions during translation. One prominent effect is the inhibition of EF-G-dependent uncoupled GTPase, i.e., a strong EF-G-dependent GTPase activity in the presence of idle ribosomes (those not active in protein synthesis, i.e., non-polysomal). However, thiostrepton blocks spontaneous (EF-G-independent) translocation as well. Furthermore, the antibiotic inhibits A-site occupation of the e-type and to a lesser extent the A-site binding of the i-type. Therefore, the prevalent effect of thiostrepton is probably an inhibition of the transition between PRE and POST states, regardless of the direction [47].

Thiostrepton binds to the 50S subunit with a remarkably high association constant ($K_a > 10^9\ M^{-1}$) [168], which is 2–4 orders of magnitude higher than the association constant for many other antibiotics and six orders of magnitude higher than that for puromycin. Thiostrepton also binds to naked 23S rRNA and this affinity is enhanced in the presence of L11; however, L11 in isolation does not bind the drug. L11 binds a fragment of 23S rRNA (nucleotides 1052–1112), as do thiostrepton and micrococcin, an antibiotic structurally related to thiostrepton (see Appendix F1), providing strong evidence that both drugs bind within this region. The producer of thiostrepton, *Streptomyces azureus*, protects its own rRNA by introducing a methyl group onto the ribose moiety of A1067, thereby causing resistance to thiostrepton (and micrococcin). This small 2′-O-methyl group decreases the binding affinity of thiostrepton by at least six orders of magnitude [168].

The 23S rRNA/L11 complex, together with the pentameric complex L10•$(L12)_4$, has been implicated in elongation factor-dependent GTP hydrolysis. An EF-G crosslink within the 70S ribosomes maps to a fragment of 23S rRNA containing A1067, and bases A1067 and A1069 are protected by EF-G in addition to those protected in the sarcin-ricin loop [169]. Although EF-Tu shows no direct protection of bases in domain II of 23S rRNA [169], a mutation of A1067 affects EF-Tu function, and residues G1041, G1068 and G1071 are shielded by aminoacyl-tRNA-bound enzymatically to the A-site with or without kirromycin [170]. Chemical and enzymatic probing studies show that thiostrepton protects 13 nucleotides between A1067 and A1098 [171]. The same set of protections were found in the presence of micrococcin with one important exception: namely that the N-1 position of A1067 was protected against dimethylsulfhate (DMS) by thiostrepton but exhibits enhanced reactivity upon micrococcin binding. Since A1067 is also strongly shielded by EF-G, this observation may well be related to the contrasting effects that thiostrepton and micrococcin have on EF-G-dependent GTPase, i.e., thiostrepton is inhibitory whereas micrococcin is stimulatory (reviewed in Ref. [64]).

The protection pattern of thiostrepton encompasses the loops of two helices of the 23S rRNA, H43 and H44. The importance of both loop regions for drug binding is

supported by the fact that methylation of A1067 confers thiostrepton resistance [168]. Similarly, mutations of the residue A1067 to U or C and, with a weaker effect, to G, result in thiostrepton resistance *in vitro*. The mutations at both A1067 and A1095 strongly reduce the binding of micrococcin and thiostrepton to the ribosome, whereas L11 binding is not affected by these mutations. Note that methylation of the ribose at position 1067 is a much smaller change when compared with a transversion at this position, and yet the effect of methylation on thiostrepton binding is much more drastic.

The L11-binding region of *E. coli* 23S rRNA can be replaced by the homologous stretch of residues from the yeast *S. cerevisiae*, with the result that these engineered ribosomes are also thiostrepton-sensitive [172]. Potentially, this raises a paradox, since yeast ribosomes are naturally resistant to thiostrepton. However, the naked yeast 26S rRNA is able to bind thiostrepton and thus the potential thiostrepton-binding site may simply be masked by proteins in the intact yeast ribosome. The exchange of the L11 binding site between *E. coli* and yeast is equivalent to the simultaneous introduction of 20 mutations between positions 1056 and 1103. Despite these differences in primary sequence, the conformation of this region is likely to be evolutionary highly conserved, since it has been demonstrated that L11 can recognize the corresponding region in the rat 28S rRNA and *vice versa* [173]. Furthermore, *E. coli* L11 and thiostrepton bind co-operatively to the *E. coli* 23S rRNA region and to the rat 28S rRNA region, if position 1878 (the equivalent of 1067 in *E. coli*) is mutated from G to A. No such co-operativity was seen with rat L12 (the *E. coli* L11 homolog). The lack of co-operativity in eukaryotic ribosomes may also play a role in thiostrepton resistance [173].

Protein L11 consists of two domains: the C-terminal part is responsible for the tight interaction with the rRNA-binding region for L11, and the N-terminal part is required for the co-operative binding of thiostrepton. Mutations in the N-terminal region (specifically, substitutions of P18S/T and P22S/T in *E. coli* L11) confer resistance to thiostrepton [174, 175], although not by affecting interaction of thiostrepton with the rRNA, but perhaps by allowing L11 the freedom to move despite the presence of thiostrepton. Interestingly, in bacterial and archaeal ribosomes, on which thiostrepton is active, P18/22 in L11 are conserved, whereas in the equivalent position in eukaryotic L11 the prolines are not conserved, consistent with their natural resistance. The crystal structure of L11 in complex with its rRNA-binding site has been solved to 2.57–2.8 Å resolution [176, 177]. It has been proposed that the sugar of A1067 and the base A1095 interact directly with thiostrepton by forming a binding pocket in conjunction with the prolyl residues of the N-terminal domain of L11 (Fig. 12.15). Unfortunately, the L11 region (as well as the pentameric L10•$(L7/L12)_4$) are highly disordered in all the available high-resolution crystal structures of the ribosomal subunits [38, 39], making determination of thiostrepton-bound 50S subunit structures more complicated.

There is some controversy over the exact step of thiostrepton action. In contrast with numerous previous results (reviewed in Ref. [28]), a recent publication purported that thiostrepton allowed binding of EF-G to the ribosome, a single translocation reaction and hydrolysis of GTP, but prevented release of EF-G.GDP [178]. These

thiostrepton-stabilized EF-G–ribosome complexes were analyzed by cryo-EM [179]. The conclusions drawn from this analysis, interpreted on the basis that the thiostrepton-stabilized EF-G was the GDP conformer, was at odds with the interpretation of the fusidic acid complexes (see Ref. [180]). In direct contradiction with this model, recent evidence was presented demonstrating that thiostrepton is, in agreement with earlier works, a strong inhibitor of EF-G-dependent GTP hydrolysis and acts by destabilizing the interaction between EF-G and the ribosome [181]. Numerous attempts were made to reconcile the two disparate results but even repeating the experiments under the conditions used by Rodnina and coworkers [178], the conclusion remained the same, namely that thiostrepton strongly inhibited GTP hydrolysis and association of EF-G with the ribosome. Additionally, thiostrepton was shown to stimulate IF2-dependent GTP hydrolysis, whereas micrococcin stimulated the GTP hydrolysis of both factors. These results can be interpreted best if thiostrepton (and micrococcin) are thought to stabilize the L11 region in a particular conformation that prevents (or reduces) stable binding of EF-G and EF-G-dependent GTP hydrolysis. In the case of micrococcin the weakened interaction of EF-G with the ribosome, although sufficient to stimulate GTP hydrolysis, results in rapid dissociation

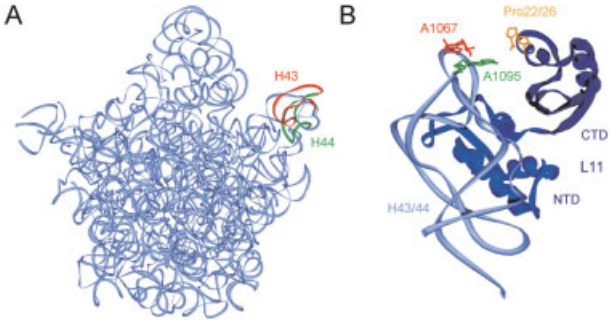

Figure 12.15 Putative thiostrepton binding site on the 50S subunit. (A) Overview of the L11-binding site on the *D. radiodurans* 50S subunit. Only 23S and 5S rRNA are shown in ribbons representation (pdb file 1kpj) with the L11-binding site, H43 (red) and H44 (green) indicated. Note this region is relatively disordered in both D50S and H50S structures with the L11 protein being totally disordered in the H50S structure (pdb 1jj2) but the CTD being present in the D50S structure (pdb 1kpj). (B) The putative thiostrepton binding site illustrated using the isolated L11-rRNA structure (pdb1mms; [177]). Ribbons representation of a fragment of RNA (light blue) that mimics the L11 binding sites. Ribosomal protein L11 is shown with the C-terminal domain (CTD, blue), which binds to the rRNA fragment and the free N-terminal domain (NTD, dark blue) indicated. Mutations in H43 (base A1067 shown in red) and H44 (with base A1095 in green) of the 23S rRNA and in L11 (Prolines at position 22 and 26 in yellow) that confer resistance to thiostrepton are indicated.

of EF-G•GDP from the ribosome, thus resulting in increased turnover and therefore accounting for the observed stimulation of GTP hydrolysis [181].

12.3.3.2 **Viomycin Blocks Coupled GTPase Activity**

Viomycin is a cyclic peptide antibiotic composed of an unusual assortment of amino acids; the non-coded tuberactidine and ureidodehydroalanine in addition to β-lysine, serine and diaminopropionic acid (as seen in Appendix F1). Viomycin (sometimes referred to as tuberactinomycin B) belongs to the tuberactinomycin family of antibiotics and has seen limited use against tuberulosis. Viomycin exhibits inhibitory characteristics similar to the aminogylcoside family of antibiotics, in particular to hygromycin B, since viomycin acts both to induce misreading as well as inhibit EF-G-dependent translocation *in vitro* [182], but not GTP hydrolysis [178]. In fact, viomycin has been shown to compete with aminoglycosides for binding to the 30S subunit and *vice versa* [183]. However, the binding site of viomycin, although still uncertain, is probably very different to that of hygromycin B, since it seems to encompass components from both the small and large subunits: Resistance to viomycin results from ribosomes that have alterations in either rRNA from the small or large subunit, although the exact location of these mutations has not been determined [184]. Protection from chemical probing by viomycin identified bases 912–915 and A1408 in the 16S rRNA and in addition bases U913 and G914 in the 23S rRNA (Ref. [128] and unpublished data cited in Ref. [185]; see Fig. 12.2). Furthermore, conformational changes in the ribosome, measured using a toeprinting assay, demonstrated that viomycin induced an effect only with 70S ribosomes and not with 30S subunits, in contrast with all the aminoglycosides tested which affected both [185]. This suggests that viomycin may not even bind the 30S subunit in the absence of the 50S and further emphasizes the differences between viomycin and the aminoglycosides. An *E. coli* mutant strain lacking N1 methylation of G745 in H35 of domain II of the 23S rRNA also exhibits 4-fold increased resistance to viomycin as well as having a markedly reduced growth rate and a large reduction in the number of 70S ribosomes [186]. Furthermore, viomycin protected G914 from kethoxal probing more efficiently in strains lacking the G745 methylation than the wild type, suggesting that the relatively moderate increase in the level of resistance conferred by the methylation probably does not reflect a specific resistance mechanism but results from conformational changes in the 50S subunit that affect the viomycin-binding site [186]. Collectively, these data suggest that viomycin binds at the interface of the ribosomal subunits; however the presence of two binding sites, one on each subunit, cannot be excluded.

Recently, viomycin has been shown to prevent the EF-G (and RRF)-mediated release of tRNA from the ribosome during ribosome recycling [187]; however, not as effectively as thiostrepton and, unlike thiostrepton, viomycin did not inhibit the release of the RRF [188]. This suggests that viomycin and thiostrepton operate using different mechanisms, i.e., maybe viomycin allows EF-G binding and GTP hydrolysis, whereas thiostrepton severely reduces the binding of EF-G (as mentioned in Sect. 12.3.3.1).

Another feature that viomycin has in common with aminoglycosides relates to competitive inhibition of several ribozymes and also of group I intron splicing (Ref. [189]; reviewed in Ref. [190]). This finding led to the provocative proposal that low-molecular-weight molecules, such as small RNAs or antibiotic progenitors, may have been present in the primordial soup and co-evolved with the modern ribosome, originally serving a regulator function [191]. Indeed, the recent findings that Ede and Pct work antagonistically to influence initiation complex formation certainly demonstrates the potential existing for such small molecule regulation (see Sects. 12.2.2 and 12.2.3).

12.3.3.3 **Spectinomycin Interferes with EF-G Binding**

Spectinomycin is sometimes listed under "aminoglycosides", but it has in fact nothing in common with this group of antibiotics, neither structurally (Appendix F1) nor functionally. The drug inhibits translocation by interfering with the binding of EF-G to the ribosome, probably by preventing the conformational changes in the ribosome associated with EF-G binding. Consistent with this idea, the binding position of spectinomycin has been located to the elbow of h34 and h35 within the head of the *T. thermophilus* 30S subunit (Fig. 12.16) [67]. Helix 34 has a putative role in trans-location of the tRNAs from the A to P-site, probably requiring a rearrangement in its interaction with neighboring helices 35 and 38. Spectinomycin makes interactions

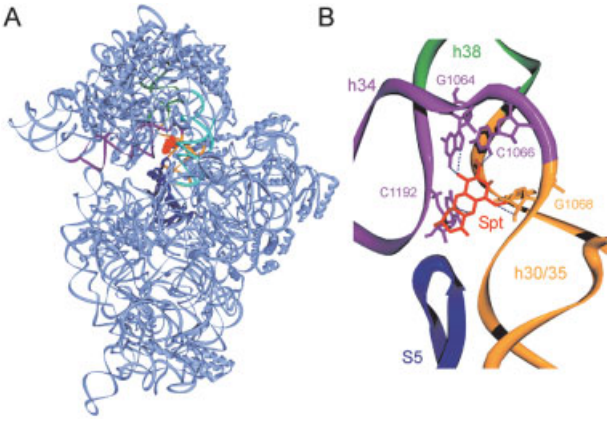

Figure 12.16 Spectinomycin binding site on the 30S subunit. (A) Overview of the spectinomycin binding site on the 30S subunit (pdb 1fjg [67]). Ribbons representation of 16S rRNA (light blue), with h34 (purple), h30/35 (yellow), h38 (green) and h28 (cyan) highlighted, as well as ribosomal protein S5 (dark blue). (B) Close-up view of the spectinomycin binding site at the elbow junction of h34 and h30, where hydrogen bond interactions (dashed blue line) between spectinomycin (Spt, red) and G1068 (h30) and C1066, G1064 and C1192 (counter clockwise) are shown. Other colours as in (A)

with three bases of h34 (G1064, C1066, and C1192) and with the phosphate of G1068 in h35, which together may stabilise this region, preventing the conformational changes necessary for translocation. This is supported by cryo-EM reconstructions of functional states that reveal movements within the head region during translocation [192].

The determined spectinomycin-binding site is in agreement with spectinomycin-resistant mutations that map within h34, specifically nucleotides G1064, C1192 and C1066 [193–196]. Furthermore, spectinomycin protects C1063 and G1064 from chemical probing [23] and overexpression of an RNA fragment resembling helix 34 confers resistance to spectinomycin [197]. The fragment is proposed to sequester the drug thereby permitting the intact ribosome to function and consequently display a spectinomycin-resistant phenotype. Surprisingly, mutations in S5 also give rise to spectinomycin resistance [198], although S5 is not required for spectinomycin binding. These mutations map to a loop in S5 that does not make direct interaction with spectinomycin; instead it stabilizes the pseudoknot region that is connected to h34 through a network of interactions. This led to the proposal that mutations in this loop, by disrupting this network of interactions, allow the head to move freely during translocation, even when spectinomycin is bound [67].

12.3.3.4 **Fusidic Acid is the Counterpart of Kirromycin**

Fusidic acid is a steroidal antibiotic (Appendix F1), which has been extensively studied since the 1960s and whose mode of action was well characterized by the mid-1970s (reviewed in Ref. [28]). Fusidic acid allows translocation and GTP hydrolysis, but prevents the associated conformational changes in EF-G, thus stabilizing the EF-G·GDP complex on the ribosome in an analogous fashion to how kirromycin prevents dissociation of EF-Tu. It is used clinically, primarily against *S. aureus*, from which most resistance mutations have been selected [199, 200]. Most resistance mutations are clustered within three distinct regions that map to the *fusA* gene, which encodes EF-G (Fig. 12.17A) [200]. According to the crystal structures of EF-G·GDP and nucleotide-free EF-G, the three mutational regions are confined to a central region of EF-G, localizing to a three-way junction between the G domain and domains III and V. It is possible that fusidic acid binds to the interface of these three domains and by restricting their movement prevents EF-G from adopting the GDP conformation (reviewed in Ref. [201]). Therefore, mutations within this region probably either facilitate the conformational changes in EF-G required for dissociation from the ribosome despite the presence of the drug, whereas others may simply prevent the drug from binding to EF-G [200].

The high occupancy and stability of the fusidic acid-bound EF-G ribosome complex has led to medium resolution cryo-EM reconstructions revealing the binding and interaction of EF-G with the ribosome [202–204]. Fusidic acid does not work on eukaryotes, but sordarin is thought to act in an analogous fashion on yeast EF2 (the homolog of EF-G). Indeed, this antifungal was used to construct stable EF2-80S yeast ribosome complexes for cryo-EM analysis (at 17.5 Å [205] and more recently at

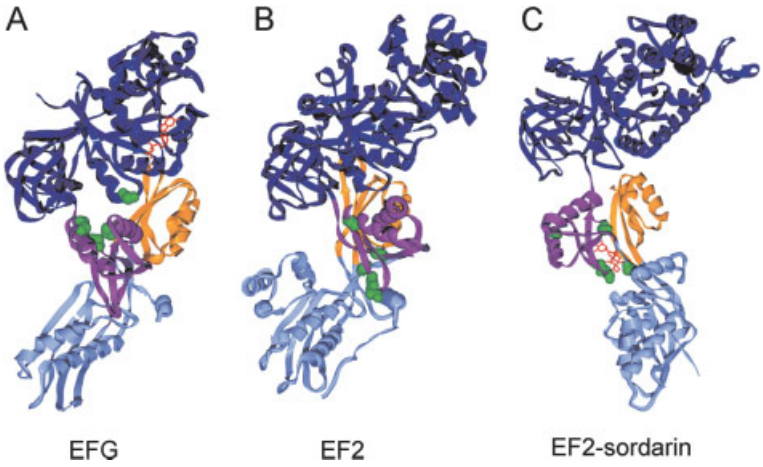

Figure 12.17 Comparison of bacterial EFG, yeast EF2 and EF2-sordarin. (A) EF-G.GDP (pdb1fmn; [200]), (B) EF2, apo form (pdb1nov; [206]), (C) EF2 bound with Sordarin (pdb1nou; [206]). Domains I, II and G domain are coloured dark blue, domain III, purple, domain IV, light blue, domain V, yellow. Residues in EF-G that confer resistance to fusidic acid (A, F90L, P405L/Q, L431Q, A435N, P436Q, H458Y) or in EF2, to sordarin (B and C; Q490E; Y512S, S523E, E524P, A562P) are coloured in green. The GDP and sordarin molecule are coloured red in A and C, respectively.

12 Å; [276]. The crystal structure of EF2 in the apo-form and in complex with sordarin were solved to 2.85 and 2.12 Å resolution, respectively [206] (Figs. 12.17B, and C). Sordarin forms hydrogen-bonds to residues Gln490, Ala562 and Phe798, thus linking domains III, IV and V. Since no contact with the G domain is made, it would seem that the binding site for sordarin and fusidic acid may differ, although the mechanism of inhibition is probably similar, i.e., preventing the conformational changes necessary to form the low-affinity state that allows EF dissociation from the ribosome. Interestingly, sordarin locates within a very enclosed binding pocket, where extensive van der Waals interactions are made, such that almost two-thirds of the surface area of the drug is buried [206]. This binding site is not present in the apo form of EF2 suggesting that sordarin binds with an induced fit.

There is good agreement between the structurally determined sordarin-binding site and mutations in EF2 that give rise to sordarin resistance: substitutions in domains III (Q490E) and IV (Y512S, S523E, E524P, A562P) as well as a deletion in domain V (*Δ*G790) have been reported to confer resistance in *S. cerevisiae* [207, 208]. Many of these substitutions are naturally occurring in plant and mammalian EF2s explaining why sordarin is a fungal-specific translation inhibitor. Additionally, sordarin resistance results from mutations of the large-subunit ribosomal protein L10e (see Table 12.6; [209]).

Table 12.6 Antibiotic resistance resulting from mutations in ribosomal proteins

Antibiotic	Ribosomal component	Mutation position[a]	Selected reference[a]
Cycloheximide	L41	Q56P	251, 252
Evernimicin	L16	See Table 12.2	See Table 12.2
Erythromycin	L4	K63E	253, 254
Erythromycin	L22	Δ_{82}MKR$_{84}$	253, 254
Quinupristin-dalfopristin and erythromycin	L22	Δ_{79}GP$_{80}$ Insertions, e.g. $_{84}$GPTLK	255
Emetine	S14	R149C R149C-R150H	256
Gentamycin	L6		257
Streptomycin	S12	P41L/S, 42Q/R, K43E, K53, R85C/H, K87R/E, P90L, G91D	258-265
Streptomycin	S4		266
Spectinomycin	S5		267, 198
Neamine	S17	H32	268, 269
Sordarin	L10e	Q137P, K T143I, A ΔS134	209
Thiostrepton	L11	P18S, T P22S, T	174, 175

a Selected examples only of amino acid mutations and corresponding references (by no means complete) presented using equivalent *E. coli* numbering except for cycloheximide resistance in eukaryotes due to L41 and sordarin resistance in some yeast due to L10e.

12.4 Inhibitors of Termination, Recycling and *trans*-Translation

The final step of protein synthesis is signalled by the presence of a stop codon in the A-site. In *E. coli,* this termination signal is recognized by the decoding termination release factors, RF1 and RF2, which mediate the release of the nascent polypeptide from the ribosome (see Chap. 9). Subsequently, RF3 binds to recycle the decoding RFs from the ribosome in a GTP-dependent manner before also dissociating (reviewed in Ref. [210]). The disassembly of the post-termination complex is accomplished by the tandem effort of two factors, the ribosome-recycling factor RRF and EF-G (reviewed in Ref. [211]). Entry into the termination of protein synthesis can also be initiated through the co-called trans-translation pathway. This pathway is evoked most often when ribosomes become stalled because the mRNA that they are translating is truncated, i.e., the mRNA does not finish with a stop codon in the A-site; instead the A-site is empty. In this specific situation, a specific transfer-messenger RNA (tmRNA) enters the ribosomal A-site to continue translation and, in doing so, frees the ribosome and tags the truncated protein for degradation (see Chap. 10).

12.4.1 Termination

As yet there are no known specific inhibitors of the termination process. A number of antibiotics that effect termination are better known as inhibitors of the elongation cycle. Members of aminoglycoside family of antibiotics, including streptomycin, have been shown to specifically inhibit RF-dependent peptidyl-tRNA hydrolysis activity without preventing the binding of the termination factors to the ribosome [212]. Comparison of the solution structure of the termination factor RF2 [213], with that of the ribosome-bound form [214, 215] suggests that, upon ribosome binding, RF2 undergoes significant conformational changes. This rearrangement is probably initiated by recognition of the stop codon in the A-site and results in the movement of domain III of RF2 into the peptidyl-transferase center to mediate peptidyl-tRNA hydrolysis. Therefore, the aminoglycoside family of antibiotics could perturb the orientation of the RF on the ribosome, preventing the correct positioning of domain III necessary to activate peptide release. Sparsomycin, which binds in the PTF center and inhibits PTF activity (see Sect. 12.3.2.2) also prevents peptide release without affecting the binding of the RFs to the ribosome [212, 216]. Interestingly, a number of antibiotics have been identified that differentially effect peptide-bond formation and peptide release, being notably less effective against the latter, especially the RF-independent release of the peptide [216], the most significant difference being seen for the lincosamides, lincomycin and clindamycin [216], all of which bind directly in the PTF [217].

In contrast, thiostrepton has been shown to inhibit the binding of both RF1 and RF2 to the ribosome [217]. This can be understood in light of the recent cryo-EM reconstructions of RF2 on the ribosome where domain I of RF2 makes extensive contact with L11 and the GTPase-associated region, where thiostrepton also binds [214, 215].

The situation with spectinomycin however is not so clear. At low concentrations (1 μM) the *in vitro* peptide release activity of RF1 and RF2 at UGA and UAA codons, respectively, is enhanced, whereas at high concentrations (100 μM) RF2 binding is inhibited [212]. Furthermore, ribosomes carrying spectinomycin-resistant mutations C1192A or C1192U inhibited ribosome binding of both RF1 and RF2 *in vitro* but RF2 was affected more severely [212]. This suggests that binding of the RFs to the ribosome may require conformational changes within the ribosome, which are prevented by the binding of a rigid spectinomycin molecule to the head of the 30s subunit.

The challenge for the future will be to develop antibiotics that are specific for the termination phase, perhaps by taking advantage of the fact that the termination factors between prokaryotes and eukaryotes are structurally unrelated [213].

12.4.2 Recycling

It seems that the majority of antibiotics that inhibit translocation; thiostrepton, viomycin, fusidic acid and aminogylcosides; also effectively inhibit RRF-dependent

ribosome recycling [187]. This is not totally unexpected since this RRF-mediated reaction is strictly dependent on EF-G. Kaji and co-workers are working on the hypothesis that during RRF-mediated ribosome recycling the role of EF-G is analogous to that during elongation, i.e., EF-G actually translocates the RRF molecule, whose structure incidentally closely resembles that of a tRNA, from the A to the P-site (see Ref. [218]). However, this model has not yet been proven. In fact, recent evidence from chemical probing experiments suggest that RRF can bind to the ribosome in a completely different orientation to that of a tRNA (reviewed in Ref. [219]).

Since no counterpart to RRF has been identified in eukaryotes, this makes ribosome recycling an attractive target for antibiotic inhibition. The goal would be to find or develop antibiotics that can specifically inhibit RRF function without affecting other steps of proteins synthesis, instead of the current situation where all antibiotics targeting this phase operate through inhibition of EF-G function. To date, no such antibiotics have been found, but with an optimistic prospect for an RRF–ribosome complex crystal structure in the near future, designing of such antibiotics may soon be within reach.

12.4.3
Trans-translation

The importance of tmRNA was questioned when deletion strains (*ΔssrA*) were generated that had growth rates similar to the wild type strain. However, under certain stress conditions, even the *ΔssrA* strain was non-viable. One of these stress conditions is the presence of protein synthesis inhibitors. Unfortunately, the *ΔssrA* strain was generated by insertion of a kanamycin resistance cassette into the tmRNA gene, making the study of aminoglycoside effects on this strain uninformative. Aminoglycosides have been shown to increase the amount of ssrA-mediated tagging [220], suggesting the effect on the *ΔssrA* strain would be severe, especially since it was not viable in the presence of a number of antibiotics that bind to the PTF center or tunnel, such as chloramphenicol, lincomycin, spiramycin, tylosin, erythromycin (as well as spectinomycin which binds to the 16S rRNA) at drug concentrations that had no significant effect on the wild type strain [221]. Such a result would not be at all surprising in the presence of aminoglycosides: since they induce misreading which can lead to ribosomal stalling, the presence of tmRNA under these conditions would be necessary to rescue the stalled ribosomes. Although more unexpected for antibiotics that target the 50S subunit, it has been recently demonstrated for chloramphenicol and the oxazolidinone linezolid that they induce frameshifting and nonsense suppression [166], probably due to perturbation in the binding of the A- and/or P-site tRNAs.

12.5
Mechanisms Causing Drug Resistance

All antibiotics discussed here (at least the *source* compounds) are typically produced in *microorganisms* as secondary metabolites. In some cases, we have already discussed

how the 'producer' survives, and many of the known resistance mechanisms are strategies that are applied by the antibiotic-producing organisms themselves and can also be found in drug-resistant microorganisms that have become a major problem in the treatment of infections. We distinguish between six different mechanisms of resistance, four of which are non-ribosome-related and are discussed briefly, whereas the remaining two are directly related to the ribosome and are therefore discussed in more detail.

12.5.1 Modification of the Antibiotic

Modification of the antibiotic can inactivate the drug or alternatively prevent its cellular uptake. Common mechanisms of inactivation include adenylation, acetylation or phosphorylation, as seen for the (i) aminogylcosides, which are modified primarily on the rings I (3′- and 4′-OH are phosphorylated and adenylated) and II (amino group at position 3 is acetylated) [222], (ii) chloramphenicol, which is acetylated by chloramphenicol-acetyltransferase, and (iii) viomycin, which is phosphorylated by a viomycin-phosphotransferase. Capreomycin (a derivative of viomycin) is both acetylated and phosphorylated in the *Streptomyces* species that produce it [223]. Alternatively, cleavage or even degradation of the drug occurs, for example, penicillin cleavage by β-lactamase. Usually, these enzymes reside in the periplasmatic space and inhibit uptake of the drugs through the cellular membrane via direct modification of the antibiotic.

12.5.2 Blockage of Transport (without Modification of the Drug)

Modification of certain membrane components can prevent drug accumulation in the cell either by passively preventing their uptake (fusidic acid, tetracycline) or actively by promoting their active efflux from the cell (tetracycline).

12.5.3 Overproduction of the Inhibited Substrate (Target Dilution)

Overproduction of the target can, in principle, sequester the antibiotic, enabling the remaining active molecules to maintain growth. This principle is observed with trimethoprim, a drug that inhibits folic acid metabolism. In this case, a strong overproduction of dihydrofolate reductase was identified as the reason for resistance. As previously mentioned, exogenous expression of an rRNA fragment containing the binding site of spectinomycin also confers resistance – most probably by a "titration" of the antibiotic.

12.5.4
Bypassing or Replacement of the Inhibited Reaction

In principle, an inhibited reaction can by bypassed or substituted by another reaction. An example is seen in a resistance mechanism against penicillin. Penicillin works by cleaving the peptidoglycans within the cell wall. Resistance can arise when peptidoglycan is substituted for another component within the cell wall; the biosynthesis of peptidoglycan is inhibited at a late step by the drug. It is clear that neither one of the elongation steps nor the elongation cycle itself can be substituted or bypassed, since the ribosome is the sole protein synthesizing enzyme in all cells.

12.5.5
Alteration of the Target Site

Many examples exist where the target site of the drugs has been altered, of which a number have been mentioned already. In *E. coli* substitutions of C912U in 16S rRNA confer resistance to streptomycin, whereas in the 23S rRNA, substitution of A1067U and any change at A2058 confer resistance to thiostrepton and erythromycin, respectively. Mutations in the A-site that confer resistance to the aminoglycosides antibiotics have been reviewed in Westhof and colleagues [224]. However, for most bacterial species it is prohibitively difficult to acquire such mutations, since the rRNA is usually encoded in multiple operons, and thus mutations must be introduced into all rRNA operons (rrn) to confer resistance. This is particularly true for *E. coli*, which has seven copies of the rrn operon. Single mutations in the rRNA operon will result in a mixture of resistant and sensitive ribosomes leaving the bacteria still susceptible to drugs that exert a dominant inhibition effect. This occurs because on bacterial polysomes, blockage of one sensitive translating ribosome on a distinct mRNA will indirectly block following ribosomes on the same mRNA (whether the following ones are resistant or susceptible). For this reason rrn operons that confer resistance to protein synthesis inhibitors are typically recessive or weakly co-dominant.

Mutations conferring resistance to these inhibitors usually arise more frequently in bacteria that harbour one (as in *H. halobium*) or two copies of the rrn operon (e.g. *Helicobacter pylori*). Species such as these have been used successfully to screen for spontaneous resistant strains when exposed to an antibiotic of interest, for example pactamycin- and evernmicin-resistant *H. halobium* strains [35, 225]. Alternatively, Squires and coworkers have constructed an *E. coli* strain with all seven of the rrn operons deleted from the genome and having a single copy expressed from an exogenous plasmid [226, 227], which has, for example, been used to select for kasugamycin-resistant mutants [14].

However, resistance can also be mediated via ribosomal proteins where all ribosomes of a cell become resistant because in bacteria ribosomal proteins are normally encoded by unique genes. A number of such mutations that give rise to antimicrobial agents exist and are summarized in Table 12.6.

Producers of antibiotics often modify the rRNA post-transcriptionally to protect themselves. This mechanism is independent of the copy number of rRNA operons. Examples include the ribose methylation of A1067 (16S rRNA, thiostrepton-resistant) and base methylation of A2058 (erythromycin-resistant). Conversely, the undermethylation of the two 2,6,dimethyl-adenines 1518 and 1519 (16S rRNA) due to a mutation in the corresponding methylase gene (*ksgA*) renders cells kasugamycin-resistant.

12.5.6
Active Protection of the Target by a Third Component

The sixth resistance mechanism involves the involvement of protein factors termed ribosome protection proteins (RPP), which by interacting with the ribosome confer resistance to tetracycline (Tet) (reviewed in more detail in Ref. [57, 228–230]). The best studied of these are Tet(O) and Tet(M) from *Campylobacter* and *Streptococcus*. These RPPs probably originated from the natural producer of oxytetracycline, *Streptomyces rimosus*, which harbors *otr*A, a RPP-like determinant, derived about 30 million years ago from the elongation factor EF-G [57]. Spread of these factors throughout the eubacteria by lateral gene transfer events was most likely facilitated by their location on mobile genetic elements.

Not surprisingly, the RPPs display significant sequence similarity to the ribosomal elongation factors, EF-G and EF-Tu, and have been shown to have GTPase activity although they cannot substitute for the elongation factors *in vivo* or *in vitro* [231]. Instead, these RPPs confer resistance to Tet by binding to the Tet-inhibited ribosome, for example, addition of purified Tet(O) to a Tet-inhibited poly(Phe) *in vitro* system could restore activity with Tet(O) shifting the IC_{50} in this system from 100 to more than 500 μM Tet [232]. This was shown to be due to the fact that Tet(O)/(M) can dislodge tetracycline from the ribosome, a function that is dependent on the presence of GTP. The interaction of Tet(O) with the ribosome has been studied using cryo-EM, revealing that Tet(O) has an overall shape similar to that of EF-G, and as expected binds at a common site [233]. Comparison of the EF-G and Tet(O) ribosomal contacts indicates that they differ primarily in the vicinity of domain IV, where EF-G contacts H69 and Tet(O) interacts with h18/34 of the 16S rRNA. This is significant since domain IV in EF-G has been implicated as an important determinant for promoting translocation of the tRNAs (see Chap. 8.4) and is therefore consistent with the lack of translocation activity for Tet(O). Similarly the interaction of domain IV of Tet(O) with h34 of the 30S subunit is consistent with its role in Tet release as h34 is a component of the primary tetracycline-binding site (see Sect. 12.3.1.1). Recent chemical probing experiments are in agreement with this proposal, since Tet(O) interactions with the 30S subunit were localized to h34 (C1214 is protected) and h44 (A1408 is enhanced) [54]. These are components of the decoding center located near to the primary tetracycline-binding site. The protection C1214 probably results from interaction of this base with Tet(O), a conclusion supported by the fact that the Tet(O)-binding site observed by cryo-EM approaches

C1214. However, since Tet(O) does not approach A1408, the enhancement of A1408 is indicative of a conformational change. Connell and coworkers [54] suggest that Tet(O) binding to the ribosome induces long-range conformational changes, possibly through S12 and h44 to allosterically release Tet from the primary binding site. This conformational change persists after Tet(O), via GTP hydrolysis, dissociates from the ribosome, so that the conformation unfavorable for Tet binding continues to provide an advantage for binding of the ternary complex to the A-site, thus relieving the Tet-induced inhibition [54].

12.6 Future Perspectives

High-resolution structures for each of ribosomal subunits have revolutionized our ability to design biochemical and genetic experiments aimed at understanding ribosome structure and function and also to interpret the results better. Furthermore, it has enabled us to reinterpret the huge wealth of data relating to the ribosome, where the interaction of antibiotics with the ribosome is no exception. The current state of the art encompasses understanding these interactions by direct determination of these antibiotic–ribosome complexes at high resolution. Already representatives for the majority of antibiotic families that inhibit the ribosome directly have been characterized and those that have not, are for sure being completed as this review goes to press. So what does the future hold? With the ever-increasing emergence of antibiotic-resistant bacteria, the search for novel and more potent antibiotics continues to be the challenge for the future. Using the available structural information for rational design of these new and improved antibiotics is the path ahead. Such approaches may include chemically linking known antibiotics to create so-called "hybrid antibiotics" – the idea being that simultaneous mutations that confer resistance to each antibiotic would be required to confer resistance to the hybrid antibiotic. For example this has been reported for CP-544372, a hybrid between a macrolide, linked through a long anchor group at the 4"-position of a cladinose sugar, to chloramphenicol [234]. By analyzing the currently available information pertaining to the interactions of particular antibiotics with the ribosome, another approach is to alter the antibiotic, for example, by chemically modifying the sidechains, in such a way that either they establish new or additional interactions, such as hydrogen-bonds, hopefully increasing their affinity for the ribosome and/or making them more effective, even against, currently resistant strains. This is the exact goal of start-up companies, such as Rib-X and RiboTargets, where specialized software (Analog and Ribodock®, respectively) is being used iteratively to develop new antibiotic agents. Recently, RiboTargets presented evidence as to the power of this approach by the design of a new aminoglycoside antibiotic, which they demonstrated by crystallography could bind to a small RNA mimic of the ribosomal decoding site [235].

References

1 E. F. Gale, E. Cundliffe, P. E. Reynolds et al.: in *The Molecular Basis of Antibiotic Action* Wiley, Bristol, UK 1972, pp. 278–379.
2 P. Moore, T. Steitz, *Annu. Rev. Biochem.* **2003**, *72*, 813–850.
3 P. B. Moore, T. A. Steitz, *Nature* **2002**, *418*, 229–235.
4 V. Ramakrishnan, *Cell* **2002**, *108*, 557–572.
5 D. N. Wilson, G. Blaha, S. R. Connell et al., *Curr. Protein Pept. Sci.* **2002**, *3*, 1–53.
6 A. Yonath, *Annu. Rev. Biophys. Biomol. Struct.* **2002**, *31*, 257–273.
7 T. Auerbach, A. Bashan, J. Harms et al., *Curr. Drug Targets Infect. Disord.* **2002**, *2*, 169–186.
8 J. M. Harms, H. Bartels, F. Schlunzen et al., *J. Cell Sci.* **2003**, *116*, 1391–1393.
9 C. O. Gualerzi, C. L. Pon, *Biochemistry* **1990**, *29*, 5881–5889.
10 M. Kozak, D. Nathans, *J. Mol. Biol.* **1972**, *70*, 41–55.
11 T. L. Helser, J. E. Davies, J. E. Dahlberg, *Nat. New Biol.* **1971**, *233*, 12–14.
12 T. L. Helser, J. E. Davies, J. E. Dahlberg, *Nat. New Biol.* **1972**, *235*, 6–9.
13 P. F. Sparling, *Science* **1970**, *167*, 56–58.
14 A. Vila-Sanjurjo, C. L. Squires, A. E. Dahlberg, *J. Mol. Biol.* **1999**, *293*, 1–8.
15 J. Woodcock, D. Moazed, M. Cannon et al., *EMBO J.* **1991**, *10*, 3099–3103.
16 K. Chin, C. S. Shean, M. E. Gottesman, *J. Bacteriol.* **1993**, *175*, 7471–7473.
17 I. Moll, U. Bläsi, *Biochem. Biophys. Res. Commun.* **2002**, *297*, 1021–1026.
18 B. Poldermans, N. Goosen, P. H. Van Knippenberg, *J. Biol. Chem.* **1979**, *254*, 9085–9089.
19 J. Tan, U. Jakob, J. C. Bardwell, *J. Bacteriol.* **2002**, *184*, 2692–2698.
20 K. Inoue, J. Alsina, J. Chen et al., *Mol. Microbiol.* **2003**, *48*, 1005–1016.
21 bläsi, p. c..,
22 G. Dinos, D. Wilson, Y. Tereoka et al., *Mol. Cell* **2004**.
23 D. Moazed, H. F. Noller, *Nature* **1987**, *327*, 389–394.
24 M. Pioletti, F. Schlunzen, J. Harms et al., *EMBO J.* **2001**, *20*, 1829–1839.
25 M. M. Yusupov, G. Z. Yusupova, A. Baucom et al., *Science* **2001**, *292*, 883–896.
26 F. Robert, L. Brakier-Gingras, *J. Biol. Chem.* **2003**, *278*, 44913–44920.
27 B. K. Bhuyan, *Biochem. Pharmacol.* **1967**, *16*, 1411–1420.
28 E. F. Gale, E. Cundliffe, P. E. Reynolds et al.: in *The Molecular Basis of Antibiotic Action* Wiley, Bristol, UK 1981, pp. 278–379.
29 D. E. Brodersen, W. M. Clemons, A. P. Carter et al., *Cell* **2000**, *103*, 1143–1154.
30 F. M. Aarestrup, L. B. Jensen, *Antimicrob. Agents Chemother.* **2000**, *44*, 3425–3427.
31 P. V. Adrian, W. Zhao, T. A. Black et al., *Antimicrob. Agents Chemother.* **2000**, *44*, 732–738.
32 P. M. McNicholas, P. A. Mann, D. J. Najarian et al., *Antimicrob. Agents Chemother.* **2001**, *45*, 79–83.
33 M. Zarazaga, C. Tenorio, R. Del Campo et al., *Antimicrob. Agents Chemother.* **2002**, *46*, 3657–3659.
34 P. V. Adrian, C. Mendrick, D. Loebenberg et al., *Antimicrob. Agents Chemother.* **2000**, *44*, 3101–3106.
35 L. Belova, T. Tenson, L. Q. Xiong et al., *Proc. Natl. Acad. Sci. USA* **2001**, *98*, 3726–3731.
36 C. B. Kofoed, B. Vester, *Antimicrob. Agents Chemother.* **2002**, *46*, 3339–3342.
37 P. A. Mann, L. Xiong, A. S. Mankin et al., *Mol. Microbiol.* **2001**, *41*, 1349–1356.
38 N. Ban, P. Nissen, J. Hansen et al., *Science* **2000**, *289*, 905–920.
39 J. Harms, F. Schluenzen, R. Zarivach et al., *Cell* **2001**, *107*, 679–688.
40 P. M. McNicholas, D. J. Najarian, P. A. Mann et al., *Antimicrob. Agents Chemother.* **2000**, *44*, 1121–1126.

41 A. La Teana, C. O. Gualerzi, A. E. Dahlberg, *RNA* **2001**, *7*, 1173–1179.
42 W. S. Champney, C. L. Tober, *Curr. Microbiol.* **2000**, *41*, 126–135.
43 W. S. Champney, *Curr. Drug Targets Infect. Disord.* **2001**, *1*, 19–36.
44 R. Mehta, W. S. Champney, *Antimicrob. Agents Chemother.* **2002**, *46*, 1546–1549.
45 H. S. Chittum, W. S. Champney, *Curr. Microbiol.* **1995**, *30*, 273–279.
46 J. Usary, W. S. Champney, *Mol. Microbiol.* **2001**, *40*, 951–962.
47 T. P. Hausner, U. Geigenmüller, K. H. Nierhaus, *J. Biol. Chem.* **1988**, *263*, 13103–13111.
48 J. P. White, C. R. Cantor, *J. Mol. Biol.* **1971**, *58*, 397–400.
49 W. Rogalski: in *The Tetracyclines (Handbook of Experimental Pharmacology)*, eds J. J. Hlavka and J. H. Boothe, Springer, Berlin 1985, pp. 179–316.
50 B. Rasmussen, H. F. Noller, G. Daubresse et al., *Antimicrob. Agents Chemother.* **1991**, *35*, 2306–2311.
51 M. M. Gerrits, M. R. de Zoete, N. L. Arents et al., *Antimicrob. Agents Chemother.* **2002**, *46*, 2996–3000.
52 J. I. Ross, E. A. Eady, J. H. Cove et al., *Antimicrob. Agents Chemother.* **1998**, *42*, 1702–1705.
53 C. A. Trieber, D. E. Taylor, *J. Bacteriol.* **2002**, *184*, 2131–2140.
54 S. R. Connell, C. A. Trieber, U. Stelzl et al., *Mol. Microbiol.* **2002**, *45*, 1463–1472.
55 J. S. Lodmell, A. E. Dahlberg, *Science* **1997**, *277*, 1262–1267.
56 I. V. Velichutina, J. Y. Hong, A. D. Mesecar et al., *J. Mol. Biol.* **2001**, *305*, 715–727.
57 S. R. Connell, D. M. Tracz, K. H. Nierhaus et al., *Antimicrob. Agents Chemother.* **2003**, *47*, 3675–3681.
58 I. Chopra, *Curr. Opin. Pharmacol.* **2001**, *1*, 464–469.
59 J. Bergeron, M. Ammirati, D. Danley et al., *Antimicrob. Agents Chemother.* **1996**, *40*, 2226–2228.
60 B. A. Rasmussen, Y. Gluzman, F. P. Tally, *Antimicrob. Agents Chemother.* **1994**, *38*, 1658–1660.
61 M. Tuckman, P. J. Petersen, S. J. Projan, *Microb. Drug Resist.* **2000**, *6*, 277–282.
62 C. G. Kurland, F. Jørgensen, A. Richter et al.: in *The Ribosome Structure, Function, and Evolution*, eds A. Dahlberg, W. E. Hill, R. A. Garrett et al., ASM Press, Washington, DC 1990, pp. 513–526.
63 A. P. Carter, W. M. Clemons, Jr., D. E. Brodersen et al., *Science* **2001**, *291*, 498–501.
64 C. M. T. Spahn, C. D. Presscott, *J. Mol. Med.* **1996**, *74*, 423–439.
65 C. G. Kurland, D. Hughes, M. Ehrenberg: in *Escherichia coli and Salmonella, Cellular and Molecular Biology*, ed. F. C. Neidhardt, ASM Press, Washington, DC 1996, pp. 979–1004,
66 J. M. Ogle, F. V. Murphy, M. J. Tarry et al., *Cell* **2002**, *111*, 721–732.
67 A. P. Carter, W. M. Clemons, D. E. Brodersen et al., *Nature* **2000**, *407*, 340–348.
68 J. M. Ogle, D. E. Brodersen, W. M. Clemons Jr et al., *Science* **2001**, *292*, 897–902.
69 D. Fourmy, M. I. Recht, S. C. Blanchard et al., *Science* **1996**, *274*, 1367–1371.
70 D. Fourmy, S. Yoshizawa, J. D. Puglisi, *J. Mol. Biol.* **1998**, *277*, 333–345.
71 S. R. Lynch, R. L. Gonzalez Jr., J. D. Puglisi et al., *Structure* **2003**, *11*, 43–53.
72 Q. Vicens, E. Westhof, *Structure (Cambridge)* **2001**, *9*, 647–658.
73 Q. Vicens, E. Westhof, *Biopolymers* **2003**, *70*, 42–57.
74 S. Yoshizawa, D. Fourmy, J. D. Puglisi, *EMBO J.* **1998**, *17*, 6437–6448.
75 Q. Vicens, E. Westhof, *J. Mol. Biol.* **2003**, *326*, 1175–1188.
76 Q. Vicens, E. Westhof, *Chem. Biol.* **2002**, *9*, 747–755.
77 R. Karimi, M. Ehrenberg, *Eur. J. Biochem.* **1994**, *226*, 355–360.
78 J. Ogle, A. Carter, V. Ramakrishnan, *TIBS* **2003**, *28*, 259–266.

79 D. Fourmy, M. I. Recht, J. D. Puglisi, *J. Mol. Biol.* **1998**, *277*, 347–362.
80 S. R. Lynch, J. D. Puglisi, *J. Mol. Biol.* **2001**, *306*, 1037–1058.
81 M. I. Recht, S. Douthwaite, J. D. Puglisi, *EMBO J.* **1999**, *18*, 3133–3138.
82 R. Kao, J. Davies: in *The Ribosome Structure, Function, Antibiotics, and Cellular Interactions*, eds R. A. Garrett, S. R. Douthwaite, A. Liljas et al., ASM Press, Washington, DC 2000, pp. 451–460.
83 I. G. Wool, A. Gluck, Y. Endo, *Trends Biochem. Sci.* **1992**, *17*, 266–269.
84 T. Hogg, J. R. Mesters, R. Hilgenfeld, *Curr. Protein Pept. Sci.* **2002**, *3*, 121–131.
85 H. Stark, M. V. Rodnina, J. Rinkeappel et al., *Nature* **1997**, *389*, 403–406.
86 M. Valle, J. Sengupta, N. K. Swami et al., *EMBO J.* **2002**, *21*, 3557–3567.
87 G. R. Andersen, S. Thirup, L. L. Spremulli et al., *J. Mol. Biol.* **2000**, *297*, 421–436.
88 R. Hilgenfeld, J. Mesters, T. Hogg: in *The Ribosome Structure, Function, Antibiotics, and Cellular Interactions*, eds R. A. Garrett, S. R. Douthwaite, A. Liljas, et al., ASM Press, Washington, DC 2000, pp. 347–357.
89 L. Vogeley, G. J. Palm, J. R. Mesters et al., *J. Biol. Chem.* **2001**, *276*, 17149–17155.
90 E. Fischer, H. Wolf, K. Hantke et al., *Proc. Natl. Acad. Sci. USA* **1977**, *74*, 4341–4345.
91 T. Watanabe, K. Izaki, H. Takahashi, *J. Antibiot. (Tokyo)* **1982**, *35*, 1141–1147.
92 T. Watanabe, T. Sugiyama, M. Takahashi et al., *J. Antibiot. (Tokyo)* **1992**, *45*, 470–475.
93 A. M. Zuurmond, L. N. Olsthoorn-Tieleman, J. Martien de Graaf et al., *J. Mol. Biol.* **1999**, *294*, 627–637.
94 S. E. Heffron, F. Jurnak, *Biochemistry* **2000**, *39*, 37–45.
95 A. Pingoud, W. Block, C. Urbanke et al., *Eur. J. Biochem.* **1982**, *123*, 261–265.
96 L. A. H. Zeef, L. Bosch, P. H. Anborgh et al., *EMBO J.* **1994**, *13*, 5113–5120.
97 P. Landini, M. Bandera, B. P. Goldstein et al., *Biochem. J.* **1992**, *283*, 649–652.
98 V. G. Mohrle, L. N. Tieleman, B. Kraal, *Biochem. Biophys. Res. Commun.* **1997**, *230*, 320–326.
99 T. P. Hausner, J. Atmadja, K. H. Nierhaus, *Biochimie* **1987**, *69*, 911–923.
100 I. G. Wool, *TIBS* **1984**, *9*, 14–17.
101 S. Yoshinari, S. Koresawa, S. Yokota et al., *Biosci. Biotechnol. Biochem.* **1997**, *61*, 324–331.
102 S. Yoshinari, S. Yokota, H. Sawamoto et al., *Eur. J. Biochem.* **1996**, *242*, 585–591.
103 T. Uchiumi, S. Honma, Y. Endo et al., *J. Biol. Chem.* **2002**, *277*, 41401–41409.
104 P. Nissen, J. Hansen, N. Ban et al., *Science* **2000**, *289*, 920–930.
105 M. Welch, J. Chastang, M. Yarus, *Biochemistry* **1995**, *34*, 385–390.
106 J. L. Hansen, T. M. Schmeing, P. B. Moore et al., *Proc. Natl. Acad. Sci. USA* **2002**, *99*, 11670–11675.
107 T. M. Schmeing, A. C. Seila, J. L. Hansen et al., *Nat. Struct. Biol.* **2002**, *9*, 225–230.
108 A. Bashan, I. Agmon, R. Zarivach et al., *Mol. Cell* **2003**, *11*, 91–102.
109 B. Ulbrich, G. Mertens, K. H. Nierhaus, *Arch. Biochem. Biophys.* **1978**, *190*, 149–154.
110 R. Suhadolnik: *Nucleoside Antibiotics* Wiley, New York 1970.
111 D. Vasquez: *Inhibitors of Protein Synthesis* Springer, Berlin, Heidelberg, New York 1979.
112 J. L. Hansen, P. B. Moore, T. A. Steitz, *J. Mol. Biol.* **2003**, *330*, 1061–1075.
113 F. Lichtenthaler, G. Trummlitz, *FEBS Lett.* **1974**, *38*, 237–242.
114 C. Rodriguez-Fonseca, R. Amils, R. A. Garrett, *J. Mol. Biol.* **1995**, *247*, 224–235.
115 B. Porse, C. Rodriguez-Fonseca, I. Leviev et al., *Biochem. Cell Biol.* **1995**, *73*, 877–885.
116 D. Moazed, H. F. Noller, *Proc. Natl. Acad. Sci. USA* **1991**, *88*, 3725–3728.

117 G. T. Tan, A. Deblasio, A. S. Mankin, *J. Mol. Biol.* **1996**, *261*, 222–230.
118 E. Lazaro, C. Rodriguezfonseca, B. Porse et al., *J. Mol. Biol.* **1996**, *261*, 231–238.
119 E. Lazaro, L. A. G. M. Vandenbroek, A. S. Felix, et al., *Biochemistry* **1991**, *30*, 9642–9648.
120 B. T. Porse, S. V. Kirillov, M. J. Awayez et al., *Proc. Natl. Acad. Sci. USA* **1999**, *96*, 9003–9008.
121 K. Fredrick, H. F. Noller, *Science* **2003**, *300*, 1159–1162.
122 I. Agmon, T. Auerbach, D. Baram et al., *Eur. J. Biochem.* **2003**, *270*, 2543–2556.
123 M. L. Celma, R. E. Monro, D. Vazquez, *FEBS Lett.* **1971**, *13*, 247–251.
124 S. Pestka, *Biochem. Biophys. Res. Commun.* **1969**, *36*, 589–595.
125 S. Pestka, *Proc. Natl. Acad. Sci. USA* **1969**, *64*, 709–714.
126 H. J. Rheinberger, K. H. Nierhaus, *Eur. J. Biochem.* **1990**, *193*, 643–650.
127 F. Schlünzen, R. Zarivach, J. Harms et al., *Nature* **2001**, *413*, 814–821.
128 D. Moazed, H. F. Noller, *Biochimie* **1987**, *69*, 879–884.
129 U. Saarma, J. Remme, *Nucleic Acids Res.* **1992**, *20*, 3147–3152.
130 B. S. Cooperman, C. J. Weitzmann, C. L. Fernandez: in *The Ribosome: Structure, Function and Evolution*, eds W. E. Hill, A. Dahlberg, R. A. Garrett et al., ASM Press, Washington, DC 1990, pp. 491–501.
131 D. Nierhaus, K. H. Nierhaus, *Proc. Natl. Acad. Sci. USA* **1973**, *70*, 2224–2228.
132 S. Kallia-Raftopoulos, D. L. Kalpaxis, *Mol. Pharmacol.* **1999**, *56*, 1042–1046.
133 J. Poehlsgaard, S. Douthwaite, *Curr. Opin. Investig. Drugs* **2003**, *4*, 140–148.
134 S. Douthwaite, *Nucleic Acids Res.* **1992**, *20*, 4717–4720.
135 J. I. Ross, E. A. Eady, J. H. Cove et al., *Antimicrob. Agents Chemother.* **1997**, *41*, 1162–1165.
136 S. Jenni, N. Ban, *Curr. Opin. Struct. Biol.* **2003**, *13*, 212–219.
137 A. S. Mankin, *Mol. Biol.* **2001**, *35*, 509–520.
138 H. Takashima, *Curr. Top. Med. Chem.* **2003**, *3*, 991–999.
139 S. M. Poulsen, C. Kofoed, B. Vester, *J. Mol. Biol.* **2000**, *304*, 471–481.
140 L. H. Hansen, P. Mauvais, S. Douthwaite, *Mol. Microbiol.* **1999**, *31*, 623–631.
141 L. Xiong, S. Shah, P. Mauvais et al., *Mol. Microbiol.* **1999**, *31*, 633–639.
142 R. Berisio, F. Schluenzen, J. Harms et al., *Nat. Struct. Biol.* **2003**, *31*, 31.
143 F. Schlunzen, J. M. Harms, F. Franceschi et al., *Structure (Cambridge)*, **2003**, *11*, 329–338.
144 R. Berisio, J. Harms, F. Schluenzen et al., *J. Bactriol* **2003**, *185*, 4276–4279.
145 J. L. Hansen, J. A. Ippolito, N. Ban et al., *Mol. Cell* **2002**, *10*, 117–128.
146 T. Tenson, M. Lovmar, M. Ehrenberg, *J. Mol. Biol.* **2003**, *330*, 1005–1014.
147 S. Douthwaite, L. H. Hansen, P. Mauvais, *Mol. Microbiol.* **2000**, *36*, 183–193.
148 J. C. Mao, M. Putterman, *J. Mol. Biol.* **1969**, *44*, 347–361.
149 S. T. Gregory, A. E. Dahlberg, *J. Mol. Biol.* **1999**, *289*, 827–834.
150 T. Tenson, M. Ehrenberg, *Cell* **2002**, *108*, 591–594.
151 H. M. Lamb, D. P. Figgitt, D. Faulds, *Drugs* **1999**, *58*, 1061–1097.
152 B. Porse, R. Garrett, *J. Mol. Biol.* **1999**, *286*, 375–387.
153 E. Nyssen, M. Di Giambattista, C. Cocito, *Biochim. Biophys. Acta* **1989**, *1009*, 39–46.
154 R. Parfait, C. Cocito, *Proc. Natl. Acad. Sci. USA* **1980**, *77*, 5492–5496.
155 N. B. Matassova, M. V. Rodnina, R. Endermann et al., *RNA* **1999**, *5*, 939–946.
156 J. R. Colca, W. G. McDonald, D. J. Waldon et al., *J. Biol. Chem.* **2003**, *10*, 10.
157 P. Sander, L. Belova, Y. G. Kidan et al., *Mol. Microbiol.* **2002**, *46*, 1295–1304.
158 C. C. Zhou, S. M. Swaney, D. L. Shinabarger et al., *Antimicrob. Agents Chemother.* **2002**, *46*, 625–629.
159 A. H. Lin, R. W. Murray, T. J. Vidmar et al., *Antimicrob. Agents Chemother.* **1997**, *41*, 2127–2131.

160 P. Kloss, L. Xiong, D. L. Shinabarger et al., *J. Mol. Biol.* **1999,** *294,* 93–101.

161 H. Aoki, L. Ke, S. M. Poppe et al., *Antimicrob. Agents Chemother.* **2002,** *46,* 1080–1085.

162 H. Burghardt, K. L. Schimz, M. Muller, *FEBS Lett.* **1998,** *425,* 40–44.

163 D. C. Eustice, P. A. Feldman, I. Zajac et al., *Antimicrob. Agents Chemother.* **1988,** *32,* 1218–1222.

164 D. L. Shinabarger, K. R. Marotti, R. W. Murray et al., *Antimicrob. Agents Chemother.* **1997,** *41,* 2132–2136.

165 S. M. Swaney, H. Aoki, M. C. Ganoza et al., *Antimicrob. Agents Chemother.* **1998,** *42,* 3251–3255.

166 J. Thompson, M. O'Connor, J. A. Mills et al., *J. Mol. Biol.* **2002,** *322,* 273–279.

167 P. Dandliker, S. Pratt, A. Nilius et al., *Antimicrob. Agents Chemother.* **2003,** *47,* 3831–3839.

168 E. Cundliffe: in *The Ribosome: Structure, Function and Evolution,* eds W. E. Hill, A. Dahlberg, R. A. Garrett et al., ASM Press, Washington, DC 1990, pp. 479–490.

169 D. Moazed, J. M. Robertson, H. F. Noller, *Nature* **1988,** *334,* 362–364.

170 D. Moazed, H. F. Noller, *Cell* **1989,** *57,* 585–597.

171 J. Egebjerg, S. Douthwaite, R. A. Garrett, *EMBO J.* **1989,** *8,* 607–611.

172 J. Thompson, W. Musters, E. Cundliffe et al., *EMBO J.* **1993,** *12,* 1499–1504.

173 T. Uchiumi, A. Wada, R. Kominami, *J. Biol. Chem.* **1995,** *270,* 29889–29893.

174 A. S. Mankin, I. Leviev, R. A. Garrett, *J. Mol. Biol.* **1994,** *244,* 151–157.

175 B. T. Porse, I. Leviev, A. S. Mankin et al., *J. Mol. Biol.* **1998,** *276,* 391–404.

176 G. L. Conn, D. E. Draper, E. E. Lattman et al., *Science* **1999,** *284,* 1171–1174.

177 B. T. Wimberly, R. Guymon, J. P. McCutcheon et al., *Cell* **1999,** *97,* 491–502.

178 M. V. Rodnina, A. Savelsbergh, N. B. Matassova et al., *Proc. Natl. Acad. Sci. USA* **1999,** *96,* 9586–9590.

179 H. Stark, M. V. Rodnina, H. J. Wieden et al., *Cell* **2000,** *100,* 301–309.

180 J. Frank, R. Agrawal, *Cold Spring Harb. Symp. Quant. Biol.* **2001,** *66,* 67–75.

181 D. M. Cameron, J. Thompson, P. E. March et al., *J. Mol. Biol.* **2002,** *319,* 27–35.

182 P. Wurmbach, K. H. Nierhaus, *Eur. J. Biochem.* **1983,** *130,* 9–12.

183 M. Misumi, T. Nishimura, T. Komai et al., *Biochem. Biophys. Res. Commun.* **1978,** *84,* 358–365.

184 T. Yamada, Y. Mizugichi, K. H. Nierhaus et al., *Nature* **1978,** *275,* 460–461.

185 O. Jerinic, S. Joseph, *J. Mol. Biol.* **2000,** *304,* 707–713.

186 C. Gustafsson, B. C. Persson, *J. Bacteriol.* **1998,** *180,* 359–365.

187 G. Hirokawa, M. C. Kiel, A. Muto et al., *EMBO J.* **2002,** *21,* 2272–2281.

188 M. Kiel, V. Raj, H. Kaji et al., *J. Biol. Chem.* **2003,** *278,* 48041–48050.

189 U. von Ahsen, J. Davies, R. Schroeder, *Nature* **1991,** *353,* 368–370.

190 R. Schroeder, C. Waldsich, H. Wank, *EMBO J.* **2000,** *19,* 1–9.

191 J. Davies, *Mol. Microbiol.* **1990,** *4,* 1227–1232.

192 J. Frank, R. K. Agrawal, *Nature* **2000,** *406,* 318–322.

193 M. F. Brink, G. Brink, M. P. Verbeet et al., *Nucleic Acids Res.* **1994,** *22,* 325–331.

194 H. Fromm, M. Efelman, D. Aviv et al., *EMBO J.* **1987,** *6,* 3233–3237.

195 U. Johanson, D. Hughes, *Nucleic Acids Res.* **1995,** *23,* 464–466.

196 Z. Svab, P. Maliga, *Mol. Gen. Genet.* **1991,** *228,* 316–319.

197 G. Thom, C. D. Prescott, *Bioorgan. Med. Chem.* **1997,** *5,* 1081–1086.

198 G. Funatsu, E. Schilitz, H. G. Wittmann, *Molec. Gen. Genet.* **1971,** *114,* 106–111.

199 S. Besier, A. Ludwig, V. Brade et al., *Mol. Microbiol.* **2003,** *47,* 463–469.

200 M. Laurberg, O. Kristensen, K. Martemyanov et al., *J. Mol. Biol.* **2000**, *303*, 593–603.

201 A. Liljas, O. Kristensen, M. Laurberg et al.: in *The Ribosome. Structure, Function, Antibiotics, and Cellular Interactions*, eds R. A. Garrett, S. R. Douthwaite, A. Liljas et al., ASM Press, Washington, DC 2000, pp. 359–365.

202 R. Agrawal, P. Penczek, R. Grassucci et al., *Proc. Natl. Acad. Sci. USA* **1998**, *95*, 6134–6138.

203 R. K. Agrawal, A. B. Heagle, P. Penczek et al., *Nat. Struct. Biol.* **1999**, *6*, 643–647.

204 R. K. Agrawal, J. Linde, J. Sengupta et al., *J. Mol. Biol.* **2001**, *311*, 777–787.

205 M. G. Gomez-Lorenzo, C. M. T. Spahn, R. K. Agrawal et al., *EMBO J.* **2000**, *19*, 2710–2718.

206 R. Jorgensen, P. A. Ortiz, A. Carr-Schmid et al., *Nat. Struct. Biol.* **2003**, *10*, 379–385.

207 M. C. Justice, M. J. Hsu, B. Tse et al., *J. Biol. Chem.* **1998**, *273*, 3148–3151.

208 M. Shastry, J. Nielsen, T. Ku et al., *Microbiology* **2001**, *147*, 383–390.

209 M. C. Justice, T. Ku, M. J. Hsu et al., *J. Biol. Chem.* **1999**, *274*, 4869–4875.

210 L. Kisselev, M. Ehrenberg, L. Frolova, *EMBO J.* **2003**, *22*, 175–182.

211 A. Kaji, M. Kiel, G. Hirokawa et al., *Cold Spring Harb. Symp. Quant. Biol.* **2001**, *66*, 515–529.

212 C. M. Brown, K. K. Mccaughan, W. P. Tate, *Nucleic Acids Res.* **1993**, *21*, 2109–2115.

213 B. Vestergaard, L. Van, G. Andersen et al., *Mol. Cell* **2001**, *8*, 1375–1382.

214 B. P. Klaholz, T. Pape, A. V. Zavialov et al., *Nature* **2003**, *421*, 90–94.

215 U. B. Rawat, A. V. Zavialov, J. Sengupta et al., *Nature* **2003**, *421*, 87–90.

216 N. Polacek, M. J. Gomez, K. Ito et al., *Mol. Cell* **2003**, *11*, 103–112.

217 N. Brot, W. P. Tate, C. T. Caskey et al., *Proc. Natl. Acad. Sci. USA* **1974**, *71*, 89–92.

218 M. Selmer, S. Al-Karadaghi, G. Hirakawa et al., *Science* **1999**, *286*, 2349–2352.

219 D. E. Brodersen, V. Ramakrishnan, *Nat. Struct. Biol.* **2003**, *10*, 78–80.

220 T. Abo, K. Ueda, T. Sunohara et al., *Genes Cells* **2002**, *7*, 629–638.

221 J. de la Cruz, A. Vioque, *RNA* **2001**, *7*, 1708–1716.

222 K. J. Shaw, P. N. Rather, R. S. Hare et al., *Microbiol. Rev.* **1993**, *57*, 138–163.

223 R. H. Skinner, E. Cundliffe, *J. Gen. Microbiol.* **1980**, *120*, 95–104.

224 P. Pfister, S. Hobbie, Q. Vicens et al., *Chembiochem.* **2003**, *4*, 1078–1088.

225 A. S. Mankin, *J. Mol. Biol.* **1997**, *274*, 8–15.

226 T. Asai, C. Condon, J. Voulgaris et al., *J. Bacteriol.* **1999**, *181*, 3803–3809.

227 T. Asai, D. Zaporojets, C. Squires et al., *Proc. Natl. Acad. Sci. USA* **1999**, *96*, 1971–1976.

228 I. Chopra, M. Roberts, *Microbiol. Mol. Biol. Rev.* **2001**, *65*, 232–260.

229 M. C. Roberts, *FEMS Microbiol. Rev.* **1996**, *19*, 1–24.

230 M. C. Roberts, *Mol. Biotechnol.* **2002**, *20*, 261–283.

231 V. Burdett, *J. Bacteriol.* **1996**, *178*, 3246–3251.

232 C. A. Trieber, N. Burkhardt, K. H. Nierhaus et al., *Biol. Chem.* **1998**, *379*, 847–855.

233 C. M. Spahn, G. Blaha, R. K. Agrawal et al., *Mol. Cell.* **2001**, *7*, 1037–1045.

234 Y. J. Wu, W. G. Su, *Curr. Med. Chem.* **2001**, *8*, 1727–1758.

235 R. J. Russell, J. B. Murray, G. Lentzen et al., *J. Am. Chem. Soc.* **2003**, *125*, 3410–3411.

236 D. Fourmy, M. I. Recht, S. C. Blanchard et al., *Science* **1996**, *274*, 1367–1371.

237 R. A. Sayle, E. J. Milner-White, *Trends Biochem. Sci.* **1995**, *20*, 374.

238 N. Guex, M. C. Peitsch, *Electrophoresis* **1997**, *18*, 2714–2723.

239 W. Humphrey, A. Dalke, K. Schulten, *J. Molec. Graphics* **1996**, *14*, 33–38.

240 F. Abdulkarim, L. Liljas, D. Hughes, *FEBS Lett.* **1994**, *352*, 118–122.

241 J. R. Mesters, L. A. H. Zeef, R. Hilgenfeld et al., *EMBO J.* **1994**, *13*, 4877–4885.

242 L. A. H. Zeef, L. Bosch, *Mol. Gen. Genet.* **1993**, *238*, 252–260.

243 C. Alexander, N. Bilgin, C. Lindschau et al., *J. Biol. Chem.* **1995,** *270,* 14541–14547.

244 M. Sosio, G. Amati, C. Cappellano et al., *Mol. Microbiol.* **1996,** *22,* 43–51.

245 K. Boon, I. Krab, A. Parmeggiani et al., *Eur. J. Biochem.* **1995,** *227,* 816–822.

246 P. Londei, J. L. Sanz, S. Altamura et al., *J. Bacteriol.* **1986,** *167,* 265–2671.

247 L. Xiong, P. Kloss, S. Douthwaite et al., *J. Bacteriol.* **2000,** *182,* 5325–5331.

248 J. Prystowsky, F. Siddiqui, J. Chosay et al., *Antimicrob. Agents Chemother.* **2001,** *45,* 2154–2156.

249 S. Tsiodras, H. S. Gold, G. Sakoulas et al., *Lancet* **2001,** *358,* 207–208.

250 J. Thompson, D. F. Kim, M. O'Connor et al., *Proc. Natl. Acad. Sci. USA* **2001,** *98,* 9002–9007.

251 L. Del Pozo, D. Abarca, J. Hoenicka et al., *Eur. J. Biochem.* **1993,** *213,* 849–587.

252 S. Kawai, S. Murao, M. Mochizuki et al., *J. Bacteriol.* **1992,** *174,* 254–262.

253 H. S. Chittum, W. S. Champney, *J. Bacteriol.* **1994,** *176,* 6192–6198.

254 H. G. Wittmann, G. Stoffler, D. Apirion et al., *Mol. Gen. Genet.* **1973,** *127,* 175–189.

255 B. Malbruny, A. Canu, B. Bozdogan et al., *Antimicrob. Agents Chemother.* **2002,** *46,* 2200–2207.

256 D. D. Rhoads, D. J. Roufa, *Mol. Cell. Biol.* **1985,** *5,* 1655–1659.

257 C. Davies, D. E. Bussiere, B. L. Golden et al., *J. Mol. Biol.* **1998,** *279,* 873–888.

258 J. Bjorkman, P. Samuelsson, D. Andersson et al., *Mol. Microbiol.* **1999,** *31,* 53–58.

259 K. Bohman, T. Ruusala, P. C. Jelene et al., *Mol. Gen. Genet.* **1984,** *198,* 90–99.

260 G. Funatsu, K. Nierhaus, H. G. Wittmann, *Biochim. Biophys. Acta* **1972,** *287,* 282–291.

261 G. Funatsu, H. G. Wittmann, *J. Mol. Biol.* **1972,** *68,* 547–550.

262 S. Galili, H. Fromm, D. Aviv et al., *Mol. Gen. Genet.* **1989,** *218,* 289–292.

263 S. Gregory, J. Cate, A. Dahlberg, *J. Mol. Biol.* **2001,** *309,* 333–338.

264 A. R. Timms, H. Steingrimsdottir, A. R. Lehmann et al., *Mol. Gen. Genet.* **1992,** *232,* 89–96.

265 U. van Acken, *Mol. Gen. Genet.* **1975,** *140,* 61–68.

266 G. Funatsu, W. Puls, E. Schiltz et al., *Molec. Gen. Genet.* **1972,** *115,* 131–139.

267 A. Bollen, T. Helser, T. Yamada et al., *Cold Spring Harb. Symp. Quant. Biol.* **1969,** *34,* 95–100.

268 A. Bollen, T. Cabezon, M. de Wilde et al., *J. Mol. Biol.* **1975,** *99,* 795–806.

269 B. L. Golden, D. W. Hoffman, V. Ramakrishnan et al., *Biochemistry* **1993,** *32,* 12812–12820.

270 J. J. Cannone, S. Subramanian, M. N. Schnare et al., *BioMed Central Bioinformatics* **2002,** *3.*

271 B. T. Wimberly, D. E. Brodersen, W. M. Clemons et al., *Nature* **2000,** *407,* 327–339.

272 M.A. Schaefer, A.O. Tastan, S. Patzke et al., *J. Biol. Chem.* **2002,** *277,* 19095–19105.

273 J.E. Wilson, T.V. Pestova, C.U. Hellen et al., *Cell* **2000,** *102,* 511–520.

274 J.M. Harms, F. Schluenzen, P. Fucini et al. *BMC Biol.* **2004,** Apr 1.

275 S.M. Swaney, D.L. Shinabarger, R.D. Schaadt et al., *Abtracts of the 38th Interscience conference on Antimicrobial Agents and Chemotherapy* **1998** Abstract C104.

276 C.M. Spahn, M.G. Gomez-Lorenzo, R.A. Grassucci et al., *EMBO J.,* **2004,** *23,* 1008–1019.

Appendix A1

Pactamycin

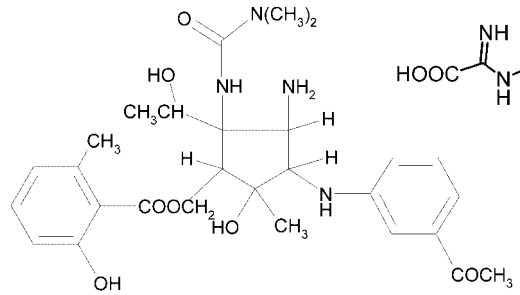

Kasugamycin

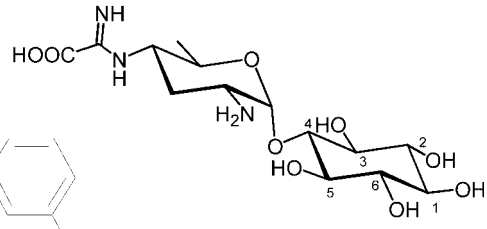

Edeine

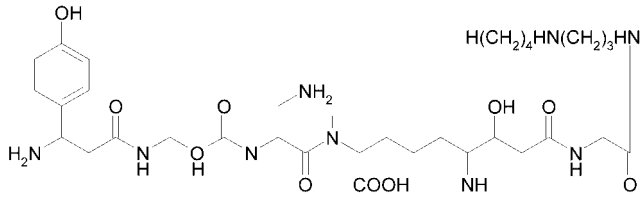

Evernimicin and Avilamycin

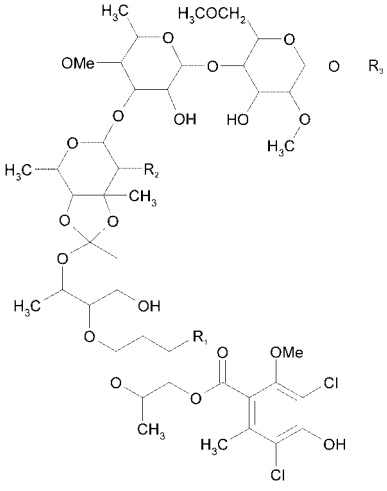

Avilamycin

R_1= OH, R_2= H

R_3=

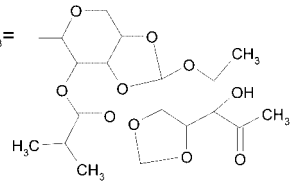

Evernimicin

R_1=

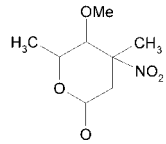

R_2= OH

R_3=

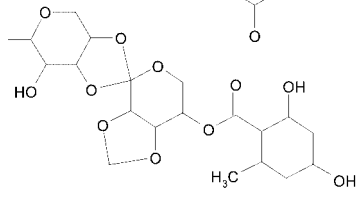

Appendix B1

Tetracyclines

Tetracycline (1953)

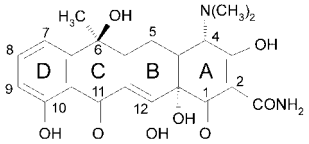

7-Chlortetracycline (1948)

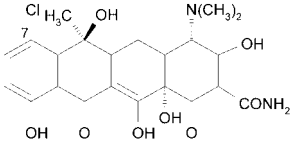

Doxycycline
(6-deoxy-tetracycline) (1967)

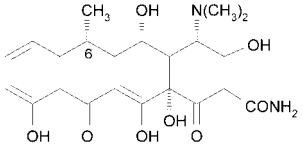

Minocycline
(7-dimethylamino-6-demethyl-6-deoxy-tetracycline) (1972)

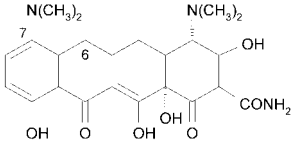

Glycylcyclines

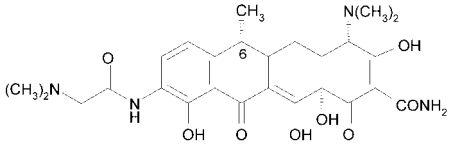

DMG-DOT
(DMG-doxycycline)
(9-(*N*,*N*-dimethylglycylamido)-6-deoxytetracycline)
(1993)

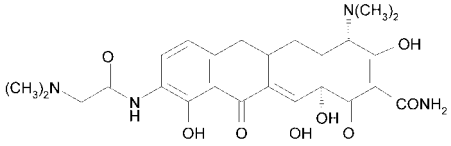

DMG-DMDOT
(9-(*N*,*N*-dimethylglycylamido)-6-demethyl-6-deoxytetracycline)
(1993)

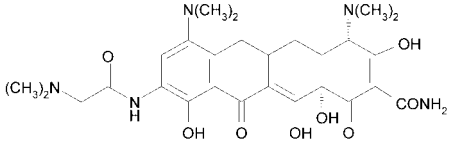

DMG-MINO
(9-(*N*,*N*-dimethylglycylamido)-minocycline)
(1993)

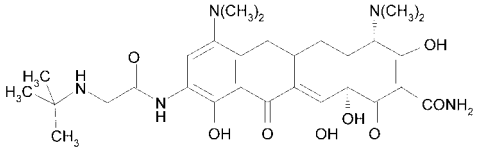

GAR-936
(tigecycline) or
(TBG-MINO) or
(9-(t-butylglycylamido)-minocycline)
(1993)

Appendix C1

Aminoglycosides: 4,5-2-DOS

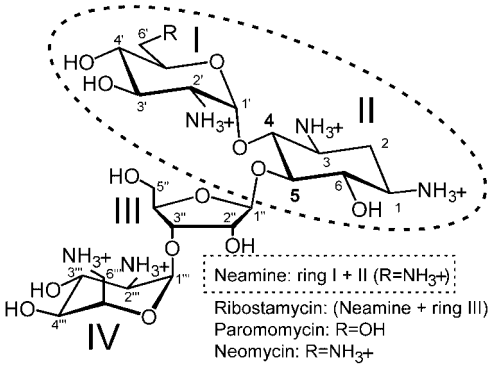

Streptomycin

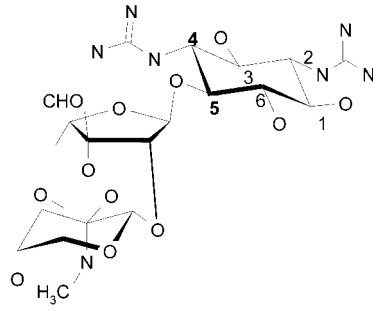

Aminoglycosides: 4,6-2-DOS

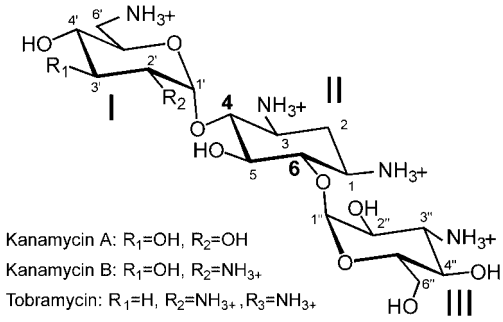

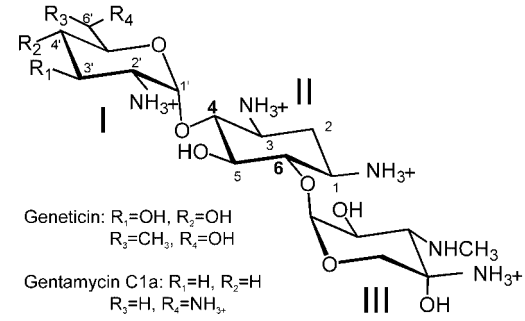

Appendix D1

Kirromycin
R=H

Aurodox (N-methyl-Kirromycin)
R=CH_3

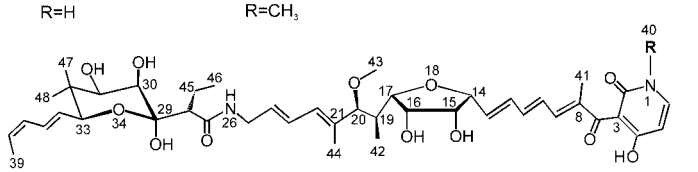

Enacyloxin IIa

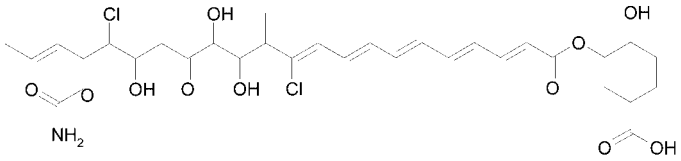

Pulvomycin

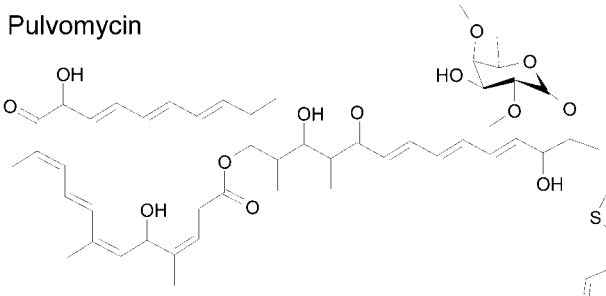

GE2770A
(MDL 62,879)

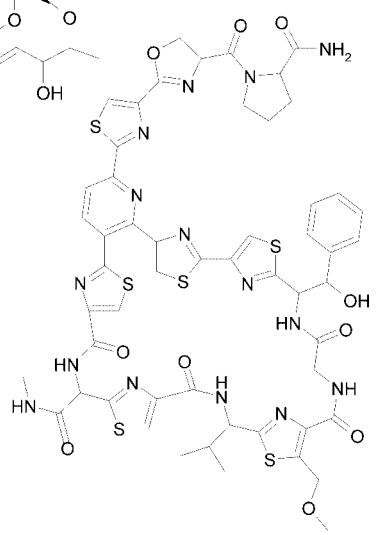

Appendix E1

Peptidyl-transferase inhibitors

Puromycin

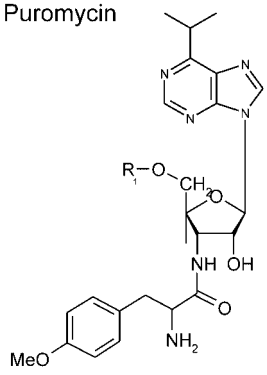

tRNA-A76

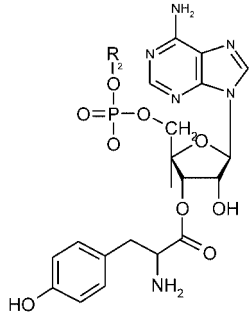

Chloramphenicol

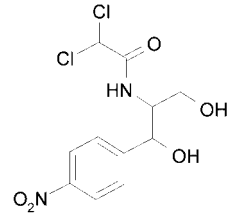

Anisomycin

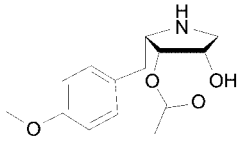

Blasticidin S

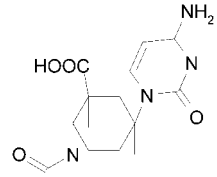

Sparsomycin

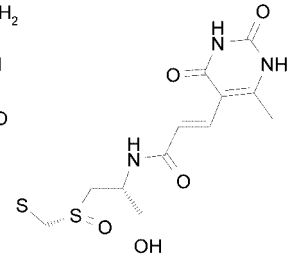

Lincosamides

Lincomycin: R= OH
Clindamycin: R= Cl

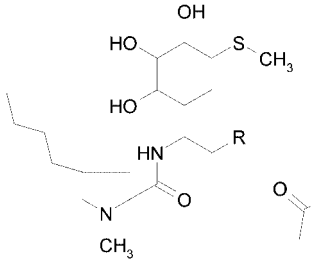

Oxazolidinones

Linezolid: R= O

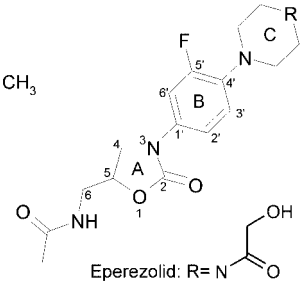

Eperezolid: R= N

NRI

A-72310

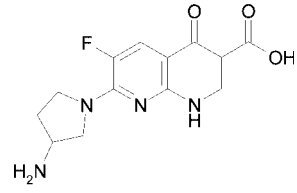

Appendix E2

Macrolides: 14 and 15 membered

Erythromycin: R_1= H, R_2= O
Clarithromycin: R_1= CH_3, R_2= O
Roxithromycin: R_1= H, R_2 = $NOCH_2O(CH_2)_2OCH_3$

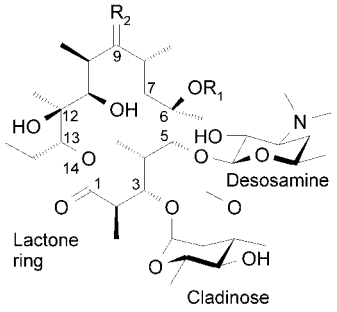

Cethromycin (ABT-773)

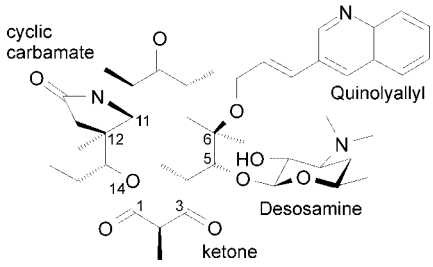

Telithromycin (HMR-3647)

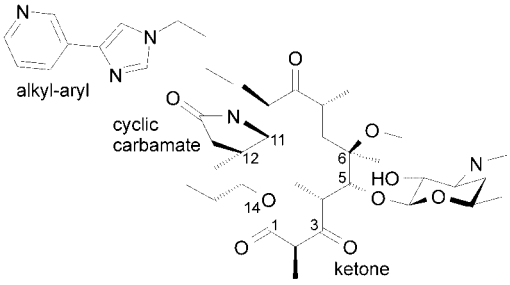

Azithromycin

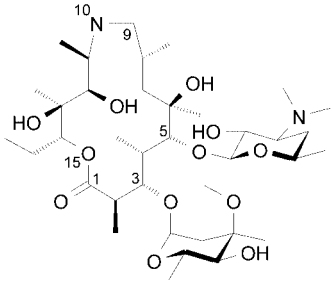

Troleandomycin

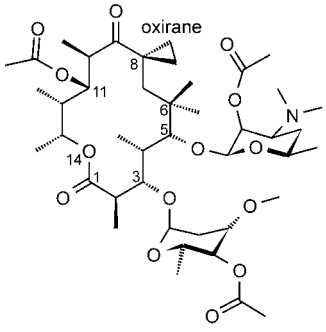

Appendix E3

Macrolides: 16 membered

Carbomycin A

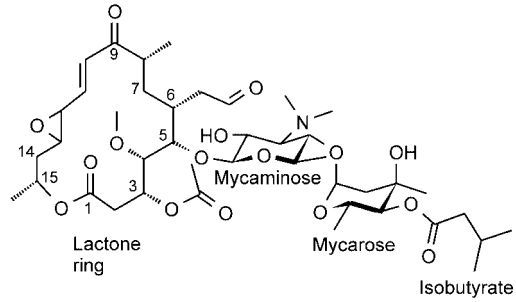

Tylosin

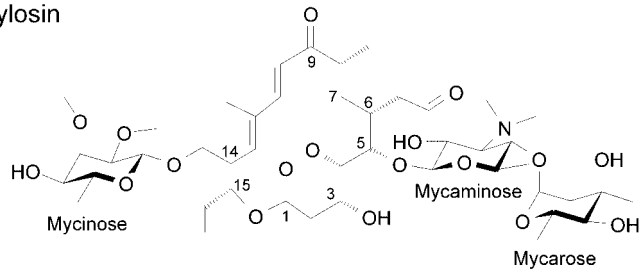

Spiramycin

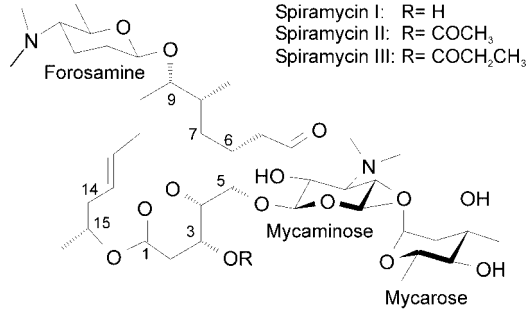

Streptogramins

Virginiamycin S (S_A)

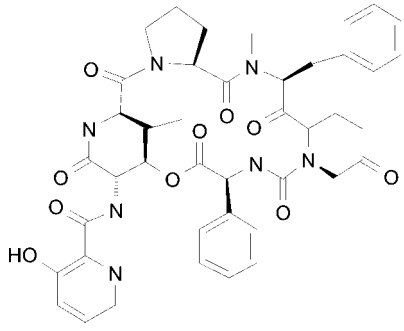

Virginiamycin M (S_B)

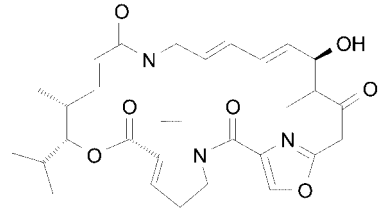

Appendix F1

Translocation inhibitors

Thiostrepton

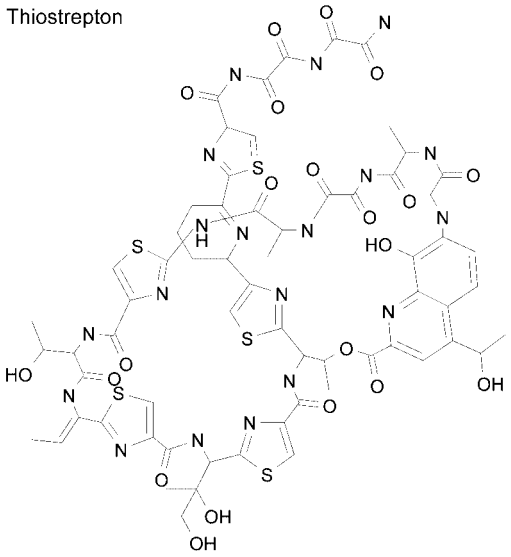

Fusidic acid

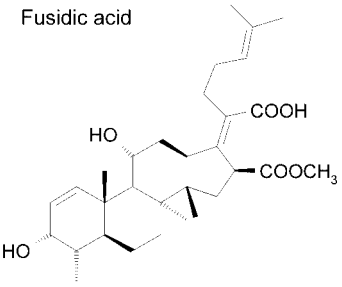

Sordarin (GM193663)

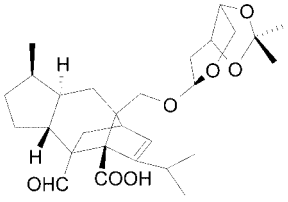

Micrococcin

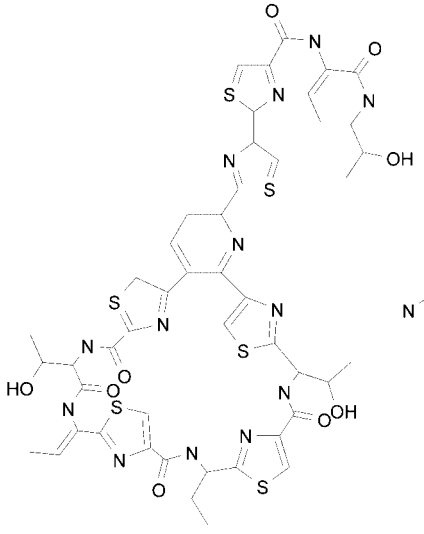

Spectinomycin

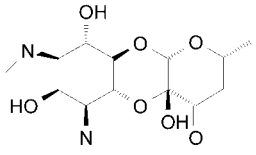

Viomycin